THE WOLF CREEK RESEARCH BASIN, YUKON TERRITORY:

26-YEARS OF HYDROLOGIC CHANGE

THE WOLF CREEK RESEARCH BASIN, YUKON TERRITORY:

26-YEARS OF HYDROLOGIC CHANGE

By: FIONA M. CHAPMAN, B.Sc (Ag. Env. Sci)

A Thesis Submitted to the School of Graduate Studies in Partial Fulfilment of the Requirements of the Degree Master of Science

MASTER OF SCIENCE (2021) MCMASTER UNIVERSITY
(EARTH AND ENVIRONMENTAL SCIENCE) HAMILTON, ONTARIO

TITLE: The Wolf Creek Research Basin, Yukon Territory: 26-years of hydrologic change

AUTHOR: Fiona M. Chapman, B.Sc. (Ag. Env. Sci.) (McGill University)

SUPERVISOR: Dr. Sean K. Carey

NUMBER OF PAGES: xiii, 104

Lay Abstract:

Increasing temperatures and changing precipitation patterns are global consequences of climate change, which are amplified in northern environments. This research looks at a long-term hydrologic dataset of the Wolf Creek Research Basin (WCRB), located near Whitehorse, Yukon. Three hydrologic variables were evaluated: air temperature, precipitation, and discharge. Each variable plays a critical role in a watershed's response to climate change. From 1993 to 2019, there was a significant increase in winter precipitation across the basin. Mean annual temperature also increased at the two lower elevation sites at a rate comparable to the rest of Yukon. Mean annual discharge has also increased, most notably in fall and winter which is reflective of an increase in groundwater contributions to the stream. This research increases our understanding of the relationships and drivers behind hydrometric changes which allows for a stronger interpretation of the response of catchments to climate change.

Abstract:

Increasing temperatures and changing precipitation patterns are global consequences of climate change, which are amplified in northern environments. Cold environments are particularly sensitive to warming due to the importance of sub-zero temperatures, which influence frozen ground status and precipitation type. The objective of this research is to evaluate the controls on the timing, rate, and volume of the major hydrological fluxes within the Wolf Creek Research Basin (WCRB), Yukon Territory and to identify any long-term changes. WCRB is a long-term hydrological observatory established in 1993 to evaluate cold region hydrological processes. Within WCRB, three long-term meteorological stations at different elevations with total precipitation measurements and several stream gauges allow a long-term (26 year) evaluation of water balance components. Increases in temperature and precipitation magnitude are consistent with climate models including CIMP6 models. There has also been a significant increase in the number of high intensity precipitation days (primarily in June, July, and August). Fall and winter discharge increased and there was an increase in mean annual baseflows. The proportion of discharge output during freshet (April 1st – July 1st) has not changed, but the timing of peak flow has shifted from late-May to mid-June. This research provides a unique opportunity to study long-term change while recognizing short-term natural variability in hydrologic data. Understanding the mechanisms within catchments will allow for a stronger interpretation of the response of catchments to changing climate regimes which can have diverse impacts on local ecosystems and prevailing geohazards in northern environments.

Acknowledgements:

First, I would like to thank my supervisor, Dr. Sean Carey for his support throughout the rollercoaster that was my masters. Sean remained optimistic and full of ideas while my initial project melted away during Spring 2020. I am grateful for his commitment to the Wolf Creek Research Basin since inauguration as this project would not have been possible without years of efforts way before I got involved.

On that note, I would also like to thank the countless people who have contributed to data collection at the WCRB. Most recently, this includes David Barrett and Tyler de Jong. Thank you for keeping the operations up and running, helping me track down miscellaneous data, and keeping us up to date on all things Yukon, within and outside of the basin.

Thank you to all the members of the Watershed Hydrology Lab group. Your eagerness to listen and help throughout my time at McMaster did not go unnoticed. Special thanks to Victor for designing an app to help with my analysis, and Graham for putting in a huge effort to foster a sense of community in our virtual reality. Seeing lab members and hearing about everyone's research through the writing club and coffee made a significant difference to working from home.

I would also like to specifically thank Arsh, Sean, and Lauren for tolerating numerous ArcGIS and R Studio woes, and contributing to quality Team B rants. Similarly, I would like to thank Joe and Renee for filtering out many less-than-intelligent questions and for their support while working our way through similar struggles.

Finally, I guess I should thank my family, Mum, Dad, Cameron, and Brandon for having me back 24/7 after they thought they got rid of me, and a special thanks Zack for being a phenomenal distraction and keeping me company for as long as he could.

Table of Contents

List of Figures

Chapter 2

Chapter 3

Chapter 4

List of Tables

Chapter 2

Chapter 3

Chapter 4

Chapter 1: Introduction

1.1 Introduction

Increasing temperatures and changing precipitation patterns are global consequences of climate change. These impacts are amplified in cold regions, with temperature increases in northern environments being twice that of the global average since 2002 (AMAP, 2017; IPCC, 2018; Laudon et al, 2013; Lyon et al., 2018, Meredith et al., 2019). Freeze-thaw cycles and precipitation phase rely on sub-zero temperatures, making high-latitude ecosystems particularly sensitive to warming (Tetzlaff et al., 2013). Consequently, increasing temperatures in northern environments have cascading effects that influence a range of hydrologic processes and have severe impacts on water quality, nutrient cycling, and aquatic ecosystems (AMAP, 2017; IPCC, 2018).

In cold regions, warmer temperatures are accompanied by reduction in snow cover and an increased frequency of intense convective storms, causing a shift from snow- to rain-driven streamflow hydrographs (DeBeer et al., 2016; Musselman et al., 2017). The combination of warmer temperatures and relative increase in rain versus snow in northern regions are leading to permafrost degradation and loss of ground ice, as well as increases in evapotranspiration (DeBeer et al., 2016). These changes influence soil water pathways and stream flow regimes, which impact the timing of peak and low-flow, water temperature, and water chemistry (AMAP, 2017; Lafrenière & Lamoureux, 2019; Lyon et al., 2018).

Despite the increased sensitivity of high-latitude watersheds to environmental change, they are extremely understudied as they are less accessible than mid-latitude catchments (Laudon et al., 2017; O'Donnel 2018). There are limited long-term hydrologic monitoring sites established in northern regions, and 40% of the previously established sites stopped recording water balance data between 2000 and 2017 (Laudon et al., 2017). Long-term data sets are essential for understanding the hydrological implications of climate change as natural variability skews short-term trends within all watersheds (St. Jacques et al., 2010). The continual measurement of long-term hydrologic data allows for the identification of trends and facilitates the evaluation of how catchments respond to changes in temperature and precipitation regimes. This in turn helps guide our understanding of process interaction and can aid in the prediction of future hydrological response to climate change.

The Wolf Creek Research Basin (WCRB) is a northern research basin (61° N, 135° W) established in 1992 and climate and water balance data collection began in 1993. The WCRB provides an important location for a long-term northern hydrologic study site due to its northern latitude, proximity to Whitehorse, Yukon, moderate size (179 km^2), altitudinal gradient (660 to 2080 masl), and ecozone variety (forest, shrub taiga, and tundra). The 26-years of hydrological data collected at the WCRB provides a unique opportunity to assess the integrated watershed scale hydrologic processes and provide insight on water balance dynamics over the course of a few decades. The long-term water balance of WCRB advances current knowledge of key hydrologic drivers in subarctic

watersheds, while considering the interconnectedness of hydrologic processes and how these processes have changed over time.

1.2 The Water Balance

Water balances provide an overview of water movement within a defined area by quantifying hydrological inputs and outputs on a watershed scale for a specified time period (Dingman, 2015). They provide an integrated view of hydrological processes and offer a comparative framework to contrast different responses across watersheds. Neglecting groundwater fluxes into and out of a watershed, the water balance is defined as:

(1) $\Delta S = P - D - E$

Where ΔS is change in storage, P is precipitation, D is total discharge, and E is evapotranspiration. Precipitation includes rain and snow (in snow-water equivalent, SWE) and other solid precipitation. The water balance can be defined volumetrically, although typically is area-normalized and reported in millimeters as this facilitates inter-catchment comparisons. To close a water balance and conserve mass, it is generally assumed that storage within a watershed does not change ($\Delta S = 0$) over the period for which the water balance is being calculated (Kane et al., 2005), therefore:

(2) $P = D + E$

Precipitation and discharge are measured and, while evapotranspiration can be directly measured using various micrometeorological techniques, it is more common for evapotranspiration to be calculated as the difference between precipitation and discharge.

Water balances are commonly calculated on seasonal or annual basis, depending on data availability and research objective. Annual water balances are typically calculated over a water year which is defined based on the start of a water cycle in a given region. For the WCRB, a water year is defined as being from 1 October to 31 September of the following calendar year, as snow typically begins to accumulate in October.

Water balances of northern watersheds are common but not abundant, and there are very few northern study sites with long-term hydrologic data sets. For example, Kane et al. (2005) compared 39 northern watersheds (>50 °N) for which water balances have been calculated but only 10 of these sites had more than 15-years of data. A range of monitored northern study sites are essential for understanding northern hydrology, as their long-term water balances quantify the variability and impact of each water balance component, and how these have changed with time.

1.2.1 Precipitation

In northern regions, total annual precipitation is often snow dominant, decreases with increasing latitude, and has significant variation inter-annually and among sites (Kane et al., 2005). Precipitation is a primary driver of catchment hydrology as it includes all inputs into a catchment, and influences the surface energy balance by the strong influence of snow on surface albedo (Woo, 2012; Yang & Kane, 2021). Precipitation regimes are altered by storm track trajectories, moisture recycling, and temperature controls on capacity of saturated air and precipitation phase (Bintanja & Andry, 2017).

Climate trends and future projections show an increase in northern precipitation, with the Arctic getting up to 50% wetter over this century, primarily as a feedback of climate warming (Barrow et al., 2004; Bintanja & Andry, 2017; DeBeer et al., 2016). Precipitation is influenced by global climate oscillations which have a control on wet and dry years, but intensified local surface evaporation due to warming and is associated with an increase in late-season and high-intensity rainfall, annually (Arp et al., 2020; Hisdal et al., 2003; Wan et al., 2015; Yang & Kane, 2021). Late-summer and early-fall rainfall increases late-season flows, generating unparalleled late-season floods, with some floods exceeding those generated by snowmelt in previously snow-dominated catchments (Arp et al., 2020). Increases in rainfall also generates substantial soil water recharge thereby increasing annual baseflow (Wittenberg, 1999).

The increase in rainfall is not expected to be paralleled in snowfall, therefore the ratio of liquid to solid precipitation is expected to increase with time (Bintanja & Andry, 2017). The intensification of rainfall has already caused shifts from snow-dominated to rain-dominated or hybrid catchments in some sub-arctic regions, and climate models predict that rain-dominance will become the norm for the majority of Arctic catchments by the end of the 21st century (Bintanja & Andry, 2017; Cunderlik & Ouarda, 2009).

1.2.2 Snow

Though a shift to rain-dominant catchments is projected, many arctic and sub-arctic catchments currently remain snow-dominated, exhibiting nival regimes, with some

having mixed flow regimes (Arp et al., 2020; Cunderlik & Ouarda, 2009). The majority of annual precipitation accumulates as snow from late-fall to early-spring and is stored on the surface until freshet, the period during which snow melts (Woo, 2012). Snow accumulation depends on total snowfall, but snow distribution is also influenced by wind, local topography, and vegetation. The distribution of snow controls the amount of snow subject to sublimation and influences the timing of melt, with up to a third of total annual snowfall being returned to the atmosphere due to the sublimation of blowing snow (Pomeroy and Gray, 1995; Rasouli et al., 2014). Wind redistributes snow from exposed areas to sheltered areas, such as leeward slopes, gullies, and in vegetation, with elevation, aspect, and vegetation cover accounting for 80-90% of variability in snow accumulation on the catchment scale (Jost et al., 2007; Pomeroy et al., 2006). For example, in the WCRB upwards of 50% of snow at the highest elevation sites, and 25% at mid-elevation sites, is redistributed by wind and 20 to 30% more snow accumulates on north than south-facing slopes (Pomeroy et al., 1999; Woo & Carey, 1999).

Vegetation also influences snow redistribution by trapping snow. Shrubs trap snow relative to their height and density, with tall shrubs retaining more snow than short shrubs; however, all shrubs capture more snow than areas dominated by moss and lichen causing snow to be blown from tundra to shrubby and forested areas (Pomeroy et al., 2006; Woo, 2012). In a WCRB sub-catchment with lichen, moss, short shrubs, and tall shrubs, the greatest SWE before snowmelt is found within tall shrubs (McCartney et al., 2006). Furthermore, vegetation shades snow and reduces sublimation. A reduction of

sublimation means more snow accumulates rather than being lost to the atmosphere, and shading delays snowmelt (Sturm et al., 2000).

The importance of vegetation controls on snow accumulation increases with shrubification in northern regions (Sturm et al., 2000). Shrubification is characterized by treelines migrating northward, tall shrubs encroaching on areas previously dominated by short shrubs, and short shrubs covering tundra previously dominated by moss and lichen (Leipe & Carey, 2021; Myers-Smith & Hik, 2017; Sturm et al., 2005). Shrubification is estimated to increase snow accumulation by sheltering and capturing snow, thereby reducing sublimation (Sturm et al., 2000). An increase in accumulated snow is expected to generate greater runoff during freshet; however, increased shading and snow captured at higher elevations may delay peak flows despite increasing temperatures (Jost et al., 2007; Pomeroy et al., 2006; Sturm et al., 2000).

1.2.3 Measuring Precipitation

Precipitation is notoriously difficult to measure, especially in northern regions, where snow and trace precipitation makes up significant portions of the water budget. Precipitation gauges underestimate snow and rain as: 1) they require a minimum amount of precipitation to be able to record a precipitation value and therefore do not reliably record small precipitation events, and 2) precipitation gauges are installed to catch vertical rainfall; however, wind influences the direction of precipitation limiting the accurate capture.

Trace precipitation (< 0.2 mm of rain, or < 0.2 cm of snow) is common in the arctic and represents a significant portion of total annual precipitation, but is often not measured by traditional rain gauges (Mekis, 2005; Milewska et al., 2019; Woo, 2012). In the Canadian Arctic, trace precipitation accounts for up to 20% of total annual precipitation yet is unaccounted for unless corrections to precipitation data are made (Mekis, 2005). In subarctic regions, trace precipitation is less important but has been shown to represent 4 to 6% of total precipitation in southwestern Yukon and therefore must be considered when measuring precipitation (Mekis, 2005). Other challenges in measuring precipitation, such as undercatch and evaporation (before measurement), further contribute to the underestimation and limit our ability to accurately estimate precipitation.

Snow is commonly measured by heated precipitation gauges, snow radar, snow pillows, and manual snow surveys. Prior to wind shields being installed on heated precipitation gauge, snow measured by gauges underestimated snow accumulation by up to four-fold due to undercatch (Liljedahl et al., 2017; Stuefer et al., 2020). The installation of wind shields approximately halved the underestimation by reducing the influence of wind close to the gauge, but the measurement remains imperfect (Liljedahl et al., 2017). Snow and rain measurements by gauges are mathematically corrected based on gauge shape and windspeed (Milewska et al., 2019; Pan et al., 2016). Snow surveys are advantageous as they consider the high spatial heterogeneity of snow accumulation, however the intensive field work requirements and lack of automated measurements

limits sampling frequency and duration with high-quality measurements generally being restricted by project duration (Pomeroy et al., 1999; Sturm & Stuefer, 2013).

Accurate precipitation measurement is challenging, but vital to be able to present a complete water balance. An underestimation of precipitation impacts the relative amount of input, output as runoff or evaporation, notably when evaporation is calculated a residual value. Long-term, the error associated with the underestimation of precipitation accumulates in the storage term (Liljedahl et al., 2017).

1.2.4 Evapotranspiration

Evapotranspiration (ET), the combination of direct evaporation and transpiration, influences the amount of water available for runoff and recharge by recycling water back into the atmosphere. ET can be measured using micrometeorological techniques, but direct measurements are sparse in northern regions due to the high cost of eddy-covariance equipped meteorological towers. Point measurements are useful notably when considering small relatively homogeneous areas, but they are unable to represent the heterogeneity across catchments (Bring et al., 2016). Large scale inter-catchment studies have moved towards remote sensing techniques to evaluate ET on regional scales (Zhang et al., 2010), but at the catchment scale, ET is commonly calculated in water balance studies as a residual (Amiro, 2009). As a residual, ET values are dependent on the accuracy of precipitation and runoff measurements and their relative representativeness across a catchment. Representative ET values are essential for closing water balances,

defining water availability, and differentiating between dry and wet catchments based on the ET to precipitation ratio (Tetzlaff et al., 2013; Thornewaite, 1948).

In general, ET decreases with latitude as less solar energy is available in high latitudes, but it is highly variable inter-annually and between sites (Kane et al., 2005). ET peaks during summer when solar radiation is greatest (Wang et al., 2013). Due to the seasonality of ET, the proportion of precipitation recycled back to the atmosphere varies. For example, Rovansek et al. (1996) found that ET exceeded precipitation after freshet in a wetland dominated watershed in Alaska, whereas ET does not exceed precipitation prior to freshet. This is echoed by a more recent study in high-elevation catchments in Switzerland which highlights that rainfall is disproportionately evaporated as compared to snow in high-elevation and northern catchments (Allen et al., 2019).

Temperature, water availability, and vegetation are the primary controls on ET, with some northern regions moving towards drier conditions despite an increase in precipitation (Hinzman et al, 2005). As the majority of ET occurs from canopy transpiration and evaporation of intercepted precipitation, an increase in leaf area index (LAI) is expected to increase total ET despite decreasing direct soil evaporation due to shading (Beringer et al., 2005; Kozii et al., 2020). This increase ET is greatest during the growing season (Beringer et al., 2005). Nicholls and Carey (accepted) further highlight the importance of vegetation in controlling ET across a Canadian subalpine watershed as ET rates are highest, and most seasonally stable, in the most vegetated sub-catchments. Shrub expansion and an increase in woody vegetation has a positive feedback with ET,

with changes in vegetation type and abundance expected to increase ET by up to 13% in the next 50 years (Pearson et al., 2013).

Direct evaporation also contributes to total ET and is dependent on the abundance of surface water. Any changes in lake or wetland size within a catchment will influence total ET by altering water availability (Hinzman et al., 2005). On a smaller scale, seasonal surface ponding also increases ET. Ponding, and therefore ET, does not occur homogeneously across catchments but depends on the ability for water to accumulate on the surface, and therefore not infiltrate into the soil. Catchments areas with low infiltration capacity, such as bedrock, clay, and ice-rich layers have greater surface ponding than areas with high infiltration capacities, such as silt or sand substrate (Carey & Woo, 1999). Ponding is most significant during freshet and influences evaporation; however, transpiration becomes more important during the growing season as soil-moisture decreases and shading increases (Carey & Woo, 1999). Due to the numerous controls on ET at the catchment scale, ET is highly variable spatially and temporally highlighting the importance of considering ET heterogeneity in water balance analyses.

1.2.5 Discharge

Stream discharge provides an effective tool to evaluate the response of watersheds to changing temperatures and precipitation patterns, as it defines catchment output and integrates hydrological variability across the watershed (Burn, 1994; Burn & Hag Elnur, 2002; Zhang et al., 2001). Total discharge consists of direct runoff and baseflow, where

baseflow is commonly thought of as the old-water or groundwater contribution to streamflow, and direct runoff taken as the proportion of new- or event-water contributing to streamflow via surface and near-surface pathways (Dingman, 2015). Historically, there was an emphasis on overland flow being a dominant form of runoff in cold regions (Freeze, 1974), but over the past several decades runoff in cold regions has identified several complex subsurface pathways including overland, matrix and preferential flow paths (e.g. Quinton and Marsh, 1999; Carey and Woo, 2000). The relative contribution of runoff mechanisms is variable spatially and temporally throughout catchments and depend on controls such as soil type, permafrost distribution, slope, and aspect (Carey & Woo, 2000; Carey & Woo, 2001; Yang & Kane, 2021).

In northern environments, the majority of discharge occurs during the freshet period as watersheds follow a nival (or snowmelt dominated) flow regime (Woo, 2012). The timing and rate of snowmelt influences surface discharge and groundwater regimes, with slower snowmelt being associated with less direct runoff than a short snowmelt period because the melt is less likely to exceed the infiltration rate (Musselman et al., 2017). As overland flow transports water faster than matrix or pipe flow, an increase in overland flow causes an increase in the amount of water reaching streams within a shorter period generating flashy hydrographs (Dingman, 2015). Areas with continuous permafrost have been shown to have more overland flow due to the decreased soil infiltration capacity; however, infiltration from snowmelt does generate pipe and matrix

flow displacing water stored in the subsurface as the active layer thaws (Carey & Woo, 1999; Dingman, 2015).

Baseflow is maintained by the groundwater input to streams, where the groundwater is recharged by precipitation infiltrating into the ground and percolating through soil (Woo, 2012). The infiltration and percolation rates are primarily controlled by soil type, saturation, and temperature, with ground below 0°C being less permeable than thawed soil, assuming the same initial conditions (Rasouli et al., 2014). Groundwater recharge is essential for maintaining baseflow and occurs most rapidly in areas with high vertical connectivity and is therefore related to permafrost distribution in northern catchments (Walvoord et al., 2012).

1.2.5.1 Trends in Discharge

Discharge can be described in terms of magnitude and event timing, with mean annual or monthly discharge and day of year (DOY) peak flow or spring onset being common descriptors (Burn & Elnur, 2002; Cayan et al., 2001; Stewart et al, 2004). There are few recorded changes in annual streamflow in northern streams, but there are significant changes in seasonal discharge. Northern streams show increases in winter and spring discharge, variable trends in summer, and little to no trends in fall discharge (Hisdal et al., 2010).

In Scandinavian catchments, there have been significant changes in the magnitude of discharge in the 40-years prior to 2002 (Hisdal et al., 2010). The same trends are

echoed by Matti et al. (2017) across 59 basins, also in Scandinavia, from 1961 to 2010. Maximum daily discharge increased in winter, spring, and fall, but decreased in summer (Hisdal et al., 2010; Matti et al., 2017). The increase in fall discharge is associated with a shift from snow- to rain- dominated hydrographs, in which a shift to earlier and smaller peak flow events are a result of increasing temperatures and earlier snowmelt (Matti et al., 2017; Vormoor et al., 2015). In north America and northern Europe, earlier snowmelts have been shown to shift freshet to earlier in the year (Burn & Elnur, 2002; Jones et al., 2015; Wasko et al., 2020), and an earlier spring onset is thought to explain trends in earlier ends to ice conditions (Burn & Elnur, 2002).

Detecting streamflow trends is challenging, notably in winter as flows are low so small deviations from the mean may be considered significant and values may be skewed due to ice jamming (Hisdal et al., 2010; Matti et al., 2017). However, increases in winter runoff over the past several decades are associated with increasing winter temperatures and late-season precipitation; trends that increase subsurface connectivity and are predicted to continue (Meredith et al., 2019; St. Jacques & Sauchyn, 2009; Walvoord et al., 2011).

1.3 Subsurface flow and connectivity

Subsurface flows and connectivity are influenced by frozen ground regimes in northern environments. Ground that has remained below 0°C for two or more consecutive years, is defined as permafrost and can be discontinuous (<90%) or continuous (>90%;

van Everdingen, 1998). Discontinuous permafrost is further classified as being extensive, widespread, or sporadic, where sporadic permafrost only occurs in isolated patches (Harris et al., 1988). Permafrost is overlain by a transition zone and an active layer (Woo, 2012). The active layer is perennial, freezing and thawing each year, whereas the transition layer is an ice-rich layer that thaws during warm years, but remains frozen during cooler summers (Shur, Hinkel, & Nelson, 2005). Permafrost and seasonally frozen ground inhibit infiltration and percolation capacities as permafrost creates a quasi-impermeable surface to subsurface flow (Carey & Quinton, 2005). Permafrost limits flow in the subsurface to the active and transition layers (supra-permafrost) and subsurface runoff connectivity increases with ground thaw. Supra-permafrost aquifers are linked to deeper waters through the presence of taliks (Woo, 2012).

Moving northward, there is a general transition from sporadic to continuous permafrost. In more southernly regions, deeper subsurface pathways are connected to the stream continuously maintaining streamflow throughout the year (Woo, 2012). As permafrost becomes more widespread, complete freezeback of the active layer may result in the cessation of streamflow during winter, and in areas where taliks are present, groundwater is at times able to maintain flows. The link between groundwater connectivity to the stream network has received considerable attention in permafrost environments, as climate warming and permafrost thaw is often used to explain changes in winter flows observed across the Canadian territories and in northern Eurasia over the

past several decades (Smith et al., 2007; St Jacques & Sauchyn, 2009; Walvoord & Striegl, 2007).

Increased baseflow is prominent in permafrost regions, as permafrost degradation thins continuous permafrost and decreases the lateral extent of discontinuous permafrost (Kane et al., 1991; St. Jacques & Sauchyn, 2009). Discontinuous permafrost, such as that found in the WCRB, is more susceptible to degradation as it is warmer and thinner than continuous permafrost (Kurylk et al., 2015). Permafrost thaw, and the resulting thickening of the active layer, has been associated with multidecadal increase in baseflow due to the greater suprapermafrost water storage and deeper flow pathways (Lyon et al., 2009; St. Jacques and Sauchyn, 2009). A decrease in lateral extent of discontinuous permafrost also increases vertical connectivity between sub- and suprapermafrost groundwater (Walvoord et al., 2012). The combination of greater suprapermafrost storage, deeper flow pathways, and increased vertical connectivity have been shown to all contribute toward the increase in baseflow in northern regions (Lyon et al., 2009; St. Jacques and Sauchyn, 2009; Walvoord et al., 2012).

1.4 External Controls on Hydrologic Trends

1.4.1 Teleconnections

Teleconnections are periodic global climate oscillations driven by sea level pressure (SLP) and sea surface temperature (SST) differentials over different parts of Pacific, Atlantic, and Arctic oceans (Bjerknes, 1969; Hurrell, 1995; Latif & Barnett,

1994). The differences in air pressure and temperature driven by ocean-atmosphere interactions influence regional weather causing wet, dry, cool, and warm years making the phase of relevant teleconnections important to consider when analyzing meteorological trends (Bjerknes, 1969; Dingman, 2015). Major teleconnections include: El Nino and the Southern oscillation (ENSO), Pacific Decadal oscillation (PDO), North Atlantic oscillation (NAO), Pacific North American oscillation (PNA), and the Arctic oscillation (AO). ENSO and NAO have been shown to significantly influence climate in northern Europe (Ahmed et al., 2021). The Yukon is commonly grouped with British Columbia (BC) and Alaska when studying the influence of teleconnections across northwestern North America, where ENSO, PDO, and AO predominantly influence climate (Ahmed et al., 2021; Fleming & Whitfield, 2010; McNeil, 2015).

ENSO is widely accepted as being the dominant global-scale teleconnection. It is driven by difference in SLP and SST between the eastern and western Pacific. The warm or positive phase is associated with high SST in the eastern Pacific which translates to warmer winter and spring temperatures with less precipitation in Canada and Alaska, and the opposite is true of cold or negative phase (Ahmed et al., 2021; Shabbar & Khandekar, 1995). PDO periods have similar effects as ENSO on northern regions (Ahmed et al., 2021). The AO is associated with the NAO, and is known to have a lesser effect on global climate than ENSO or PDO (Ambaum et al., 2001). AO phase depends on the strength of the polar vortex, with the positive phase representing strong polar vortex and the negative phase describing a weaker polar vortex (McNeil, 2015). A strong polar vortex retains the

cold air mass around the pole, resulting in colder temperatures across Arctic regions, whereas a weaker vortex leads to the dispersion of the cold air mass, allowing for warmer temperatures in northern regions (McNeil, 2015).

The duration of positive and negative phases of global oscillation varies by teleconnection. ENSO oscillates between El Nino (warm) and La Nina (cool) events over a 3- to 5-year period. The PDO period is less well defined than the ENSO period and typically fluctuates between 20 and 30 years (Whitfield et al., 2010). The periodicity of AO has not been defined (Bridgman & Oliver, 2004). The affects of ENSO and PDO are strongest during constructive phases whereas, though ENSO remains a primary control, the influence of a warm or cool phase has been shown to be weak during destructive pairings (Gershunov & Barnett, 1998; Whitfield et al., 2010).

Contrasting hydrological processes with teleconnections is typically considered on at least a regional scale (>10 000km^2), as these are large-scale processes that may not be accurately expressed within small catchments (Kane et al., 2005). However, local-scale watershed studies such as at the Malcolm Knapp Research Forest in southwestern BC and at a range of watersheds (15 to 220 km^2) in southeastern Alaska, have shown significant relationships between catchment hydrology and ENSO and/or PDO, notably during constructive cycles (Kiffney et al., 2002; Neal et al., 2002). Therefore, it remains important to identify relevant teleconnections when discussing meteorological and hydrological trends, in order to differentiate between trends due to teleconnection phases, and changes as a response to climate change (Bierknes, 1969).

1.4.2 Variation in temperature trends at elevation

Previous work in large mountainous regions suggest that climate change is occurring faster at higher elevations (Giorgi et al., 1997; Mountain Research Initiative EDW Working Group, 2015; Wang et al., 2014). However, the impact of climate change has been shown to have a decreasing or no elevation-dependency in smaller mountain ranges of up to 2000 m (Aigang et al., 2010; Pepin & Lundquist, 2008). There is a lack of research around small mountainous regions in northern environments, and the relative effect of climate change on high elevations in northern regions is therefore unclear.

The positive elevation-dependency of climate change is associated with the relationship of warming and snow-albedo feedbacks. The difference in temperature changes at elevation has been found to be strongest in the winter, when the snow-albedo feedback occurs (Beniston, 1997; Rangwala & Miller, 2012). As snow melts at high elevations due to increases in winter and spring temperatures, the albedo decreases due to the reduced snow cover, causing increased warming (i.e., the earlier the snowmelt the more the warming). However, snow accumulation does not always increase with elevation in mountainous areas in northern regions, other studies therefore emphasize the importance of the zero-degree isotherm, and suggest that the greatest warming occurs around this isotherm due to its increased sensitivity to temperature relative to areas with mean temperatures significantly above or below freezing (Mountain Research Initiative EDW Working Group, 2015).

1.5 Research Objectives

The objective of this thesis is threefold: (1) provide a long-term dataset of mean daily temperature, windspeed, precipitation, and discharge in a subarctic watershed, (2) examine water balance fluxes and seasonal to annual trends in climate and key hydrometric variables between 1993 and 2019, and (3) assess controls on inter-annual variability and catchment response. This work aims to understand the mechanisms that drive streamflow in a subarctic watershed and provide insight into how future changes in climate may influence streamflow response in the region.

Chapter 2: Site Description and Methods

2.1 The Wolf Creek Research Basin – climate, location, and sub-catchments

The Wolf Creek Research Basin (WCRB; 60°31'N, 135°31'W) is located near Whitehorse, Yukon Territory and was established in 1992 on the traditional territory of the Kwanlin Dün First Nation, Ta'an Kwach'an Council, and Carcross/Tagish First Nation. It is a sub-watershed within the Yukon River watershed (Smith, Meikle, & Roots, 2004) and it has a subarctic continental climate. It is part of Canada's Boreal Cordillera ecozone (Smith, Meikle, & Roots, 2004) with the dominant vegetation being white spruce, aspen, willow, birch, and lichen at different elevations. Temperature decreases and precipitation increases with elevation across the basin, with sporadic permafrost (0-50%) at low elevation and discontinuous permafrost (50-90%) at high elevation (Lewkowicz and Endie, 2004; Ramage et al., 2020).

The WCRB has an area of ~179 km^2 (Rasouli et al., 2014) and is subdivided into 3 ecosections (Smith et al., 2004), each with a representative weather station from which long-term meteorological data is derived. These ecosections are boreal forest (22%), shrub tundra and taiga (58%), and alpine tundra (20%), and change over an altitudinal gradient from 660 m to 1000 m, 1000 m to 1500 m, and 1500 m to 2080 m above sea level (masl; Rasouli et al., 2019; figure 1a). Each of these ecosections contains a study site: Alpine (Alp), Buckbrush (BBS), and Forest (WCF), where weather stations are installed. The Alpine, Buckbrush, and Forest stations are located at 1615 masl, 1250 masl and 750 masl, respectively. At the highest elevation, Alpine is windblown with the dominant vegetation being moss and lichen (Figure 1.1). Buckbrush has dense willow (*Salix spp*.) and dwarf birch (*Betula nana*) shrubs, ranging from 0.5 m to 2 m in height (figure 1c) and white spruce (*Picea glauca*), up to 20 m tall, surrounds the Forest station with some scattered aspen (*Populus spp.*) throughout (Figure 1.1).

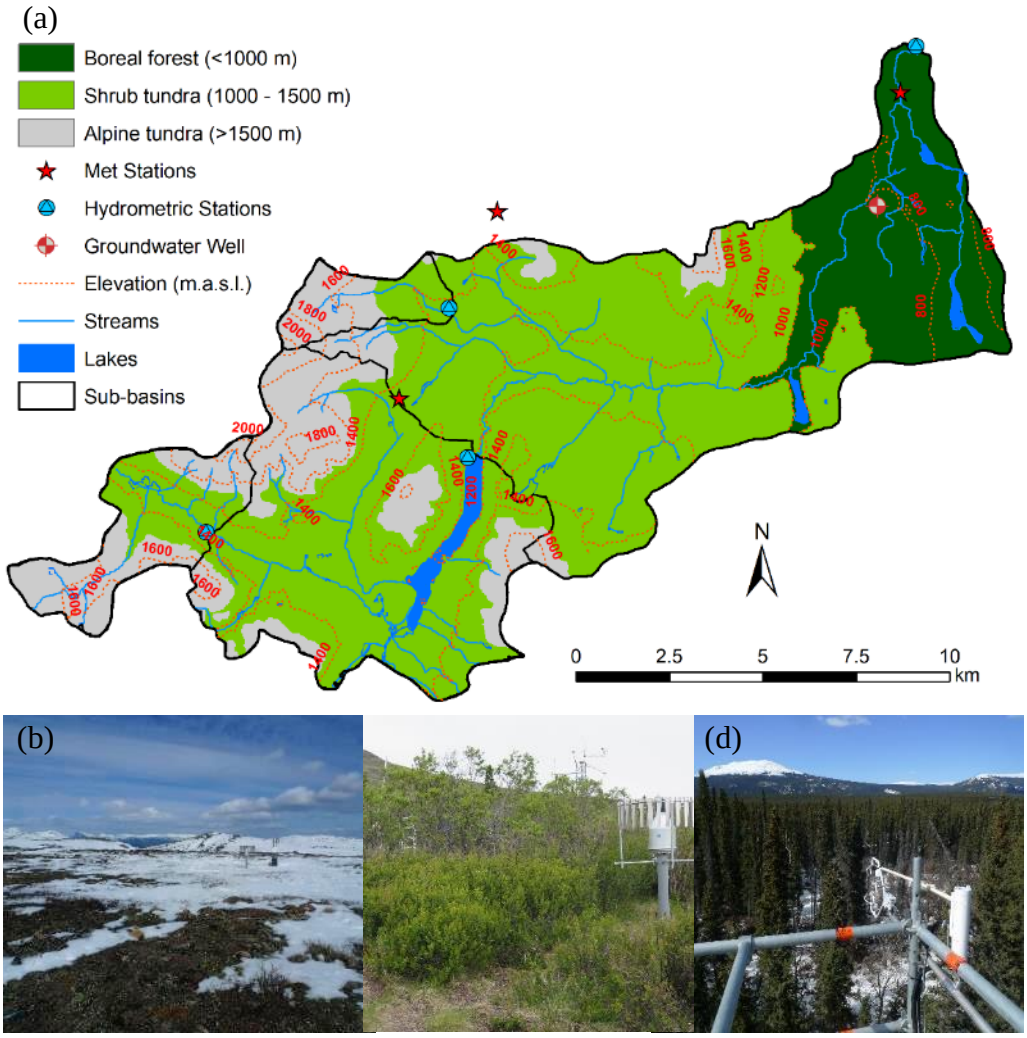

Figure 1.1: (a) The WCRB divided by ecosection (top), and a visualization of each ecosection: (b) Alpine (bottom left), (c) Buckbrush (bottom middle), and (d) Forest (bottom right) (Map credits: S. Leipe)

2.2 Instrumentation and data corrections

All data from 1993 to 2014 was obtained from the hydrometrical data published by Rasouli et al. (2019). Most instruments used to collect the 1993 to 2014 data remained consistent for the collection of 2015 to 2019 data with instruments listed in Tables 2.1 and 2.2 below. The windspeed and temperature data published by Rasouli et al. (2019) was

100% complete for each study site and no adjustments were required. The precipitation data was complete; however, a conversion error was identified over select time periods at the Alpine site: 2012-05-15 to 2012-09-28, 2013-05-01 to 2013-10-11, and 2014-05-09 to 2014-09-30. This has been corrected (multiplied by 10) in the revised data set. The streamflow data is available from 1993-04-29 to 2014-09-11. The portion of data used was from 1993-10-01 to 2014-09-11, and was 92.7% complete. The missing values were filled with streamflow data recorded, but not included in the initial publication. After filling in the data, it was 95.4% complete. The remainder of the data was completed using linear interpolation.

Table 2.1: Instruments used in 1993-2014 dataset. Table modified from Tables 2 and 3 published by Rasouli et al., 2019.

Variable	Site	Sensor	Height [m]	Mean	Record Period
Precipitation [mm]	Alpine	Texas TE525 TBRG Geonor T200B	1.87	384	1993-2014 daily
	Buckbrush	Texas TE525 TBRG Standpipe OTT Pluvio version 200 Geonor T200B	4.76	403	1993-2014 daily
	Forest	Texas TE525 TBRG Geonor T200B	21.34 1.75	278	1993-2014 daily
Air Temperature [°C]	Alpine	Vaisala HMP35CF HM45C212 (post-2005)	2.05 2.05	-3.5	1993-2014 hourly
	Buckbrush	Vaisala HMP35CF HMP45-212 (post-2005)	2.6 2.6	-1.9	1993-2014 hourly
	Forest	Vaisala HMP35CF HMP45-212 (post-2007)	21.34 21.34	-1.4	1993-2014 hourly
Wind speed [m s^{-1}]	Alpine	NRG 40 cup anemometer NRG 200P	2.75 2.75	3.6	1993-2014 hourly
	Buckbrush	NRG 40 cup anemometer RM Young 5103	4.6 4.98	1.8	1993-2014 hourly
	Forest	NRG 40 cup anemometer RM Young 5103	19.82 20	1.4	1993-2014 hourly
Streamflow [m^3 s^{-1}]	Alaska Highway	Various Instrumentation	—	0.78	1993-2014 hourly

Table 2.2: instruments used to collect 2014-2019 climate and hydrometric data at 3 long-term climate and hydrometric stations in WCRB.

Variable	Site	Sensor	Height [m]	Mean	Completeness [%]	Record Period
Precipitation [mm]	Alpine	Geonor T200B	1.75	409	93.6	2015-2019 every 30min
	Buckbrush	OTT Pluvio version 200	1.75	403	85.5	2015-2019 every 30min
	Forest	Geonor T200B	1.75	274	90.9	2015-2019 every 30min
Air Temperature [°C]	Alpine	Vaisala HM45C212	2.05	-3.2	99.9	2015-2019 every 30min
	Buckbrush	Vaisala HMP45-212	2.60	-1.7	99.4	2015-2019 every 30min
	Forest	Vaisala HMP45-212	3.00	-1.28	91.1	2015-2019 every 30min
Wind speed [m s^{-1}]	Alpine	RM Young 5103	3.00		99.9	2015-2019 every 30min
	Buckbrush	RM Young 5103	5.00		91.9	2015-2019 every 30min
	Forest	RM Young 5103	20.0		92.8	2015-2019 every 30min
Streamflow [m^3 s^{-1}]	Alaska Highway	Various Instrumentation	—	0.81	96.2%*	2015-2019
Snow Depth [cm]	Alpine	Sonic Range Sensor	1.67	—		1993-2014
	Buckbrush	Snow Pillow	0	—		
	Forest	Sonic Range Sensor	1.67	—		

*Percent completeness of 1993 to 2019 streamflow data once 1993 to 2014 data was also filled.

2.2.1 Wind measurements

Wind speed from 2015 to 2019 was collected by an R.M. Young 5103 at Forest, Buckbrush, and Alpine (Table 2.2). The 2015 to 2019 Alpine, Buckbrush, and Forest windspeed data was 99.9%, 91.9%, and 92.8% complete, respectively. Linear interpolation was used to complete the one missing value from the Alpine windspeed dataset. Linear regressions between Alpine, Buckbrush and Forest derived from the 2015-2019 windspeed data were then used to complete the missing windspeed data at Buckbrush and Forest. The equations used for this correction are:

(1) $W_s^{BBS} = 0.423 * W_s^{Alp} + 0.508$, $R^2 = 0.51$

(2) $W_s^{WCF} = 0.136 * W_s^{Alp} + 0.711$, $R^2 = 0.30$

Where W_s^{Alp}, W_s^{BBS}, W_s^{WCF} are windspeeds [m s^{-1}] at Alpine, Buckbrush, and Forest, respectively.

2.2.2 Temperature measurements

Temperature from 2015 to 2019 was collected with a Vaisala HM45C212 thermometers at Alpine, and Vaisala HMP45-212 thermometers at Buckbrush and Forest (Table 2.2). The 2015 to 2019 Alpine, Buckbrush, and Forest temperature data was 99.9%, 99.4%, and 91.1% complete, respectively. The air temperature recorded by the Whitehorse Auto tower downloaded from the Government of Canada meteorological database was 100% complete from 2015 to 2019. A linear regression between Alpine and Whitehorse Auto was used to complete the temperature data at Alpine. Linear

regressions, based on the 2015 to 2019 data, between Alpine, Buckbrush, and Forest were then used to complete the temperature data at Buckbrush, and Forest.

(3) T_{Alp} = 0.706*T_{White} + 3.04, R^2 = 0.88

(4) T_{BBS} = 1.030*T_{Alp} + 1.55, R^2 = 0.98

(5) T_{WCF} = 1.220*T_{Alp} + 2.41, R^2 = 0.87

Where T_{Alp}, T_{BBS}, T_{WCF}, and T_{White} are the air temperatures at Alpine, Buckbrush, Forest, and the Whitehorse Auto tower, respectively.

All mean temperature values were calculated using the gap filled data, and the temperature across the WCRB was calculated by taking the area weighted average across the three ecosections.

2.2.3 Precipitation measurements

The 2015 to 2019 rainfall and snow were recorded with the Geonor T200B gauge at the Alpine site, OTT Pluvio version 200 gauge at the Buckbrush site, and the Geonor T200B gauge at the Forest site (Table 2.2). Each precipitation gauge had multiple load cells (up to three), and the average value from the cells was used as the total precipitation value for each site. A daily average air temperature of 0˚C was used as a threshold temperature for precipitation phase, with precipitation recorded above a daily average temperature of 0˚C defined as rain, and below 0˚C was snow. The effectiveness of snow capture by a precipitation gauge is highly wind dependent and equations have been derived to correct for wind effects based on the shape of the snow gauge (Pan et al.,

2016). The correction equations (equations 6 and 7) derived by Pan et al. (2016) based on Smith (2007) were used to correct precipitation below 0˚C for both the Geonor T200B gauge and OTT Pluvio version 200 gauge for wind:

(6) $P_{corr} = P_{obs}/CE$

(7) $CE = 1.18e^{-0.18*Ws}$

where P_{corr} is the corrected rainfall, P_{obs} is the measured rainfall, CE is the wind influence depending on wind speed, W_s.

The Alpine, Buckbrush, and Forest 2015 to 2019 precipitation datasets were 93.6%, 85.5%, 90.9% complete, respectively. Once precipitation was corrected for temperature and wind, missing data at each site was filled using a linear regression, derived based on the 2015 to 2019 precipitation data, with the site to which it was most strongly correlated. The Alpine missing data was filled in using a linear regression between the daily precipitation at Alpine and the daily precipitation at the Whitehorse auto tower between 2015 to 2019. The completed Alpine data was then used to complete the Buckbrush and Forest precipitation datasets.

(8) $P_{Alp} = 0.519 + 0.733*P_{White}$, $R^2 = 0.29$

(9) $P_{WCF} = 0.239 + 0.376*P_{Alp}$, $R^2 = 0.36$

(10) $P_{BBS} = 0.397 + 0.656*P_{Alp}$, $R^2 = 0.43$

Where P_{Alp}, P_{BBS}, and P_{WCF} are precipitation (mm), where snow recorded at the snow water equivalence, at Alpine, Buckbrush, and Forest, respectively.

The cumulative annual precipitation at each site is calculated using the gap filled data, and the precipitation across the WCRB was calculated by taking the weighted average across the three ecosections.

2.2.4 Outflow measurements

Daily mean discharge was measured at the outlet of the WCRB. Stage was recorded every 15 minutes using various pressure tranducers that have changed since 1993, and discharge was calculated based on the relationship between stage and point discharge measurements. Point discharge measurements were taken at the outlet intermittently using both stage-area methods and dilution gauging. The dataset containing 2015 to 2019 streamflow data is the same dataset that was used to complete the 1993 to 2014 data. After combining all continuous streamflow data, the 1993 to 2019 streamflow data was 96.2% complete and the remainder of the data was linearly interpolated. However, years with more than 10 consecutive days of missing streamflow data during freshet were removed due to the inability to accurately interpolate data. All cumulative discharge at the WCRB outlet is calculated using the gap filled data, excluding 2009, 2010, and 2011.

Table 2.3: Summary of the completeness of available streamflow data at the WCRB outlet. These are based on water years (1 October to 30 September). Years not shown in table were 100% complete.

Year	Completeness (%)	Dates Missing	Days Missing	Dataset
1994	96.4	11 May – 24 May 15 June 21 June – 22 June	13	Linearly interpolated
1997	97.0	29 April – 8 May	11	Linearly interpolated
2009	78.4	21 March – 4 May 23 May – 25 June	79	Removed from dataset
2010	47.4	13 October – 26 April	192	Removed from dataset
2011	84.4	26 October – 9 December 21 April – 2 May	57	Removed from dataset
2017	96.2	8 October – 21 October	14	Linearly interpolated

2.3 Analysis Methods

All analysis was completed in R-studio based on daily average values. For all statistical analysis, trends with a p-value < 0.1 were considered significant. In the WCRB, a water year was defined as 1 October to 31 September, and this is the period over which all mean and cumulative annual values are calculated. The seasonal values presented define spring as March, April, and May, summer as June, July, and August, fall as September, October, and November, and winter as December, January, and February.

2.3.1 Water Balance components

The data included in the overall water balance was evaluated for completeness. Precipitation was calculated as the weighted mean of the study sites and was only included if the datasets were able to be filled based on a linear regression between sites such that no more than 10 consecutive days of the data was missing during freshet. The precipitation for the 2015 water year was removed as the data was only 63.3% complete. Discharge at the WCRB outlet was only included if more than 85% of the data was recorded; 2009, 2010, and 2011 are therefore not included (Table 2.3).

2.3.2 Time series analysis

Ordinary least squares (OLS) regressions were used for all time-series analysis concerning the timing of events. The timing of peak flows, spring onset, and snowmelt, as well as the percentage of total annual discharge during freshet and annual runoff ratio were regressed by year to evaluate changes over time. The runoff ratio was defined as:

$$(11)\ R = \frac{Q}{P}$$

Where R is the runoff ratio, Q is total annual discharge, and P is total annual precipitation.

The modified Mann-Kendall test using trend free pre-whitening (Hussain & Mahmud, 2019) was used for time-series analysis of the total annual flow and temperature, as well as mean annual temperature. Both precipitation and flow are non-parametrically distributed and showed some autocorrelation. The same test was applied to the temperature data for direct comparison between major trend data over time. An application developed by Weigang Tang, McMaster University was used to apply the modified Mann-Kendall test using trend free pre-whitening (Yue & Wang, 2002).

2.3.3 Defining streamflow parameters

Spring onset, the start date of freshet flows, is defined by the day of minimum cumulative departure from the mean flow (Cayan et al., 2001), where the mean flow is the average discharge for the water year ($\bar{Q}$), and the cumulative departure is ($Q_{departure}$):

$$(11)\ Q_{departure} = (\sum_t Q) - \bar{Q}$$

The day of minimum cumulative departure is the day where $Q_{departure}$ is the most negative.

The last day of snowmelt was determined for Forest, Buckbrush, and Alpine. It was defined as the first day of year that the snow radar at Forest and Alpine, and the snow pillow at Buckbrush, read 0 cm.

The peak flow dates were selected based on maximum flows that occurred between March and July of the respective years. All annual peak flows fall within these dates with the exception of 2016. The annual peak flow for 2016 occurred on September 13th, and was caused by the intentional breakage of a large beaver dam upstream. As a result, this DOY of peak flow is not reflective of the regular hydrological regime, and the date of peak flow caused by the streams hydrological response to climate factors occurs during freshet, on the June 16th, 2016.

Baseflow was also calculated and represents the groundwater contribution to the stream. The Lyne-Hollick baseflow filter from the "Hydrostats" R-package was used to determine baseflow. The Lyne and Hollick (1979) approach applies a digital filter for baseflow separation, by differentiating between quick response and original stream flow. As winter flows are purely groundwater driven in the WCRB, baseflow was compared to mean annual winter flows.

Days with high intensity flow and precipitation were also identified, and are considered to be any day above the 98th percentile of their respective datasets. Therefore, a high intensity flow day was defined as any day with cumulative discharge greater than or equal to 1.6 mm, and a high intensity precipitation day was defined as any day with a cumulative precipitation greater than or equal to 9.6 mm.

Chapter 3: Results

3.1 Long-term Meteorological Data

3.1.1 Temperature

The mean annual temperature (± standard deviation) across the watershed from 1993-2019 was -1.9°C (± 1.1°C), and declines with elevation (Table 3.1). The mean annual temperature was -1.3°C (± 1.1°C) at the Forest station, followed by -1.7°C (± 1.0°C) and -3.2°C (± 1.0°C) at Buckbrush and Alpine, respectively. The mean seasonal temperature at each site indicated colder temperatures at the Forest site in the winter due to persistent inversions. Due to these inversions, the coldest day at Forest had a mean daily temperature of -46.5°C on 2 January 1997, whereas Buckbrush and Alpine were -29.2°C and -26.6°C, respectively, on the same day. Alpine and Buckbrush reached the maximum recorded daily temperature of 21.1°C and 21.3°C, respectively on 29 July 2009. The temperature at Forest on the same day was 22.1°C. The average mean annual and seasonal daily temperatures are presented in Table 3.1, with mean annual temperatures presented in Figure 3.1. The mean annual temperature was greater than 0°C at Forest in 2015, 2016, and 2019, and at Buckbrush in 2016 and 2019.

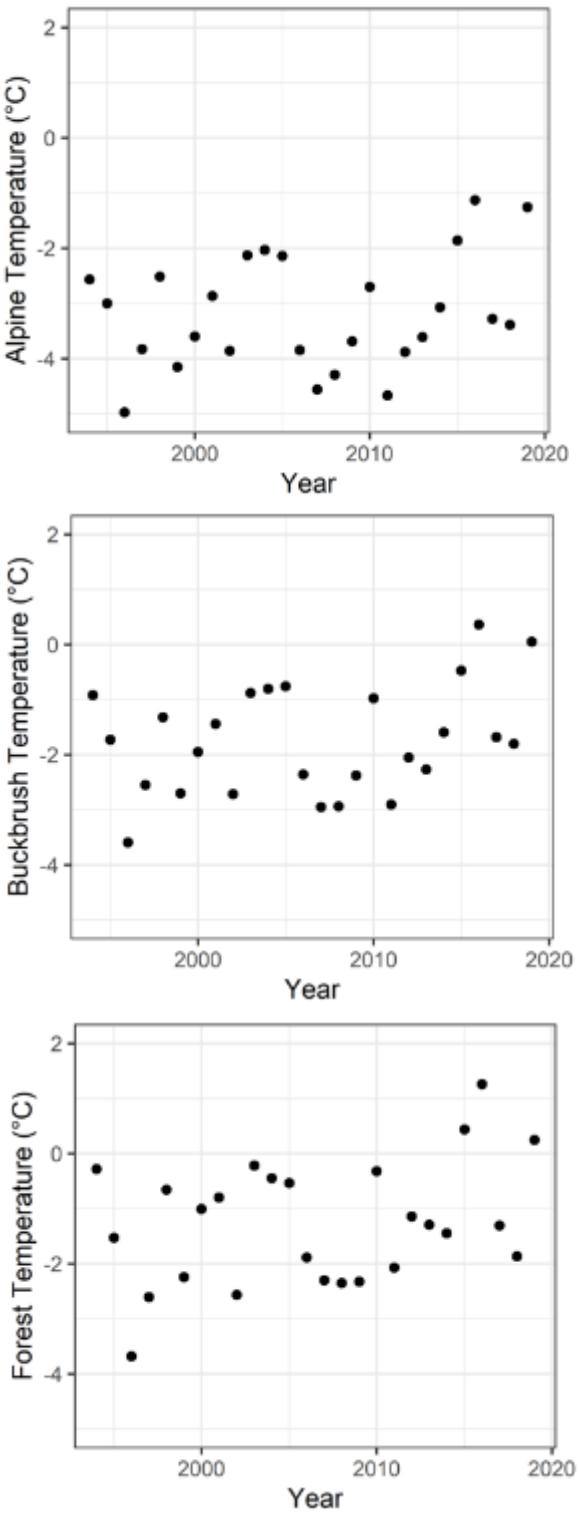

Figure 3.1: Mean annual air temperature at Alpine (top), Buckbrush (middle), and Forest (bottom) study sites in the WCRB from 1993 to 2019.

Table 3.1: Mean annual, seasonal, and extreme daily temperatures at each study site across the WCRB from 1993-2019. Spring, Summer, Fall, and Winter are defined as March to May, June to August, September to November, December to February, respectively.

	Forest	Buckbrush	Alpine	WCRB (Weighted Mean)
Mean Annual Temperature	-1.3°C (± 1.1°C)	-1.7°C (± 1.0°C)	-3.2°C (± 1.0°C)	-1.9°C (± 1.1°C)
Mean Spring Temperature	-0.3°C (± 1.7°C)	-2.4°C ± 1.7°C	-4.4°C ± 1.7°C	-2.3°C (± 1.7°C)
Mean Summer Temperature	12.4°C (± 1.0°C)	9.6°C (± 1.1°C)	7.9°C (± 1.2°C)	9.9°C (± 1.1°C)
Mean Fall Temperature	-1.8°C (± 2.4°C)	-2.5°C (± 2.2°C)	-3.9°C (± 2.2°C)	-2.6°C (± 2.2°C)
Mean Winter Temperature	-15.3°C (± 2.6°C)	-11.6°C (± 2.0°C)	-12.2°C (± 2.0°C)	-12.5°C (± 2.1°C)
Minimum Mean Daily Temperature	-46.5°C	-34.0°C	-36.1°C	-35.5°C
Date Minimum Mean Daily Temperature	2 January 1997	12 January 1996	12 January 1996	31 January 2008
Maximum Mean Daily Temperature	23.0°C	21.3°C	21.1°C	21.4°C
Date Maximum Mean Daily Temperature	19 June 2004	29 July 2009	29 July 2009	29 July 2009

Overall, the warmest year was 2016 with a mean annual temperature of 0.26°C, and the coldest year was 1996 at -3.89°C. There was some variation of warmest and coldest years among sites, but this variation was insignificant and warm years at high elevation typically represented warm years at lower elevation (Figure 3.2). All seasons and sites were significantly correlated, but deviations increased with altitude difference (i.e., warm, and cold years are most consistent between Alpine and Buckbrush and more variable between Alpine and Forest). Additionally, the relative spring and summer temperatures were most highly correlated whereas there was more variation in fall and winter. The greatest inconsistency occurred during winter between Alpine and Forest (slope = 0.87); though these relative temperatures remained highly correlated. Winter temperatures were most variable among these sites due to winter temperature inversions present at Forest causing cooler years at lower altitudes that were not representative of temperature at the higher elevation sites.

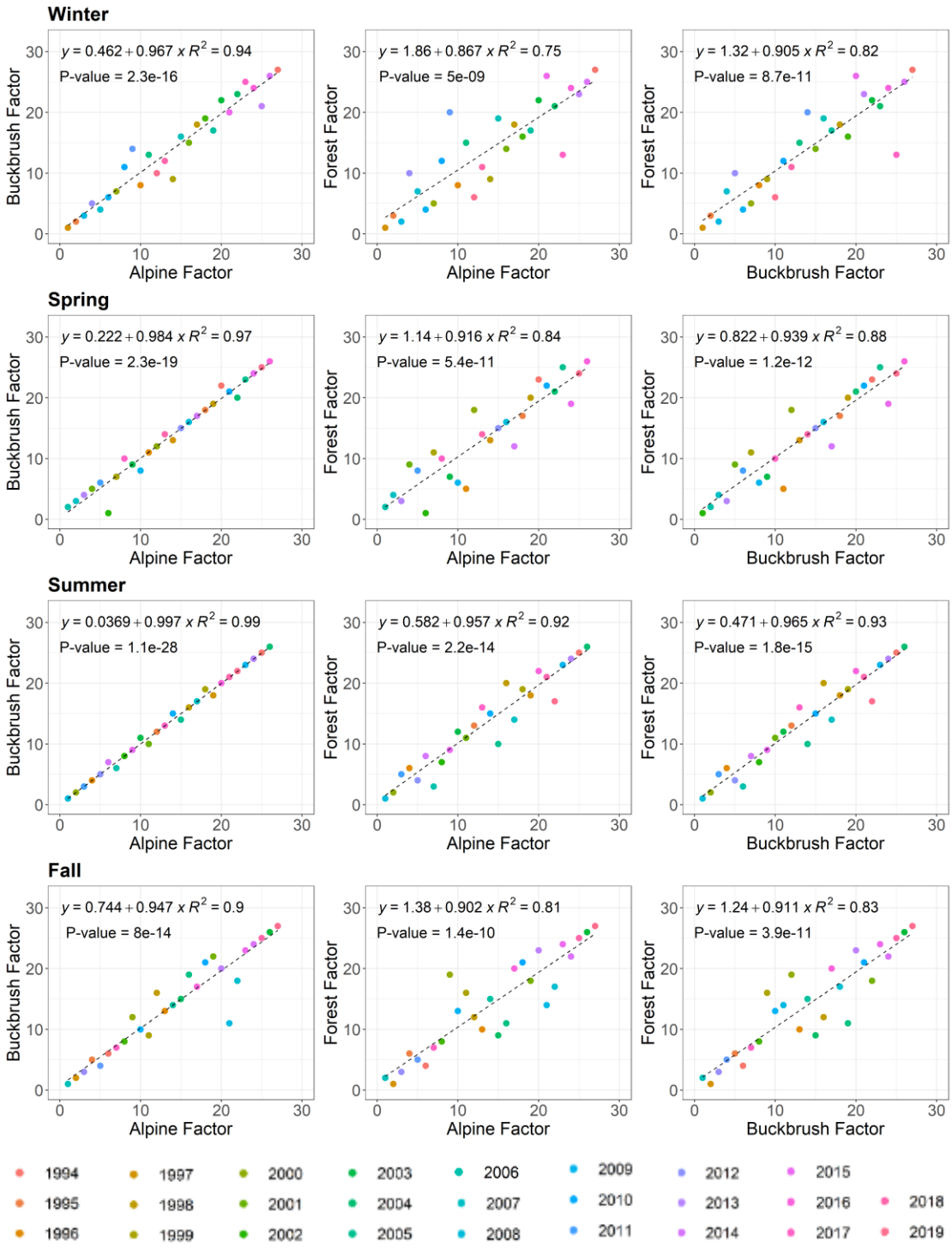

Figure 3.2: Ranking of temperatures between warm and cold seasons by site (Alpine, Buckbrush, Forest); where 1 = coldest year and 26 = warmest year.

3.1.2 Precipitation

Annual precipitation over 26 years at Forest was 261 mm (± 65 mm), 389 mm (± 95 mm) at Buckbrush, and 394 mm (± 96 mm) at Alpine. The relative amount of precipitation falling as snow within each ecosection increased with elevation, with 38% snow at Forest, to 45% at Buckbrush, and 54% at Alpine. The greatest snowfall occurred in 2009 at 264 cm, making up 59% of total precipitation, whereas the least amount of snow fell in 2001 at 115 cm consisting of only 30% of total precipitation. On average 45% **(**± 7%) of mean annual precipitation was snow. Across the basin and scaled by ecosection area, 1998 was the lowest precipitation year with 214 mm (56% snow), and 2000 had the most precipitation with 525 mm (35% snow)**.** The majority (8 out of 10) of years with high precipitation (more than 225 mm rain per year; top 10 of 25 years) received less than the average (45%) relative precipitation as snow, whereas only 3 of the remaining 15 years (less than 225 mm of rain per year), received less than the average relative precipitation as snow.

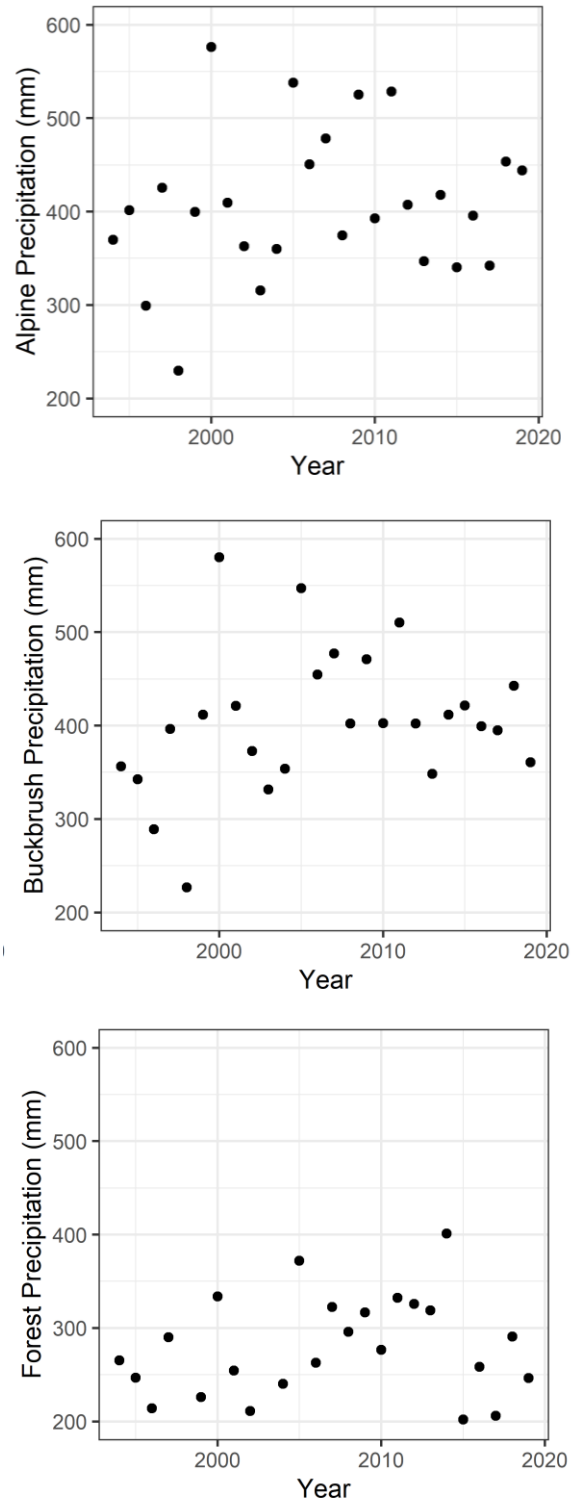

Figure 3.3: Cumulative annual precipitation at Alpine (top), Buckbrush (middle), and Forest (bottom) study sites within the WCRB from 1993 to 2019.

Table 3.2: Mean annual and seasonal precipitation at each study site across the WCRB from 1993-2019. Spring, Summer, Fall, and Winter are defined as March to May, June to August, September to November, December to February, respectively

	Forest	Buckbrush	Alpine	WCRB (Weighted Mean)
Annual				
Mean Annual Precipitation	261 mm (± 65 mm)	389 mm (± 95 mm)	394 mm (± 96 mm)	362 mm (± 86 mm)
Mean Annual Snowfall	100 mm (± 31 mm)	173 mm (± 46 mm)	211 mm (± 57 mm)	162 mm (± 44 mm)
Spring				
Mean Spring Precipitation	37 mm (± 13 mm)	56 mm (± 16 mm)	60 mm (± 21 mm)	53 mm (± 15 mm)
Mean Spring Snowfall	17 mm (± 11 mm)	35 mm (± 14 mm)	49.3 mm (± 21 mm)	33 mm (± 13 mm)
Summer				
Mean Summer Precipitation	113 mm (± 30 mm)	158 mm (± 49 mm)	147 mm (± 45 mm)	146 mm (± 43 mm)
Mean Summer Snowfall	NA	NA	3 mm (± 4 mm)	NA
Fall				
Mean Fall Precipitation	69 mm (± 27 mm)	107 mm (± 35 mm)	114 mm (± 42 mm)	100 mm (± 34 mm)
Mean Fall Snowfall	33 mm (± 17 mm)	67 mm (± 25 mm)	83 mm (± 32 mm)	62 mm (± 24 mm)
Winter				
Mean Winter Precipitation	49 mm (± 17 mm)	76 mm (±22 mm)	80 mm (± 27 mm)	71 mm (± 21 mm)
Mean Winter Snowfall	49 mm (± 17 mm)	75 mm (± 21 mm)	80 mm (± 27 mm)	70 mm (±21 mm)

As per the temperature data, there was some consistency in the relative magnitude of precipitation among sites. Years with high precipitation at Alpine typically also had high precipitation at Buckbrush and Forest (Figure 3.4). The correlation of precipitation rankings suggests that large precipitation days occurred at the watershed scale; however, there were a few notable outliers. For example, in 2013 Forest ranked 24th of 25, receiving the 2nd most recorded rainfall (228 mm), whereas Alpine site ranked 9th of 25, receiving the 16th most rainfall (165 mm). This difference was driven by a handful of high intensity rainfall days that were concentrated on the Forest site. This includes a high intensity precipitation from 20 July to 21 July 2013 which contributed 43 mm of rainfall to Forest, but only 8 mm to Alpine. Other large events limited to Forest occurred on 1 June 2013 (16 mm), 16 September 2013 (11 mm), and 29 September 2013 (11 mm). However, despite the difference in ranking some large rainfall events were limited to Alpine on 22 July 2013 (18 mm), 2 June 2013 (13 mm), 17 September 2013 (11 mm). Note the three largest daily rainfall events at Alpine (listed) all occurred the day after high intensity rainfall limited to Forest. Despite some outliers, high rainfall years are consistent between sites, as are high snowfall years (Figure 3.4). However, there was no correlation between high rainfall and high snowfall years (Figure 3.5).

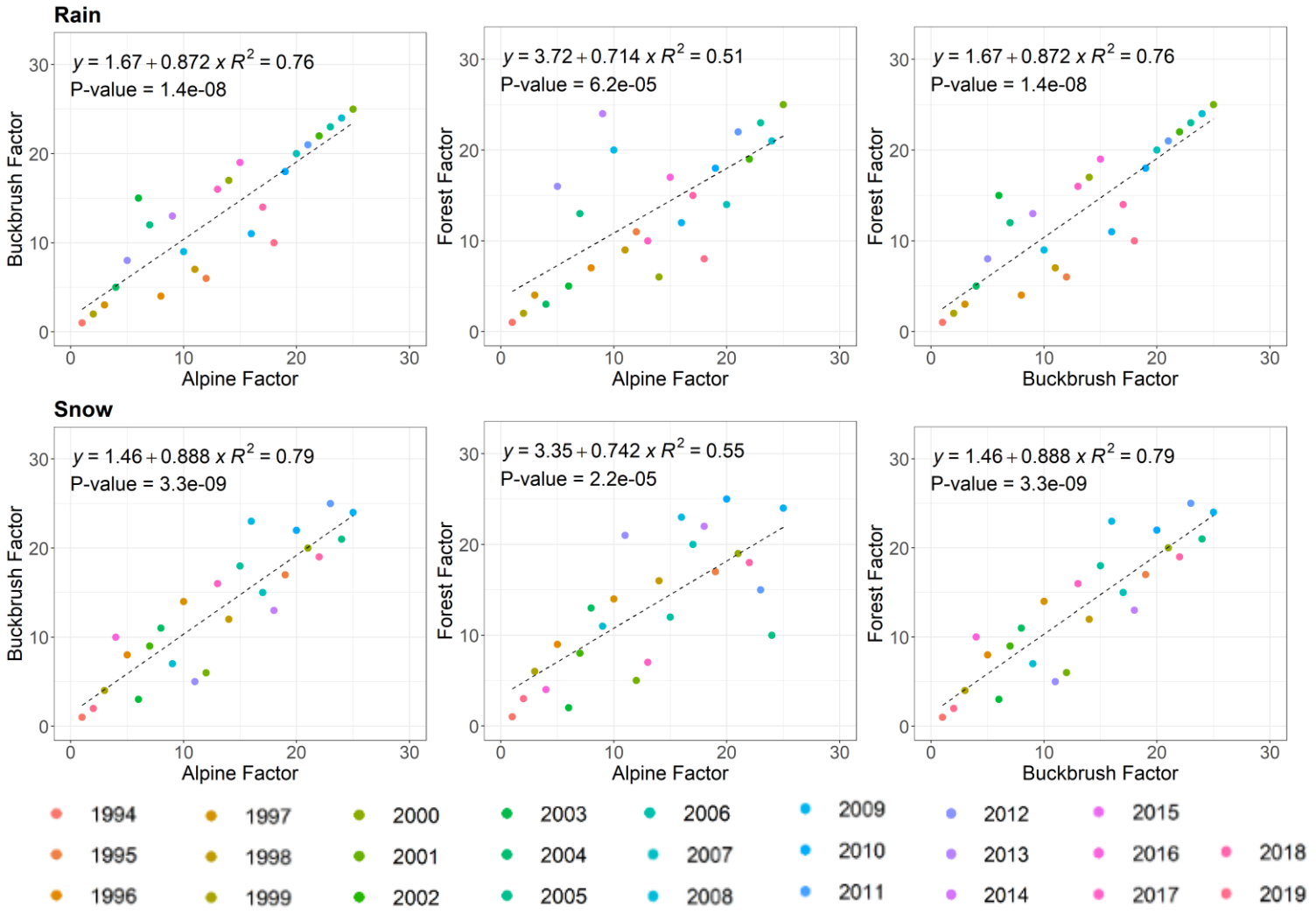

Figure 3.4: Comparison of ranking of rainfall magnitude across sites (Alpine, Buckbrush, and Forest), where 1 = least rainfall and 25 = most rainfall (top row), and snowfall magnitude where 1 = least snowfall and 25 = most snowfall (bottom row).

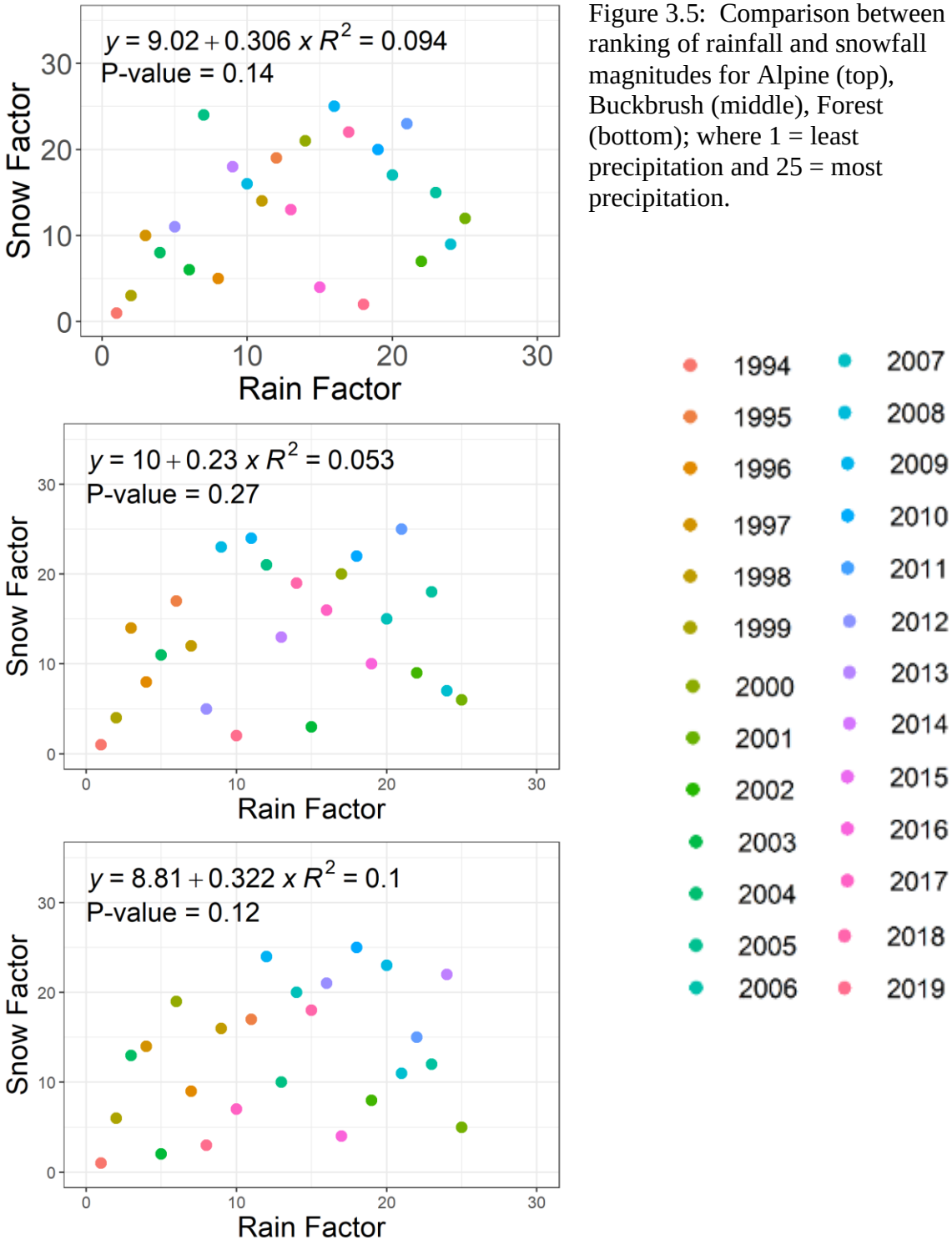

Figure 3.5: Comparison between ranking of rainfall and snowfall magnitudes for Alpine (top), Buckbrush (middle), Forest (bottom); where 1 = least precipitation and 25 = most precipitation.

The cumulative monthly precipitation from October to April was dominated by snow (> 70%). The relative abundance of snowfall in May was 21.9% and was 14.1% in September. Snowfall from June to September was negligible (< 2%) and did not contribute to precipitation storage over winter. The greatest difference in precipitation type among elevations occurred during the shoulder months: April to May, and September to October (Figure 3.5). For example, in April, the Alpine station received 97.3% of the precipitation as snow, whereas the precipitation at Forest received 51.1% snow (Figure 3.6).

Across the basin, there have been almost twice as many days with no precipitation as days with precipitation. Of the days with precipitation, the majority of events at each site were low intensity and contributed less than 2.5 mm per day (Figure 3.7). These findings are consistent across all ecosections, however there was a slightly higher frequency of high intensity precipitation (> 9.6 mm per day) at the higher elevation sites (Buckbrush and Alpine) as compared to Forest. The largest recorded precipitation days were 55.8 mm at Alpine on 18 November 1994, 44.5 mm at Buckbrush on 1 July 2010, and 38.8 mm at Forest on 4 July 2014.

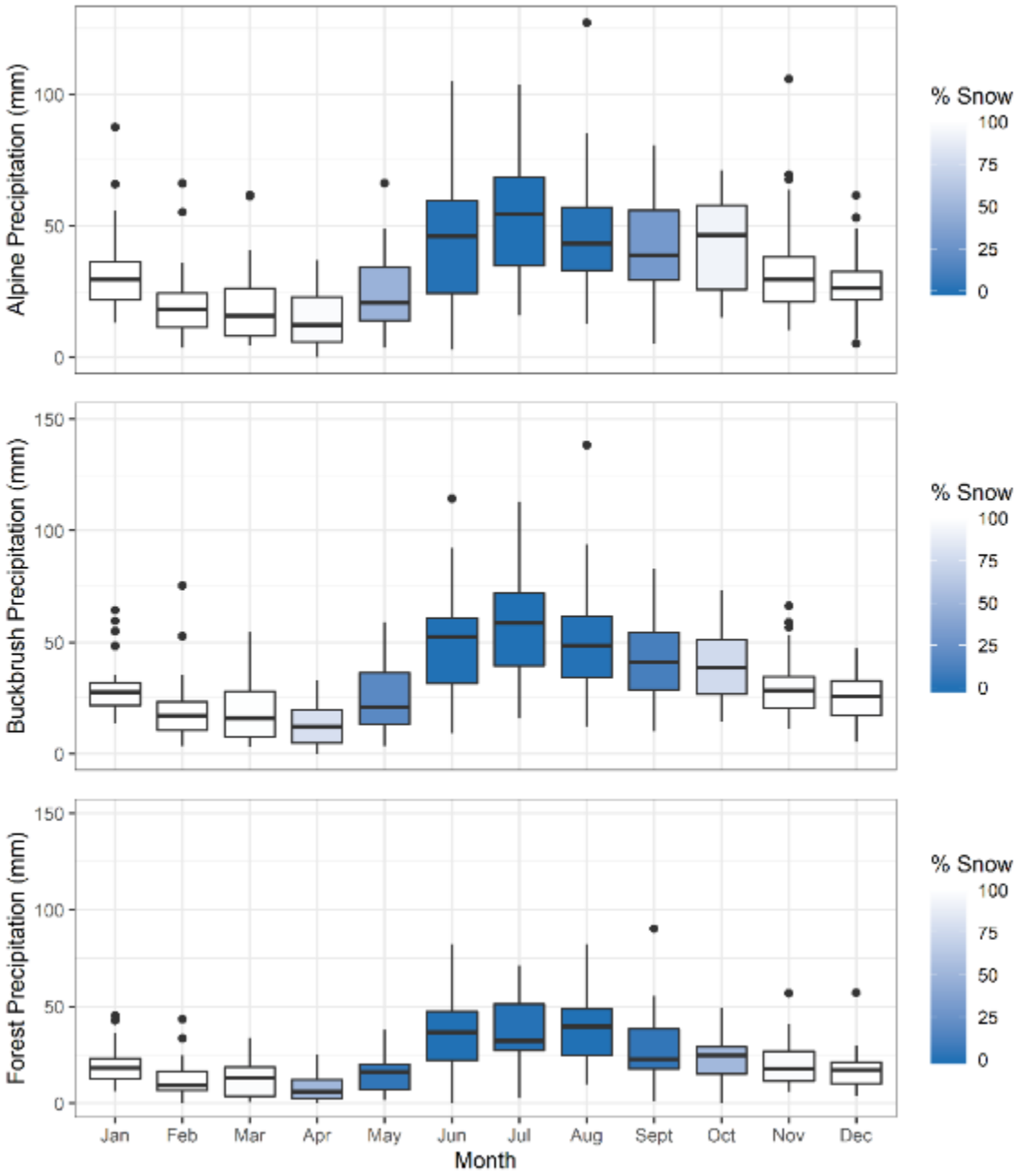

Figure 3.6: Mean monthly cumulative precipitation at Alpine, Buckbrush, and Forest. The fill shows the mean percentage of monthly precipitation as snowfall is shown. The percentages of snow distribution by season are presented in Table A.1 (Appendix A).

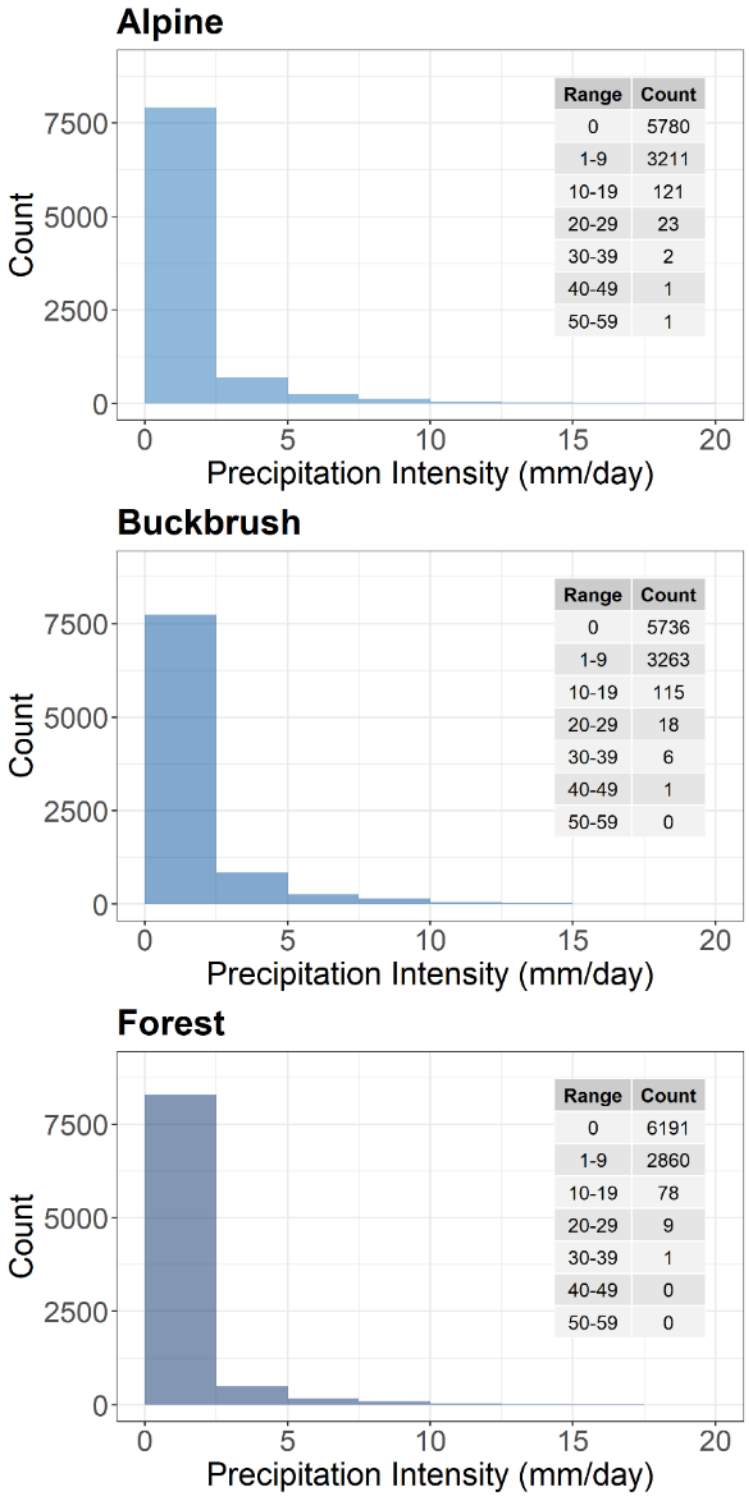

Figure 3.7: Frequency of daily precipitation binned by 2.5 mm within Alpine (top), Buckbrush (middle), and Forest (bottom) ecosections in the WCRB. The associated tables are grouped by 10 mm to demonstrate the frequency of large precipitation days otherwise not visible on the figure.

3.1.3 Discharge

The mean annual discharge at the WCRB outlet was 131.6 mm (± 41.1 mm) (Figure 3.8), with seasonal discharge of 14.1 mm (± 4.5 mm) in winter (December to February), 28.1 mm (± 8.3 mm) in spring (March to May), 57.3 mm (±27.8 mm) in summer (June to August), and 29.8 mm (±14.5 mm) in fall (September to November). Overall, the greatest seasonal discharge occurred during summer (Figure 3.9).

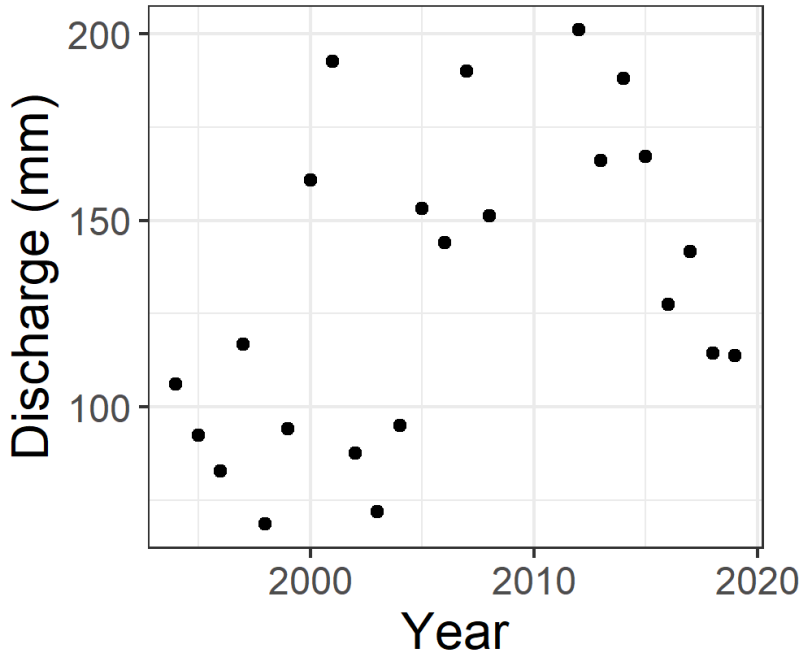

Figure 3.8: Cumulative annual discharge from 1993 to 2019 at the WCRB outlet.

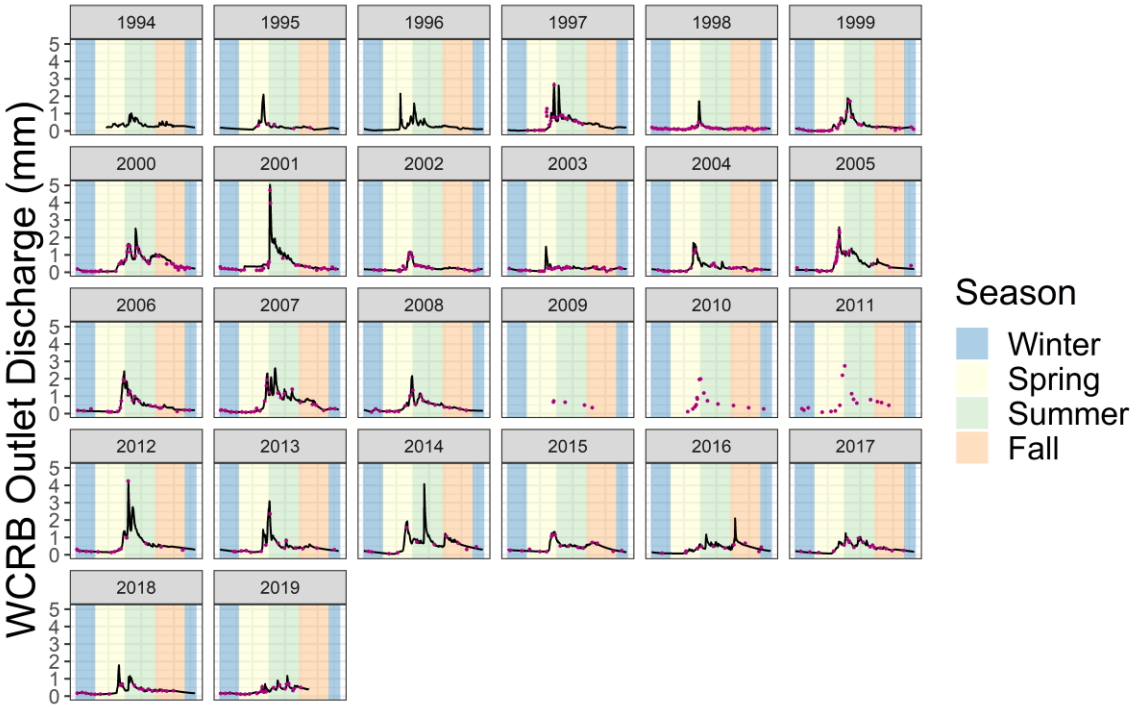

Figure 3.9: Continuous daily discharge (black lines) at the WCRB outlet. Point measurements (blue dots) are used to confirm accuracy of continuous flow measurements. Discharge data is plotted from 1 January to 31 December. The 2009, 2010, and 2011 water year (1 October to 30 September) data have more than 10 consecutive days of missing data during freshet (Table 2.1), including during freshet; the continuous data for these years was removed.

The freshet period was denoted by the annual onset of spring flows (section 2.3.3). On average, spring onset occurred around early May (DOY 127 ± 10 days) and was driven by snowmelt; however, the number of days between the end of snowmelt as measured at each site and spring onset was highly variable. Spring onset occurred 9 days (± 13 days) before the end of spring melt at Forest, 12 days (± 18 days) at Buckbrush, and 8 days (± 14 days) at Alpine (Figure 3.10).

The annual peak flow usually occurred during the freshet period between mid-May and mid-June (DOY 152, ± 22 days). On average, peak flow occurred 12 days (± 22 days) after the end of snowmelt at Forest, 16 days (± 39 days) at Buckbrush, and 12 days (± 25 days) at Alpine (Figure 3.11). There is no relation between the end of snowmelt as measured at the individual sites and the date of peak flow.

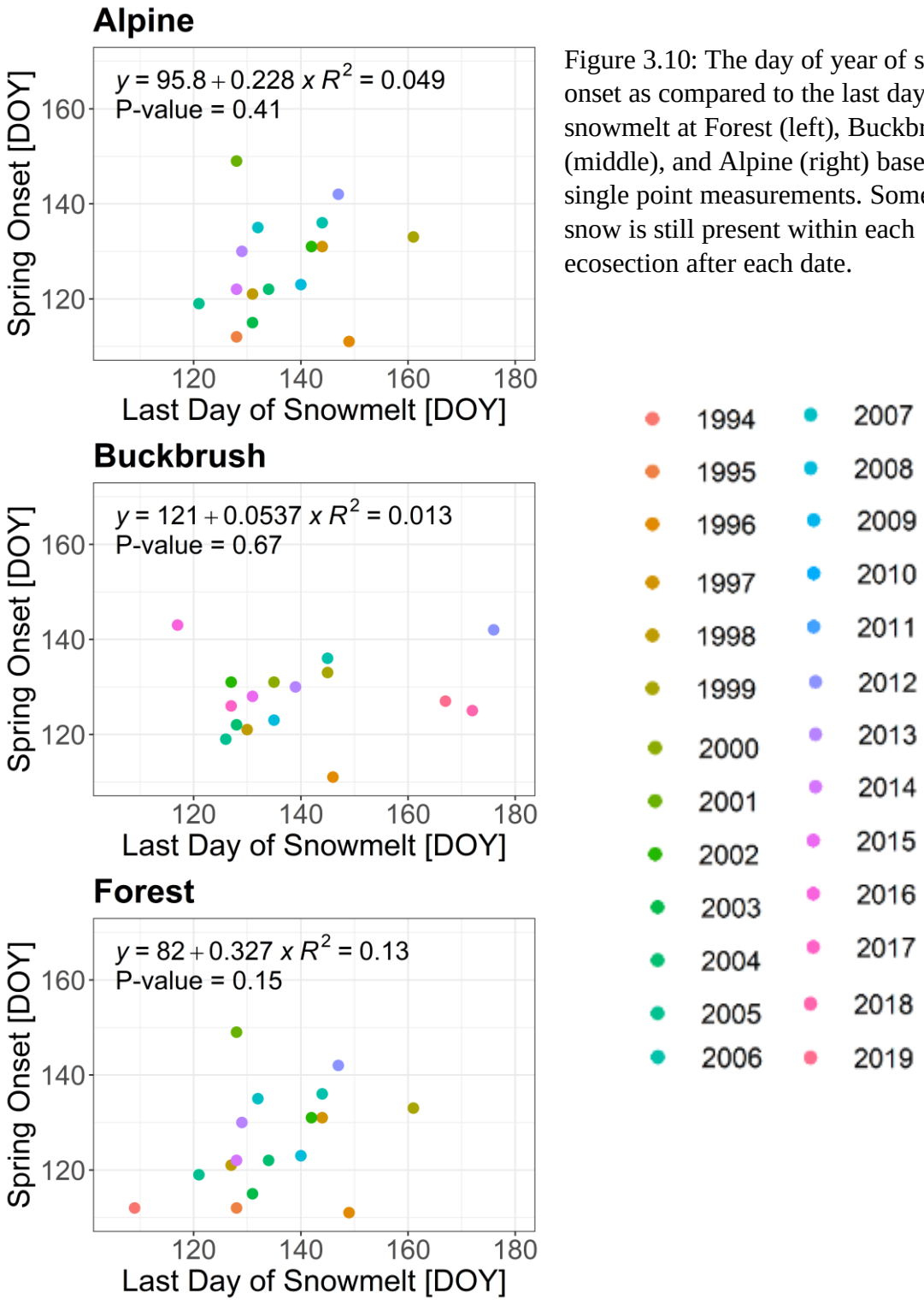

Figure 3.10: The day of year of spring onset as compared to the last day of snowmelt at Forest (left), Buckbrush (middle), and Alpine (right) based on single point measurements. Some snow is still present within each ecosection after each date.

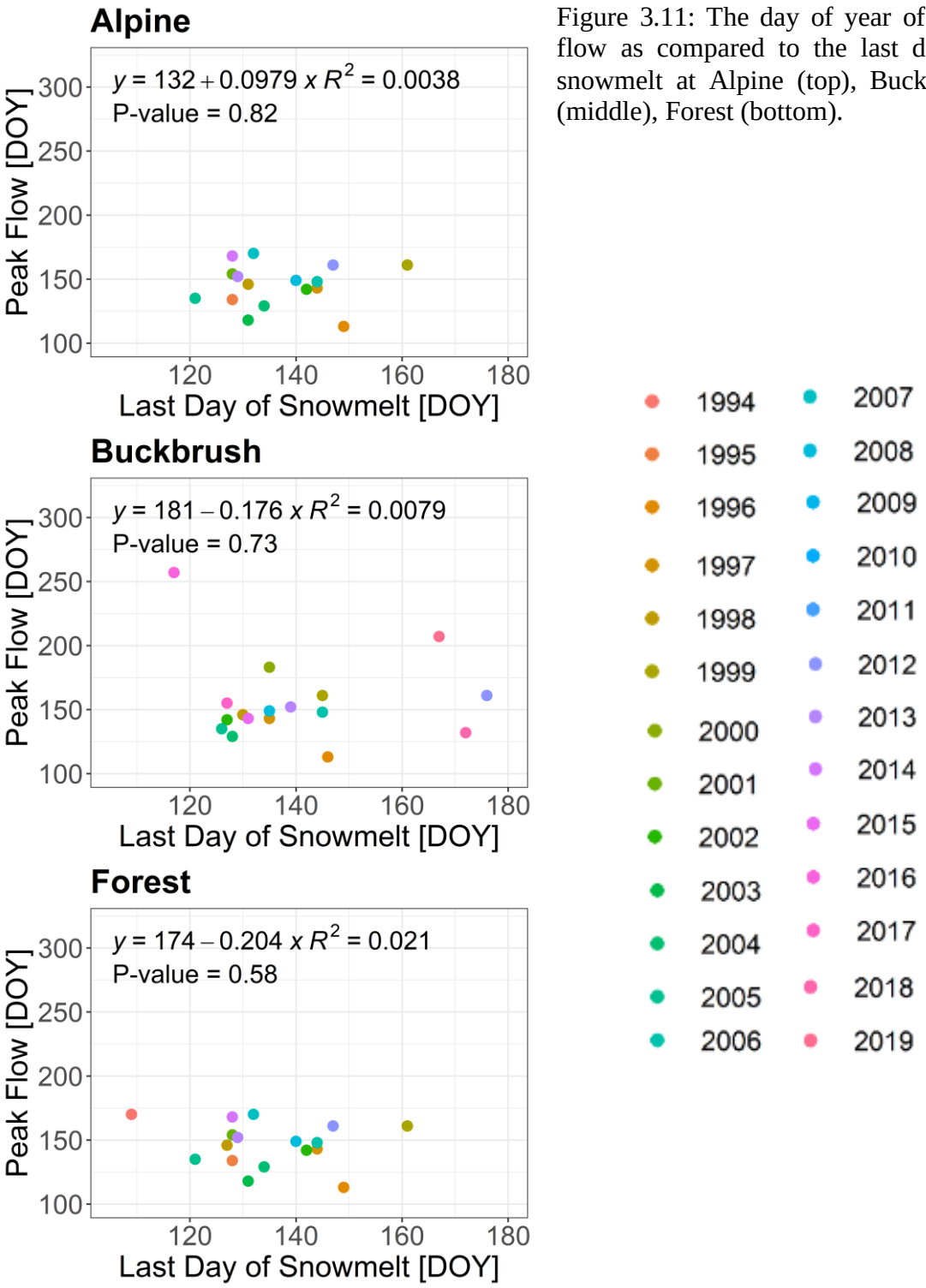

Figure 3.11: The day of year of peak flow as compared to the last day of snowmelt at Alpine (top), Buckbrush (middle), Forest (bottom).

3.1.3.1 Beaver Dam Event

Peak flows occur during freshet, with one exception: 13 September 2016, with a total daily discharge of 2.1 mm (Figure 3.9). This peak flow occurred after three weeks (34 to 36 WOY) of rainfall totalling 80.0 mm. During this period, there were two high intensity precipitation events, 26 August 2016 (20.3 mm) and 9 September 2016 (25.0mm). Despite the high intensity rain events, the high intensity flow event was not a result of the rainfall. On 12 September 2016, a large beaver dam was removed from the Coal Lake outlet generating high flows throughout the WCRB. Based on the timing and duration of the high intensity flow event with respect to the high intensity rain events and beaver dam breakage, it was concluded that the precipitation did not generate the high intensity flow. However, the high intensity precipitation events did cause small and short-lived peaks in discharge and likely contributed to the higher flow levels post-peak discharge (Figure 3.12). The increased discharge after the peak was likely maintained due to the significant precipitation throughout the basin prior to the breakage, as well as by any lag of lake discharge post-dam breakage. The time it takes for the flow to return to mean seasonal flow is unknown due to incomplete discharge data for fall 2016.

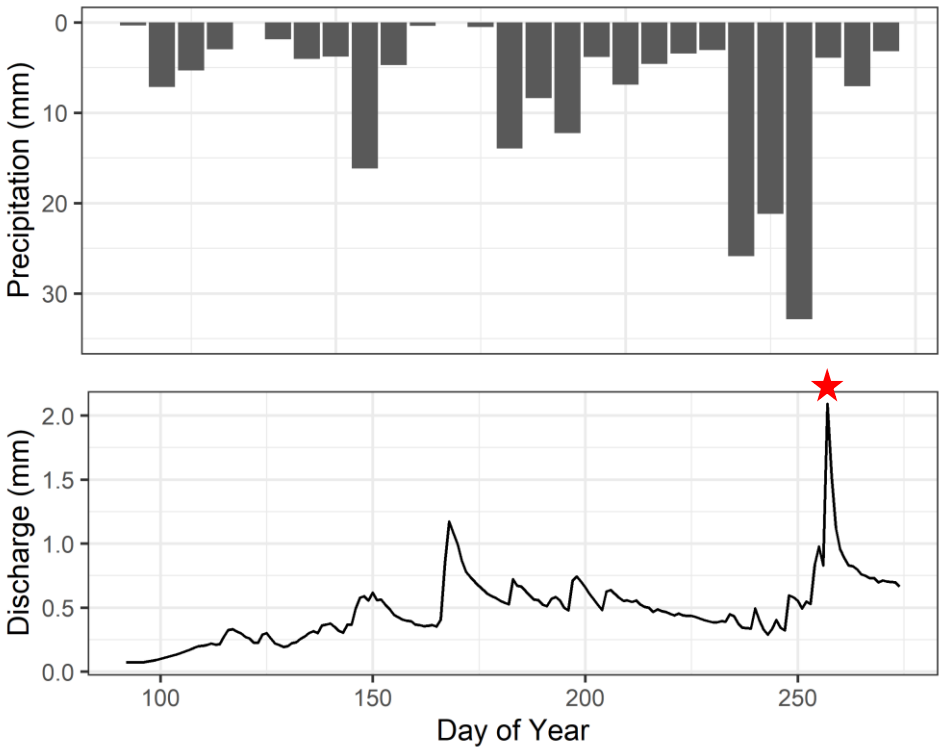

Figure 3.12: Hydrograph of daily discharge rates and cumulative weekly precipitation from 1 April 2016 to 31 September 2016: a late-season high intensity flow event year. The red star represents peak discharge primarily generated by beaver dam breakage upstream.

3.2 Water Balance

The 26-year water balance reflects the variation in cumulative annual precipitation and discharge at the WCRB outlet from 1993 to 2019. Evapotranspiration (calculated as a residual) was the greatest flux from the watershed, comprising 65.0% (± 8.5%) of total output, while discharge made up 35.0% (± 8.5%). The ET values calculated as a residual are greater than the measured values published by Nicholls and Carey (2021) by 13% from 2017 to 2019 when averaged across the basin. The mean annual ET over 26 years was 239 mm (± 52 mm). ET was lowest in 1998 (145 mm), and greatest in 2000 (364 mm). ET cannot be calculated by site as runoff ratio is only considered at the outlet. Rain represented 55.5% (± 7.2%) of annual precipitation, and snow made up 44.5% (± 7.2%) across the WCRB, but varied by ecosection and elevation (Figure 3.13).

.

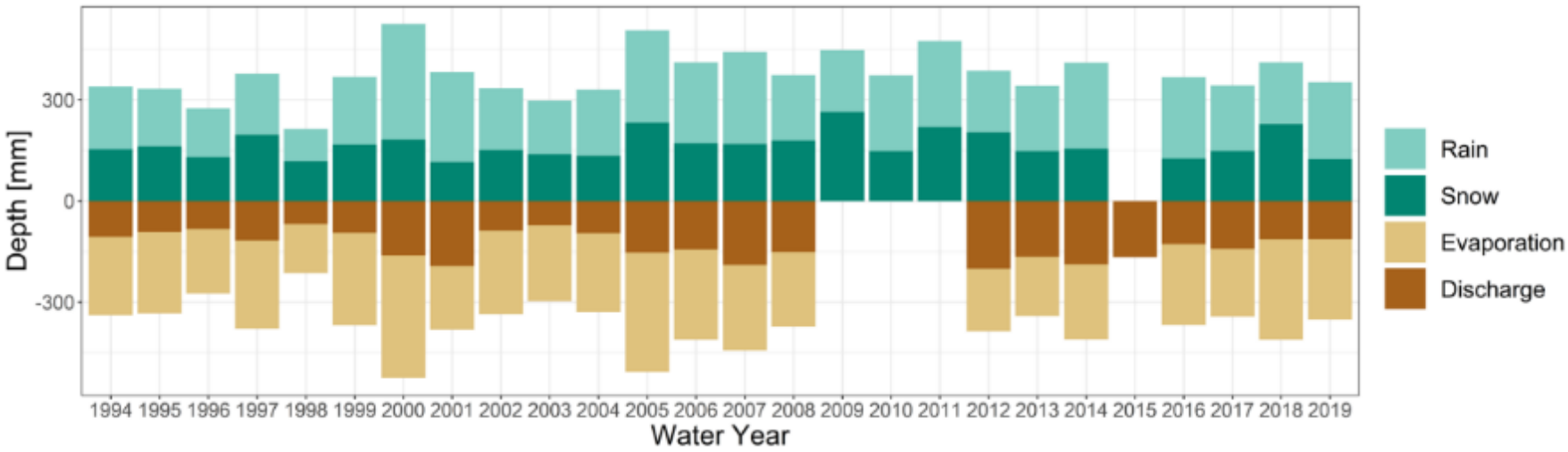

Figure 3.13: Water balance components of WCRB from 1993 to 2019. Missing columns are due to incomplete dataset

Chapter 4: Hydrometric Trend Analysis

4.1 Temporal Trends

4.1.1 Climate Parameters

The climate variables analyzed for temporal change were air temperature and precipitation. On a seasonal basis, there was a slight increase in fall air temperature within each ecosection at a rate ranging from 0.054°C per year Alpine to 0.081°C per year at Forest; this increase in air temperature remained significant when considering the weighted mean across the basin with an increase of 0.06°C per year (Table 4.1). Winter temperatures also increased significantly at Buckbrush (0.07°C per year) and averaged across the basin (0.08°C per year). There were significant increases in air temperature in January (one degree Celsius every 4.3 years) and May (one degree Celsius every 9.2 years) on the catchment scale (Table 4.1). Significant annual increases in air temperature were observed at Buckbrush, Forest, and averaged across the catchment, but not at the highest elevation (Alpine).

Table 4.1: Mann-Kendall test using trend free pre-whitening to detect statistically significant changes in mean annual, seasonal, and monthly air temperatures by site and across the catchment. The Sen slope describes the slope of the change, and the p-value describes the significance of the change. Trends highlighted in dark green were significant to the $p < 0.05$, whereas trends highlighted in light green were significant to the $p < 0.10$.

Month	Alpine: Sen	Alpine: p	BBS: Sen	BBS: p	WCF: Sen	WCF: p	WC: Sen	WC: p
Jan	0.15	0.13	0.23	0.02	0.34	0.004	0.23	0.02
Feb	0.02	0.69	0.02	0.87	-0.006	0.53	0.03	0.76
March	0.03	0.87	0.03	0.56	0.02	0.87	0.03	0.66
April	-0.03	0.83	-0.01	0.80	-0.02	0.87	-0.02	0.91
May	0.12	0.04	0.12	0.03	0.11	0.03	0.11	0.04
June	-0.01	0.62	-0.01	0.83	-0.01	0.87	-0.01	0.73
July	0.01	0.41	-0.003	0.50	-0.001	0.66	0.005	0.41
Aug	0.01	0.44	0.03	0.23	0.04	0.18	0.02	0.27
Sept	0.05	0.32	0.06	0.13	0.03	0.66	0.05	0.32
Oct	0.04	0.20	0.04	0.27	0.03	0.34	0.03	0.27
Nov	0.04	0.53	0.03	0.44	0.08	0.27	0.03	0.41
Dec	0.02	0.44	0.02	0.50	0.002	0.62	0.01	0.44
Winter	0.06	0.16	0.07	0.10	0.09	0.11	0.08	0.09
Spring	0.02	0.41	0.03	0.22	0.02	0.41	0.03	0.34
Summer	0.01	0.47	0.02	0.32	0.008	0.41	0.01	0.34
Fall	0.05	0.03	0.05	0.08	0.08	0.03	0.06	0.03
Annual	0.04	0.13	0.05	0.05	0.05	0.06	0.04	0.08

There were fewer significant changes in precipitation compared to air temperature; however, there was a significant increase in annual precipitation of 2.2 mm per year at Alpine, and sporadic increases in precipitation by season and ecosection. Notably, January precipitation increased significantly at both higher elevation sites (Alpine and Buckbrush) by 0.7 mm and 0.4 mm per year, respectively. This translates to a significant increase in January precipitation across the basin at a rate of 0.4 mm per year.

Alpine also had an increase in fall and annual precipitation (1.2 mm per year), whereas Forest had an increase in summer precipitation (1.9 mm per year), yet these trends were specific to these ecosections and were not significant on the catchment scale (Table 4.2). The variation in precipitation and air temperature between years is represented in Figures 3.3 and 3.9.

Table 4.2: Mann-Kendall test using trend free pre-whitening to detect statistically significant changes in cumulative annual and monthly precipitation by site and across the catchment. Trends highlighted in dark green were significant to the $p < 0.05$, whereas trends highlighted in light green were significant to the $p < 0.10$.

Month	Alpine: Sen	Alpine: p	BBS: Sen	BBS: p	WCF: Sen	WCF: p	WC: Sen	WC: p
Jan	0.70	0.004	0.36	0.03	-0.01	0.71	0.36	0.05
Feb	0.16	0.47	0.07	0.64	0.06	0.60	0.02	0.64
March	-0.10	0.90	-0.14	0.67	-0.07	0.86	-0.11	0.75
April	0.42	0.09	0.25	0.19	0.14	0.39	0.25	0.17
May	-0.28	0.29	-0.001	0.90	0.20	0.64	-0.03	0.82
June	0.57	0.33	0.69	0.19	1.06	0.006	0.84	0.11
July	-0.14	0.36	-0.21	0.47	0.25	0.60	-0.05	0.54
Aug	0.58	0.60	1.03	0.29	0.78	0.26	0.80	0.31
Sept	0.43	0.31	0.25	0.54	0.05	0.67	0.21	0.41
Oct	0.51	0.36	-0.02	0.86	-0.13	0.64	-0.05	0.98
Nov	0.44	0.16	0.31	0.57	0.23	0.54	0.28	0.50
Dec	0.20	0.39	-0.12	0.86	-0.06	0.90	-0.10	0.60
Winter	1.31	0.11	0.99	0.11	0.60	0.60	0.95	0.2
Spring	0.27	0.50	0.24	0.90	0.28	0.75	0.10	0.82
Summer	0.78	0.64	1.75	0.24	1.89	0.07	1.62	0.22
Fall	1.24	0.50	-0.005	0.60	0.40	0.98	0.25	0.90
Annual	2.24	0.50	2.05	0.47	2.51	0.13	2.12	0.29

Precipitation was divided into rain and snow. The change in relative abundance of snow and the absolute snowfall was assessed using OLS regression. Based on the regression, neither the percent of annual precipitation as snow across the WCRB, nor the annual snowfall significantly changed between 1993 and 2019 (Figure 4.1).

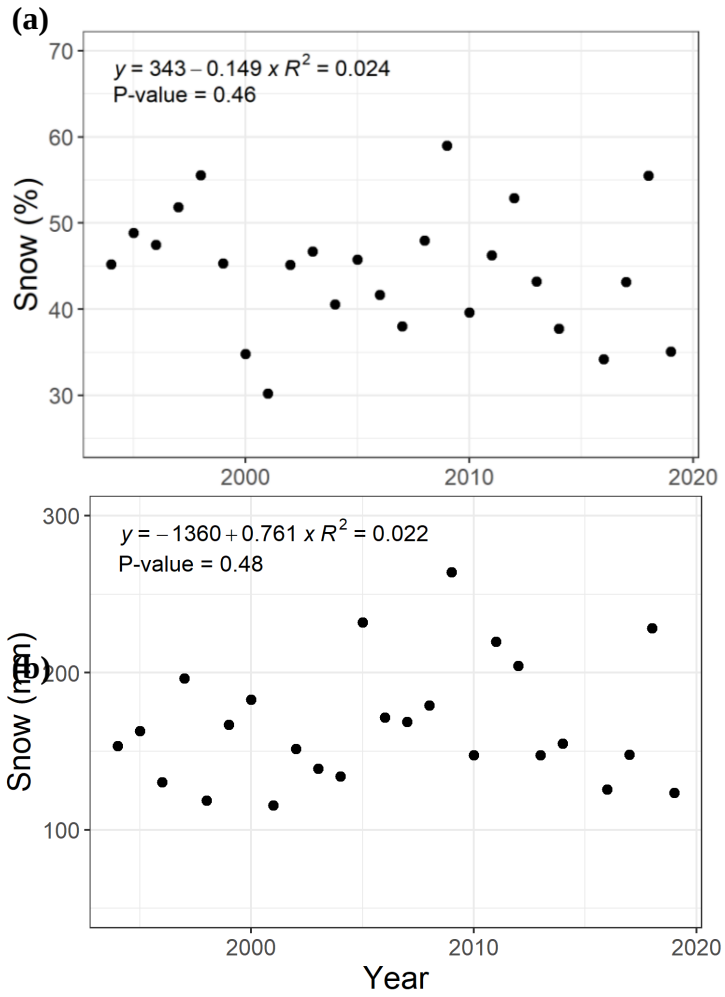

Figure 4.1: The distribution of (a) percent of total annual precipitation as snow and (b) absolute snowfall over time.

High intensity precipitation days (> 9.6 mm per day; 98th percentile) occurred between May and October, with most days occurring between June and September (Figure 4.2). Although a greater number of high intensity precipitation days occurred in June compared to September, there was not a significant difference and high intensity rainfall events did not favour early or late-season (Figure 4.3). The frequency of precipitation events within the 98th percentile (> 9.6 mm per day) increased significantly from 1993 to 2019 (Figure 4.3).

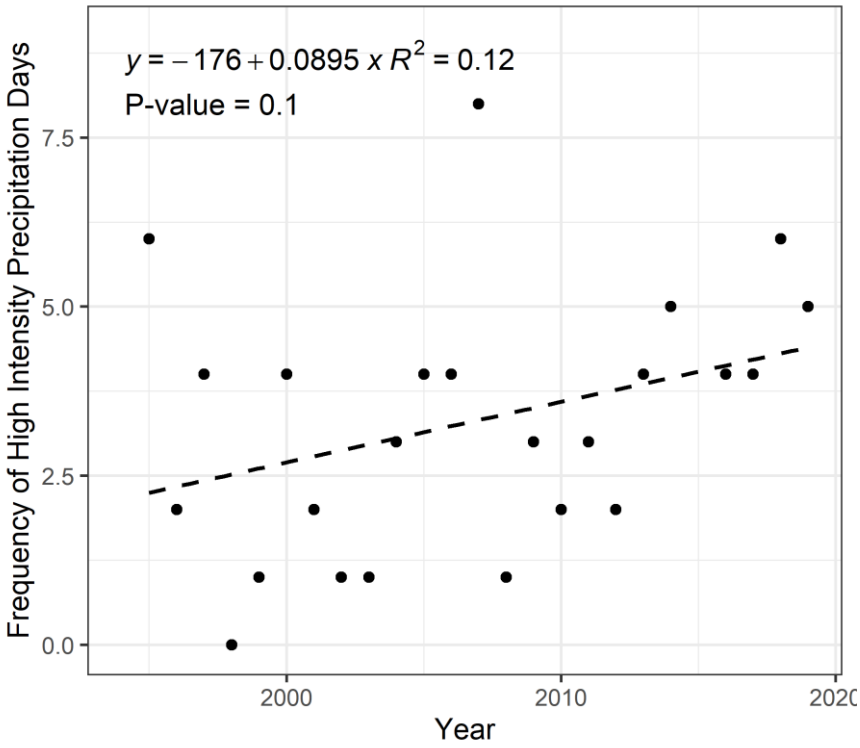

Figure 4.2: The frequency of high intensity precipitation days (>9.6 mm per day; 98th percentile) from 1993 to 2019.

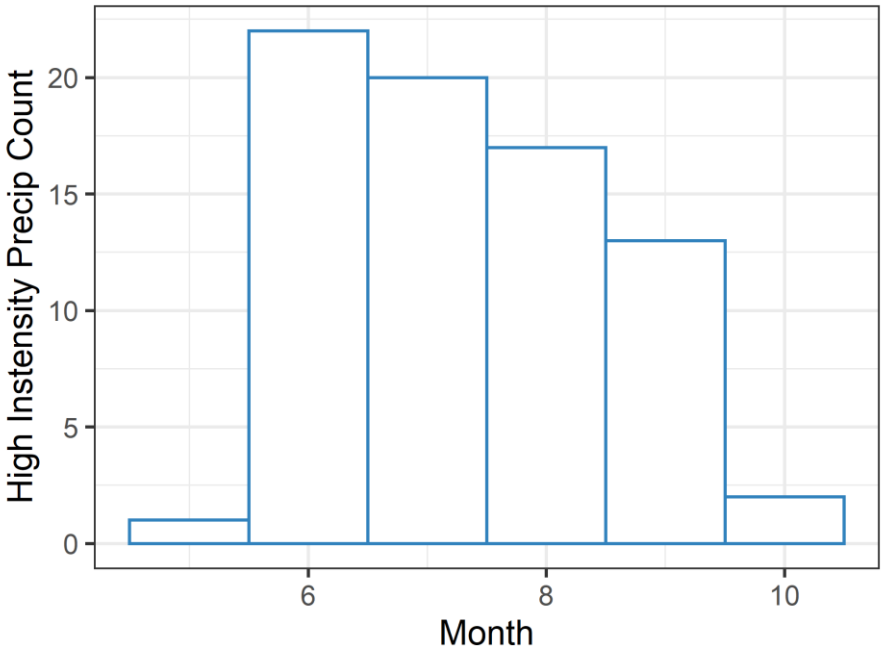

Figure 4.3: Monthly distribution of high intensity precipitation days (>9.6mm per day; 98th percentile)

Snow accumulation occurred at each site from October to April. In September, 31% of precipitation at Alpine was snowfall and snow accumulation continued at Alpine and Buckbrush in May with 49% and 18% snowfall, respectively (Figure 3.3). The mean timing of melt was DOY 135 (± 12 days) at Forest, DOY 139 (± 13 days) at Buckbrush, and DOY 134 (± 14 days) at Alpine. There was no shift in the last day of snowmelt at any site across the basin (Figure 4.4).

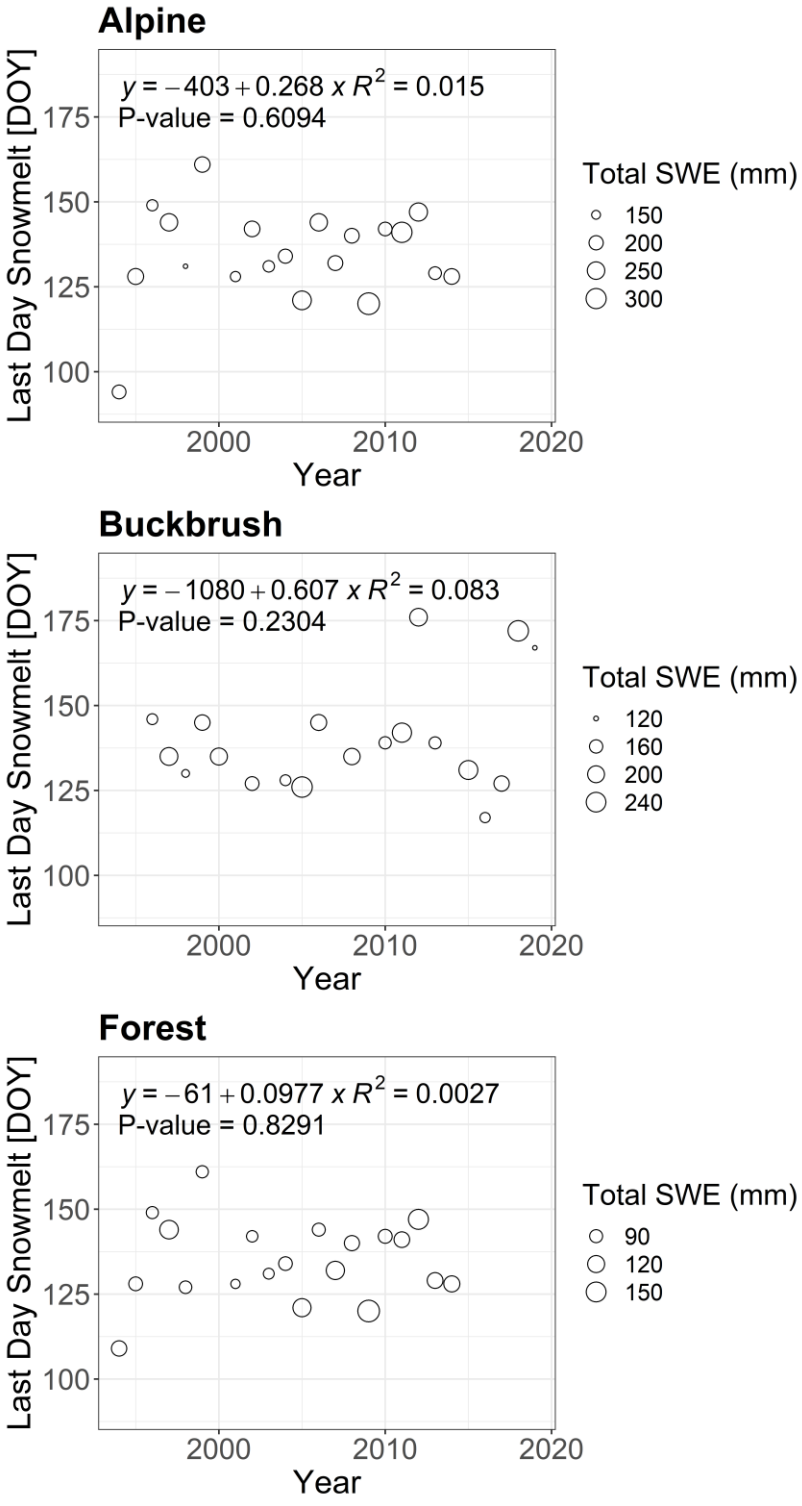

Figure 4.4: Last day of snowmelt at (a) Alpine snow radar (top), (b) Buckbrush snow pillow (middle), and (c) Forest snow radar (bottom).

4.1.3 Discharge magnitude and timing trends

Discharge magnitude and timing metrics have changed significantly with time. There were trends in the timing of peak flow, spring onset, and the percentage of total annual flow during freshet. The magnitude of annual streamflow increased significantly by 2.59 mm per year on average. This value is slightly greater than the mean increase in precipitation of 2.12 mm per year. The increase in flows was reflected on a monthly scale, with significant increases in discharge from August through March (Table 4.3). These monthly flow increases were reflected in the seasonal data with significant increases during fall and winter but there was no significant increase in discharge in spring or summer despite a significant increase in August flow (Table 4.3).

Table 4.3: Modified Mann-Kendall test using trend free pre-whitening to detect statistically significant changes in mean annual and mean monthly flows at the WCRB outlet. Trends highlighted in dark green were significant to the $p < 0.05$, whereas trends highlighted in light green were significant to the $p < 0.10$.

Month	Sen Slope	MK P-Value
January	0.11	0.02
February	0.13	0.01
March	0.08	0.08
April	0.05	0.43
May	0.30	0.65
June	0.12	0.96
July	0.40	0.18
August	0.41	0.04
September	0.36	0.02
October	0.38	0.003
November	0.28	0.001
December	0.11	0.04
Winter	0.40	0.03
Spring	0.42	0.37
Summer	1.04	0.26
Fall	0.87	0.08
Annual	2.59	0.10

High intensity flow days (> 1.6 mm per day; 98th percentile) occurred between April and July, with the majority of events occurring between May and July. There was not a significant difference between the number of number of high intensity flow days in May and June ($p = 0.054$), but there was a significant difference between the number of high intensity flow days in June and July ($p = 5.5E\text{-}11$) and May and July ($p = 9.3E\text{-}7$) (Figure 4.5). High intensity flow days primarily occurred during freshet. The single high intensity flow days that occurred in September was associated with the Beaver Dam

breakage described in section 3.1.3.1. There was no significant increase in the frequency of high intensity flow days (>1.6 mm per day) from 1993 to 2019 (Figure 4.6).

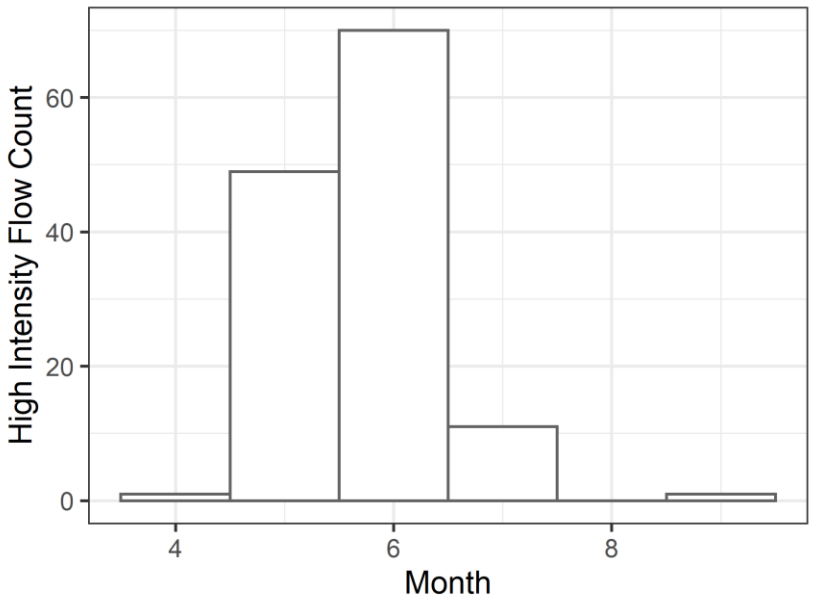

Figure 4.5: Monthly distribution of high intensity precipitation days (>1.6 mm per day; 98th percentile)

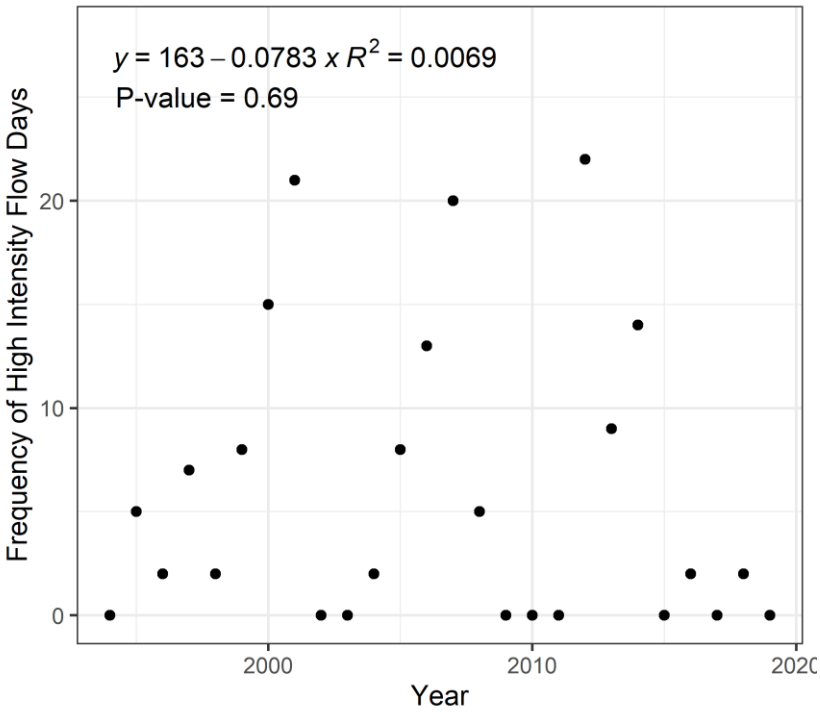

Figure 4.6: The frequency of high intensity flow days (1.6 mm per day; 98th percentile)

Based on OLS regression, there was a significant (p-value = 0.1) delay in the timing of peak flow, but no significant shift in the DOY of spring onset (Figure 4.6). Peak flow was delayed by 25 days between 1993 and 2019 (Figure 4.7). In the WCRB, most discharge occurred during spring and early summer, with an average of 40.2% (± 7.7%) of flow output during freshet (April to June). A greater proportion of discharge occurred during freshet (April to June) in high flow years relative to low flow years, which typically had lower freshet flows. Overall, there was not a significant change in the percent of cumulative annual flows that occurred during freshet (Figure 4.8). Interestingly, freshet discharge is significantly correlated (p = 0.035) with antecedent fall rainfall, but not with the total snowfall (measured in SWE) (Figure 4.9).

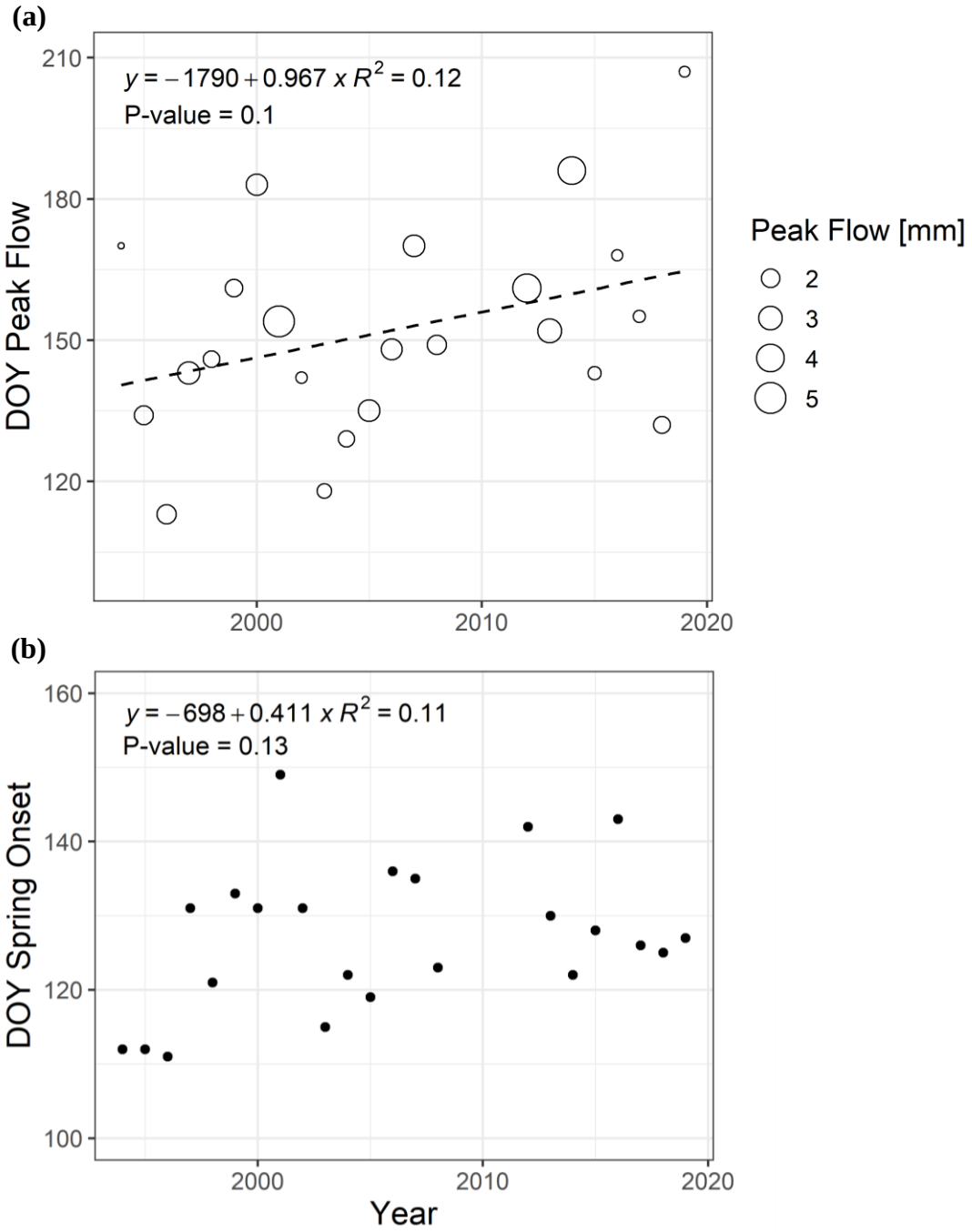

Figure 4.7: Day of year of (a) peak flow during freshet (March-July) at the WCRB outlet delayed by 1 day per year, and (b) onset of freshet flows which has a smaller and insignificant delay (0.4 days).

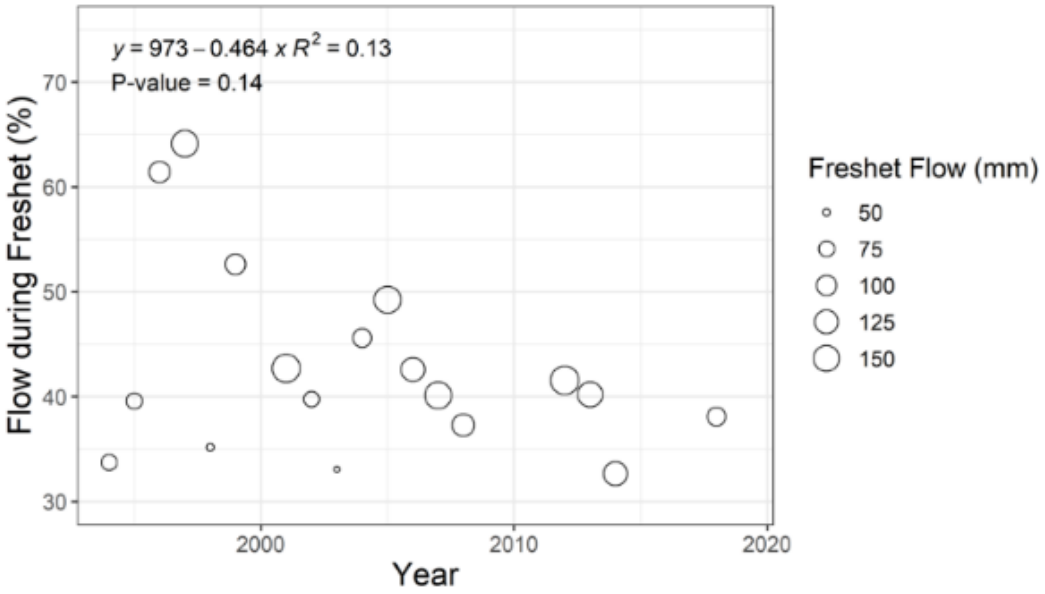

Figure 4.8: Percentage of total annual discharge output during freshet for each year, where the start of freshet was defined by the total flow that occurred in April, May, and June.

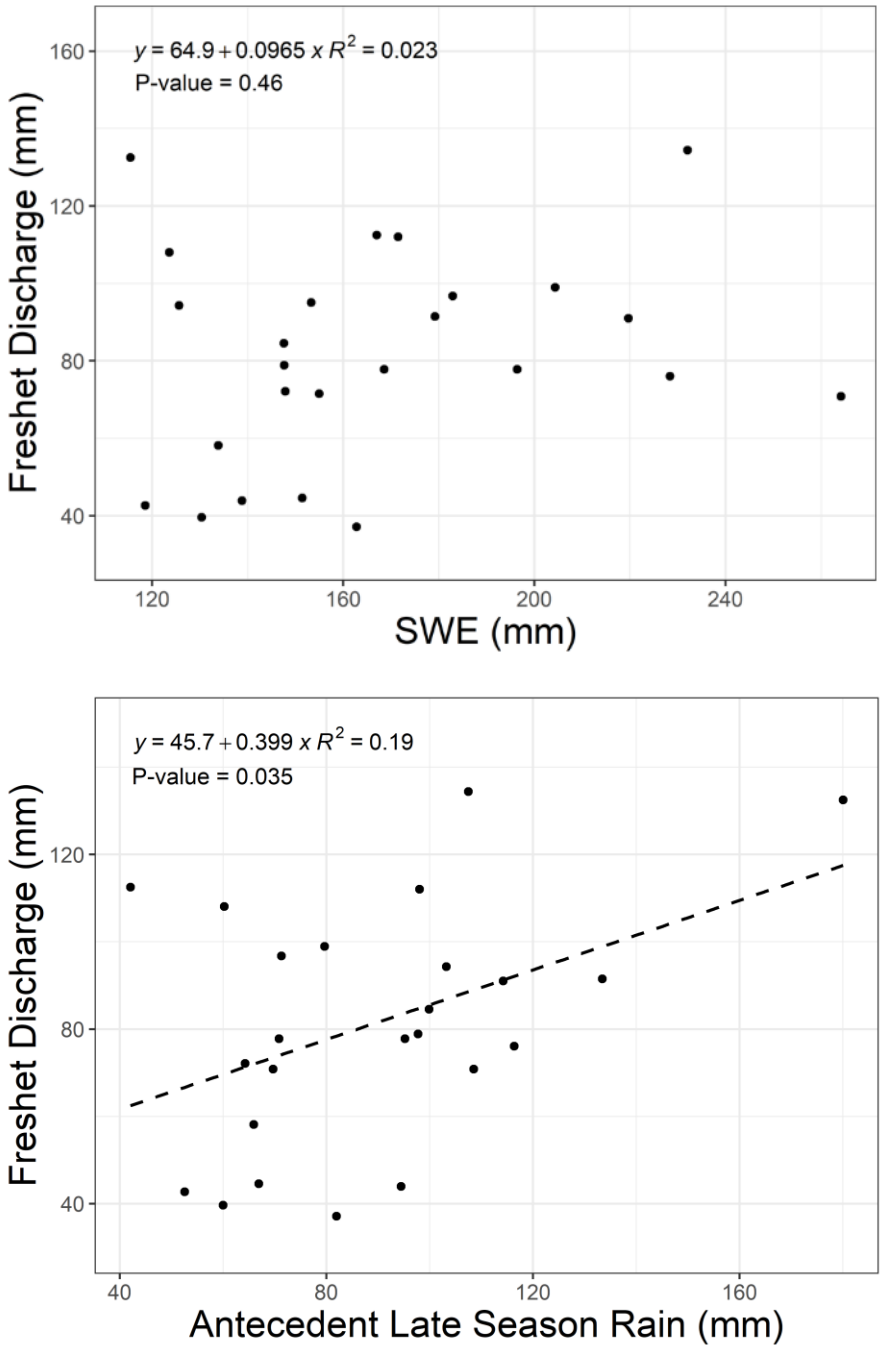

Figure 4.9: Cumulative discharge during freshet (April, May, and June) compared to snowfall in snow water equivalence (SWE) (top), and (b) cumulative late-season (August, September, and October) of the previous year (bottom).

4.14 Baseflow

The mean calculated daily baseflow (Lyne-Hollick method) was 0.19 mm (± 0.06 mm). This was correlated with winter flow point measurements (Figure 4.10) which had a mean value of 0.18 mm (± 0.06 mm). This correlation affirms that the Lyne-Hollick method is an appropriate method for calculating annual baseflow in the WCRB. Mean daily baseflow significantly increased from 1993 to 2019 (Figure 4.11) and was correlated with antecedent fall precipitation (Figure 4.12).

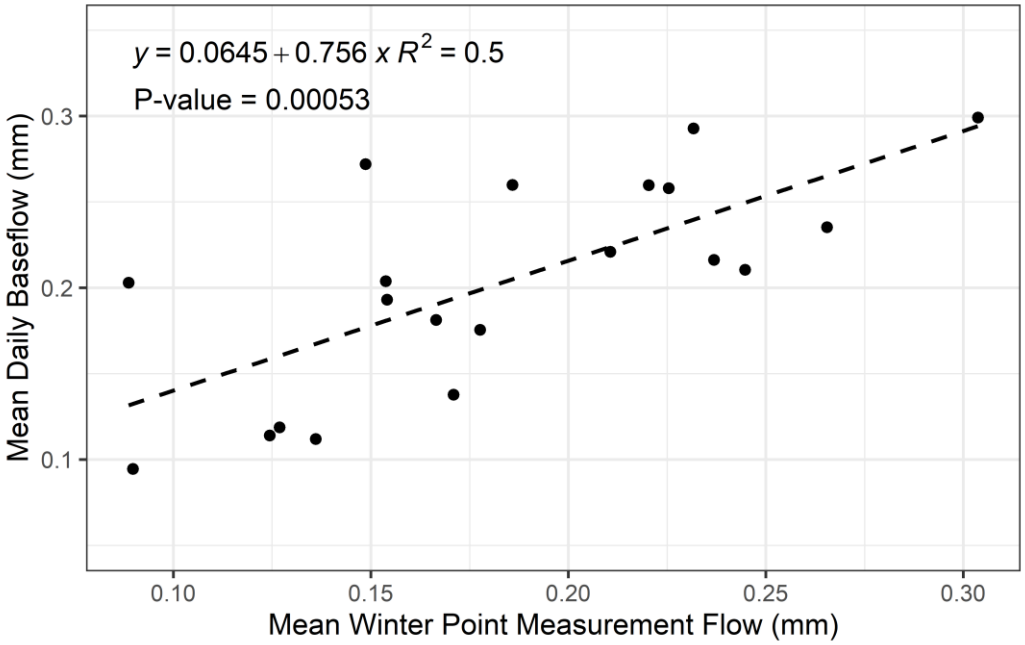

Figure 4.10: Comparison of mean daily point flow measurements over winter and the calculated (Lyne-Hollick method) mean daily baseflow used for further analysis.

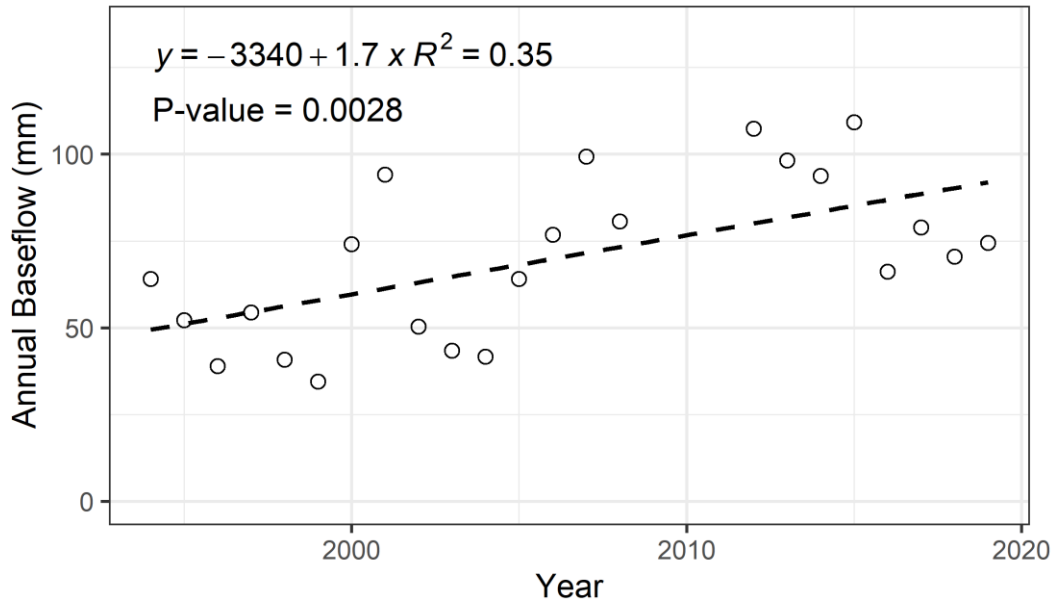

Figure 4.11: Change in calculated mean annual baseflow (Lyne-Hollick method) from 1993 to 2019.

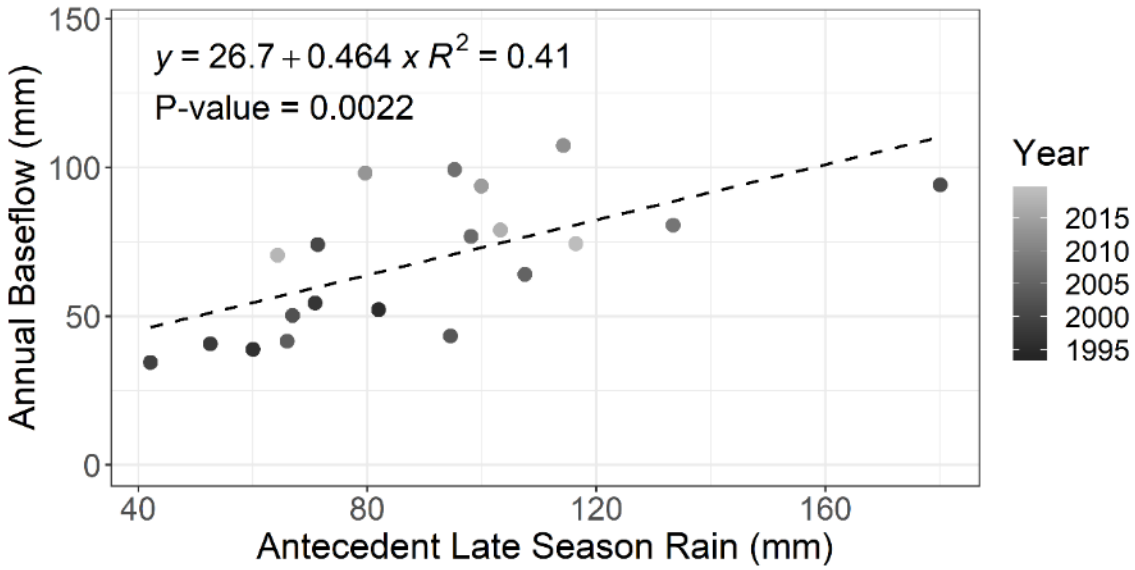

Figure 4.12: mean annual baseflow compared to antecedent late-season (August to October) rainfall.

4.1.5 Runoff Ratios

In the WCRB, the average annual runoff ratio was 34% (± 8%) and did not increase significantly between 1993 and 2019 (Figure 4.13). There were periods of above average runoff ratio from 2007 to 2008 and 2012 to 2014 with peak runoff ratio at 52% in 2012, and the lowest runoff ratio of 41% in 2008. Prior to 2007, the last time runoff ratio exceeded 50% was in 2001. The minimum runoff ratio was 24% in 2003. Runoff ratio was significantly correlated with baseflow (Figure 4.14) and with antecedent late-season (August, September, and October) rainfall (Figure 4.15).

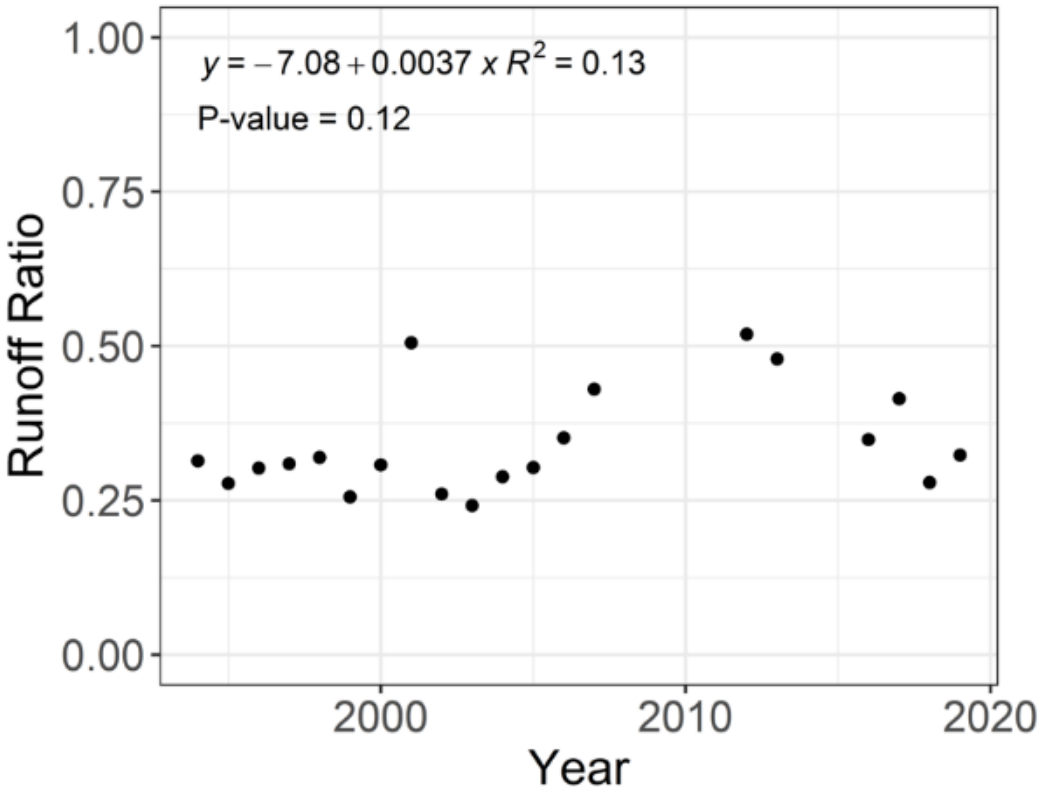

Figure 4.13: Annual runoff ratio based on total annual precipitation and discharge at the WCRB outlet.

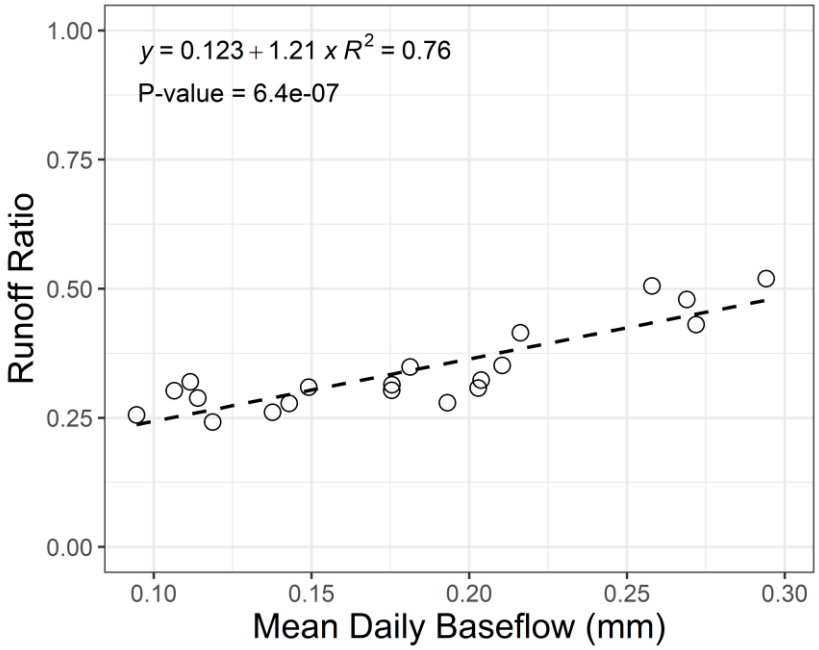

Figure 4.14: Relationship between mean annual runoff ratio and mean annual baseflow

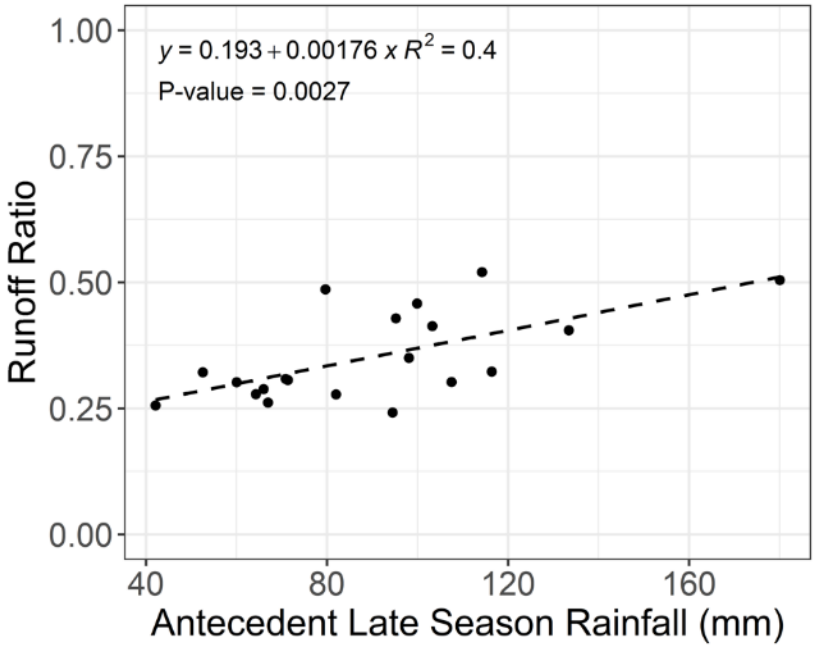

Figure 4.15: Relationship between mean annual runoff ratio and antecedent late-season (August, September, and October) rainfall, where the antecedent late-season rainfall was used as a proxy for antecedent soil moisture content before freeze.

4.2 Teleconnections

Three temporal parameters: temperature, precipitation, and flow were compared to five global pressure oscillations: Arctic oscillation (AO), El Nino southern oscillation (ENSO), North Atlantic oscillation (NAO), Pacific decadal oscillation (PDO), and Pacific North American pattern (PNA). Precipitation, flow, and temperature were each most closely correlated to PDO and ENSO (Figure 4.16), though previous work in western Canada also suggests a strong correlation with PNA which is influenced by both the PDO and ENSO cycles (Bonsal & Shabbar, 2011). There was no correlation between precipitation and flow with PNA, but WCRB temperature and PNA index have a Pearson correlation of 0.31 (Figure 4.16).

Precipitation and flow were both positively correlated with ENSO ($r_{ENSO\text{-}precip}$ = 0.29 and $r_{ENSO\text{-}flow}$ = 0.39), and negatively correlated with PDO ($r_{PDO\text{-}precip}$ = -0.36 and $r_{PDO\text{-}flow}$ = -0.49), whereas temperature was negatively correlated with ENSO ($r_{ENSO\text{-}temp}$ = -0.55) and positively correlated with PDO ($r_{PDO\text{-}temp}$ = 0.33; Figure 4.16). The strongest hydrometric correlations to ENSO and PDO occurred in fall through winter (i.e., $r_{ENSO\text{-}precip\text{-}Fall}$ = -0.54) with little correlation during summer ($r_{ENSO\text{-}precip\text{-}Summer}$ = -0.05; Figure 4.17). Some parameters, most notably flow, were more highly correlated with the respective oscillation value from the previous year.

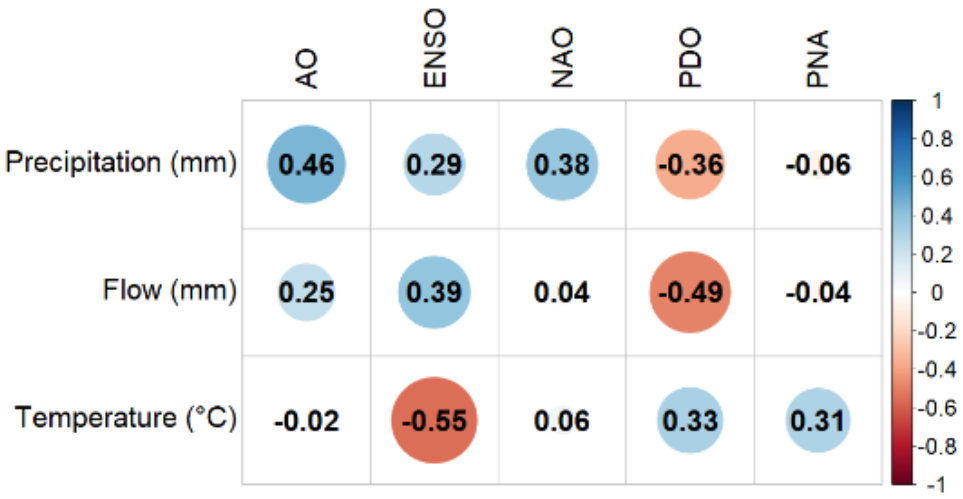

Figure 4.16: Correlation between stream and meteorological variables. All data was based on the annual values for their respective water years. The correlation values presented are the Pearson correlation coefficient (R).

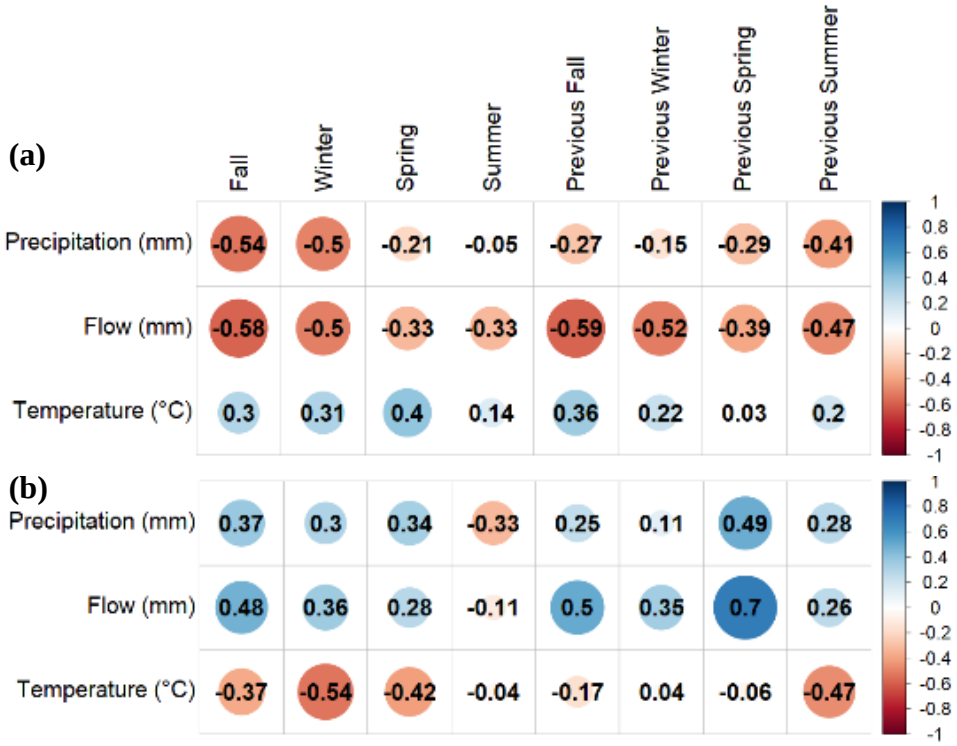

Figure 4.17: Seasonal and 1-year lagged seasonal correlation of precipitation, flow, temperature with (a) PDO and (b) ENSO. The correlation values presented *are* the Pearson correlation coefficient (R).

A negative ENSO phase resulted in a mean temperature of -1.4°C, mean precipitation of 354 mm, and mean discharge of 116 mm, whereas a positive ENSO phase resulted in a mean temperature of -2.4°C, mean precipitation of 392 mm, and a mean discharge of 149 mm.

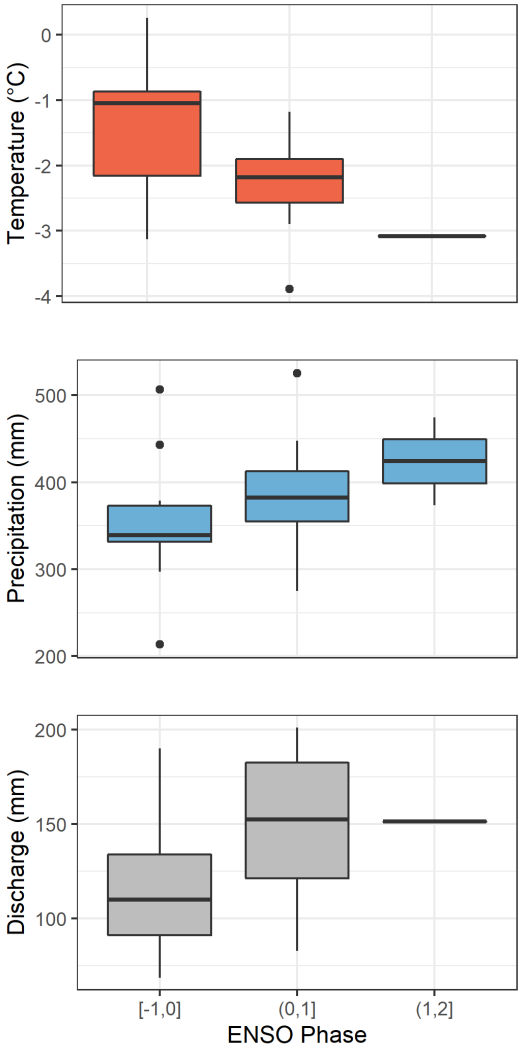

Figure 4.18: Visual representation ENSO phase influence (binned by 1 intervals) on temperature, precipitation, and discharge in the WCRB from 1993 to 2019.

Chapter 5: Discussion

The 26-year hydrometeorological dataset at the WCRB provided an opportunity to study long-term changes in the western Canadian subarctic. The dataset also furthered our understanding of large-scale interactions and assessed controls on inter-annual variability and catchment response. This analysis provided insight into how future changes in climate may further influence streamflow response in the region.

5.1 Comparing regional data to local meteorological trends

5.1.1 Temperature

Widespread projected increases in temperature in northern regions (AMAP, 2017; IPCC, 2018), were reflected annually at the watershed scale (Table 4.1). Increase in annual temperatures were aligned with climate models such as the Coupled Model Intercomparison Project Phase 6 (CMIP6). The CMIP6 modelled an increase of 5°C, or 0.06°C per year, in the northern hemisphere between 2016 and 2100 under the strongest emission scenario (Semmler et al., 2020). This is comparable with the annual increase in temperature of 0.04°C across the WCRB from 1993 to 2019 despite spatial variation within the basin. The annual temperature at Buckbrush and Forest increased at rates similar to both Box et al. (2019) and the Government of Yukon (2020) who reported temperature increases of 0.06°C per year across the arctic, and 0.04°C per year across Yukon, respectively. By site, the greatest significant increases in temperature occurred in the fall at Forest (0.08°C per year), and in winter at Buckbrush (0.07°C per year). This is also consistent with temperature increases reported in Yukon and other northern

environments who report the greatest increases in temperatures during the cold season (October to May) (Box et al., 2019; Government of Yukon, 2020). The results from the WCRB resemble global and territorial changes despite being observed at a much smaller scale.

5.1.2 Precipitation

Changes in precipitation are more pronounced but not significant in the WCRB than elsewhere in Yukon, where territorial increases in annual precipitation of 6% have been reported over the last 50 years (Government of Yukon, 2020). The CMIP6 modelled an increase in precipitation of more than 40% over the Arctic is simulated over the 21st century (Semmler et al., 2020). In the WCRB, precipitation increased at 2.12 mm per year should this trend continue to 2100 total annual precipitation would be approximately 572 mm, an increase of 59% relative to the start of the century.

Like temperature, the cold season has experienced the most consistent changes in precipitation with an increase of 0.4 mm per year across the basin in January ($p = 0.05$) (Table 4.2). This differs from reported territorial precipitation patterns, where changes in summer precipitation is typically more severe than changes in winter precipitation (Government of Yukon, 2020; Hisdal et al., 2006). The lowest elevation in WCRB is the only site which experienced a significant increase in summer precipitation at 1.9 mm per year, or 6% ($p = 0.07$) from 1993 to 2019. Though changes in the total annual and seasonal magnitude of precipitation are variable across ecosections, the frequency of high

intensity precipitation days has increased (Figure 4.2). The increase in high intensity precipitation days is evident across northern regions (Arp et al., 2020; Kane et al., 2003; Kane et al., 2008). High intensity precipitation days (>9.6 mm per day) occurred primarily as rainfall from June through September recharging groundwater and contributing to some event flow.

5.2 Temporal changes in streamflow

5.2.1 Observed long-term changes in freshet flows

5.2.1.1 Magnitude

The greatest flow within a brief period in the WCRB occurs during freshet due to snowmelt which is consistent across northern streams with nival flow regimes (Woo, 2012). Despite an increase in winter precipitation across the WCRB from 1993 to 2019 (Table 4.2) freshet flows (April, May, and June) did not increase (Table 4.3) and the percent of annual discharge output during freshet declined but was not statistically significant ($p = 0.14$) during the same period. While freshet discharge is dominated by snowmelt, the flow can be separated into baseflow and event-flow. An increase in calculated baseflow (section 4.1.5) and no shift in total freshet flows (Table 4.3) may suggest a decrease in event-flow during freshet. This is supported by the strong relation between freshet discharge and antecedent late-season rain (Figure 4.9) which also influences annual baseflow (Figure 4.12).

5.2.2.2 Timing

Despite widespread advancing of spring onset and peak flow across Nordic environments (Burn, 1994; Burn & Elnur, 2002; Jones et al., 2015; Zhang et al., 2014, Semmens & Ramage, 2013), there was no significant shift in spring onset and a notable delay in peak flow at the WCRB. Spring onset in the WCRB is delayed by 0.4 days per year but is not statistically significant ($p = 0.13$), whereas average spring onset across Canada was 0.3 days earlier per year (Jones et al., 2015). Similarly, peak flow during

freshet occurred on average 1 day later each year in the WCRB, or almost 4 weeks later since spring 1994 ($p = 0.10$). The delay in peak flow is contrary to other nival streams in west-central Canada (0.03 to 0.8 days per year earlier) (Burn, 1994).

The delay in peak flows in the WCRB may be resultant from: (1) increased snow accumulation, (2) delayed timing of snowmelt, (3) a slower melt rate, and/or (4) longer transport pathways.

(1) An increase in snow accumulation would delay snowmelt as more energy would be required to warm the pack before the initiation of melt. There was an increase in January precipitation at Alpine and Buckbrush (Table 4.2), but no significant increase over winter. Therefore, increased snow accumulation may contribute to the delay but is likely not the sole cause.

(2) The timing of melt has been associated with the timing of freshet flows in west-central Canada and in the Yukon River basin, with earlier melt generating an earlier onset (Burn & Elnur, 2002; Semmens & Ramage, 2013). In the WCRB the last day of snowmelt was determined by point measurements at Forest, Buckbrush, or Alpine and has not changed (Figure 4.7). Though this date does not consider changes in snow distribution or timing of melt across the catchment as a whole, a shift in the timing of melt is not thought to be causing the delay in peak flow onset in the WCRB.

(3) Snow distribution has changed in the WCRB due to shrubification occurring at ~5.6% per year (Leipe and Carey, 2021) in the taiga ecosection. Resultant from

shrubification, snow previously blown to lower elevation in the WCRB can be captured and stored at higher elevations (Essery & Pomeroy, 2004; Rasouli et al., 2020). Since temperature decreases with elevation in the WCRB (Figure 3.1), and higher elevation sites accumulate snow earlier to later in the year (Figure 3.3) the melt rate across the basin is expected to decrease, potentially contributing to the delay in spring onset and peak flows.

(4). Snow captured at higher elevation due to shrubification increases the travel distance for snowmelt to the stream (Anderson et al., 2010; Essery & Pomeroy, 2004). This could have occurred in WCRB as observed shrubification could retain snow at higher elevation. Snowmelt pathways can also be lengthened because of permafrost thaw and increased active layer depth (Lyon et al., 2009). In the WCRB, as the active layer thickens subsurface drainage becomes slower as flow pathways are deeper and go through less permeable soils rather than more conductive surface organic matter (Carey et al., 2013; Carey & Quinton, 2005). It is uncertain, however, if permafrost thaw has occurred over the study period.

5.2.2 Changes in baseflow

Catchment wetness is a control on connectivity throughout northern basins, with increases in subsurface storage and connectivity allowing more water to reach the stream year-round by activating subsurface flow pathways (Ala-aho et al., 2018; Connon et al., 2014). Increased subsurface storage and connectivity has been associated with increased

baseflows in western Siberia and the Northwest territories (Ala-aho et al., 2018; Connon et al., 2014; St. Jacques & Sauchyn, 2009). It is therefore hypothesized that subsurface storage and connectivity is likely a control on baseflow in the Yukon River Basin (Walvoord et al., 2007) and also in the WCRB (Figure 4.12).

Across the WCRB, the mean snow to precipitation ratio was 0.45 **(**± 0.07) (section 3.1.2). Based on boreal headwater catchment research in Finland, the WCRB snow to precipitation ratio is above the threshold (0.35) wherein summer baseflow is more sensitive to snow conditions than temperature and rainfall (Merio et al., 2019). However, the snow to precipitation ratio at Forest (0.38) fluctuates around the threshold suggesting that, though changes in snow may be theoretically dominant across the basin, the Forest contribution to baseflow may be more sensitive to rain than snow depending on the year.

5.2.3 Changes in runoff ratio

In the WCRB, there was a strong correlation between runoff ratios and baseflow, and consistent with the baseflow and antecedent late-season rainfall (Figure 4.16) runoff ratios and antecedent late-season rainfall were also correlated (Figure 4.12). This suggests that the underlying controls on baseflow may be related to those driving runoff ratios.

Thaw depth is expected to increase and permafrost distribution is expected to decrease with time as a result of permafrost degradation (DeBeer et al., 2016). Previous work in the WCRB has shown that hillslopes underlain by permafrost have higher runoff ratios than those not underlain by permafrost (Carey and Woo, 1999, 2001). This suggests

that a decrease in permafrost distribution, and an increase in thaw depth on a larger scale may result in a decrease in runoff ratio.

5.2.4 Influence of precipitation on streamflow

In the WCRB, summer and early-fall high intensity rainfall generated observable increases in discharge, but the resultant increased flows did not generate flood conditions at the outlet. For example, the flow conditions generated by two days of heavy rainfall in summer 2004 (19.9 mm in two days) increased pre-event flows from 0.4 mm per day to 0.6 mm per day. These flow conditions (0.6 mm per day) are approximately 3 times less than those generated by snowmelt the same year which peaked at 1.7 mm on 8 May 2004. Flood conditions in the WCRB are therefore not currently generated by high-intensity rainfall. Increased discharge in the late-summer and fall however, has been shown to enhance riverbank erosion as bank materials are looser than during freshet flows (Arp et al., 2020). Further increase in summer and fall discharge is expected as more high intensity precipitation is expected in northern regions (DeBeer et al., 2016).

5.3 External forces on water balance response

5.3.1 Elevation-dependent warming

Contrary to larger scale studies, the WCRB showed decreased sensitivity to warming as elevation increases (Giorgi et al., 1997; Williamson et al., 2020). Forest and Buckbrush experienced greater temperature changes over monthly, seasonal, and annual scales than Alpine (Table 4.1). On the continental scale, snow-albedo feedback and water vapor feedback are two mechanism used to explain increased sensitivity with elevation (Williamson et al., 2020). These mechanisms are not applicable to the WCRB due to the small scale and elevation range (750 to 1615 masl), however, the 0°C isotherm has been identified as a climate-sensitive zone at both continental and regional scales (Giorgi et al., 1996). In mid-elevation mountain studies commonly used to understand elevation-dependency the 0°C isotherm is approached with elevation (Pepin & Seidel, 2005; Wang et al., 2014) whereas located at high-latitude the mean annual temperature is below 0°C across the WCRB, and is closest to the 0°C isotherm at the lowest elevation. Though the increased sensitivity at lower elevation contradicts the theory of rapid upslope warming, it supports the theory that maximum warming in northern catchments occurs around the 0°C isotherm.

Increased vegetation may also contribute to reducing the rate of warming at higher elevation in the WCRB. Increases in vegetation extent and density decreases the albedo, increases surface roughness, and increases net radiation (Bounoua et al., 2010). However, increased ET from more plant cover may result in a net cooling because of increased

evaporation (Betts et al., 1997). Currently, in the WCRB this mechanism likely has a greater influence at the mid- elevation as vegetation change is more pronounced at Buckbrush than Alpine, but vegetation cover is expected to expand over time as temperature and precipitation increase (Piao et al., 2006). This negative feedback therefore may strengthen with changes in plant cover.

5.3.2 Influence of teleconnections on catchment hydrology

The WCRB dataset is spatially and temporally smaller than is generally used for teleconnection correlation studies. The WCRB is also located inland where correlation with teleconnections is typically less intense than coastal regions (McNeil, 2015), but precipitation, discharge, and temperature each had some correlation with PDO and ENSO cycles. Both PDO and ENSO are calculated based on climate anomalies with which there is significant autocorrelation, but current year precipitation and temperature correlations are most strongly correlated with current PDO or ENSO of the same year, whereas flow correlations are equal to or more strongly correlated with the previous season PDO and ENSO phase. The lagged correlation between discharge and teleconnection may be a result of stream discharge being driven by stored water which has been shown to be dependent on the previous year's precipitation (Figure 4.12).

5.3.2.1 Pacific Decadal Oscillation

The negative correlation between precipitation, flow, and PDO phase in the WCRB (Figure 4.14) is consistent with other studies across Alaska, Yukon, and

northwestern British Columbia (Fleming and Whitfield, 2010; Neal et al., 2002). However, previous work in these regions has shown that the relative intensity and positions (north or south of normal) of the Siberian and Alaskan storm tracks defined by PDO phase and position of the Aleutian low had the greatest association with precipitation than just the PDO phase (Rodionov et al., 2007). A positive PDO phase was associated with a southward shift of storm tracks causing increased precipitation around southern coastal Alaska but not inland (Rohrer et al., 2019; Simpson et al., 2002) and a negative PDO phase is associated with a northward shift in storm tracks increasing precipitation in and around the WCRB (Rohrer et al., 2019). The position of storm tracks is the physical mechanism that explains why the WCRB has a negative correlation between PDO phase and precipitation and flow. The correlation between PDO and WCRB hydrometrics is strongest in winter. The weak correlation in summer is likely explained by the weak Aleutian low during that season, as the strength of a PDO cycle and the movement and intensity of storm tracks are associated with the position and strength of the Aleutian low (Rodionov et al., 2007).

Snow accumulation on Mt. Logan, Yukon was greatest when the Aleutian low was shifted east relative to its normal center as more moist warm air is brought into western Canada (Rupper et al., 2004). Northern North America precipitation is highly dependent on the Alaskan and Siberian storm tracks (Rodionov et al., 2007). The Alaskan storm track carries moisture from the western Pacific to the Gulf of Alaska, whereas the Siberian storm track moves moisture northward from western Pacific to Siberia (Overland

& Pease, 1981). A strong Aleutian low generates frequent storms along the Alaskan storm track transporting moisture towards southern Alaska and Yukon causing more precipitation around the WCRB (Rodionov et al., 2007). Weak or divided Aleutian low, notably when located east of mean position, leads to either storms that are concentrated in the Gulf of Alaska or few and weak storms that do not deliver significant precipitation to the Yukon (Rodionov et al., 2007).

5.3.2.2 El Niño Southern Oscillation

Precipitation and flow in the WCRB are primarily positively correlated with ENSO phase, while temperature is negatively correlated, and the correlations are strongest from fall to spring (Figure 4.15). Most of the seasonal trends have Pearson correlations coefficients of 0.25 to 0.5 which is consistent across northwestern North America though relations are typically stronger in British Columbia than interior Yukon (Fleming & Whitfield, 2010; McNeil, 2015; Shabbar & Khandekar, 1996). However, similar to PDO these correlations are weakest during summer with summer precipitation having the opposite correlation with ENSO phase than other seasons. ENSO is based on equatorial Pacific Sea Surface Temperature (SST). The increased precipitation seen in the WCRB during El Niño (positive) is consistent with warmer equatorial Pacific temperatures as trade winds weaken and more moisture is transported to northwestern North America (Fleming & Whitfield, 2010). Conversely, La Niña (negative) is associated with less precipitation and increased temperature around the WCRB as westerlies strengthen with cooler equatorial Pacific temperatures.

5.4 Future research

This research provides a holistic overview of the WCRB water balance over a 26-year period, based on which interactions within the basin are discussed using a wide-angled understanding of the major processes. Future research would complement this work by focusing on interactions centered around specific processes. (1) Baseflow and antecedent soil moisture were at the forefront of this project findings, yet late-season precipitation was used as a proxy for soil moisture and no direct values were presented. The increase in baseflow is thought to be a result of increased soil moisture with increases in fall precipitation being consistent across all sites. A direct analysis of soil moisture data across the WCRB would solidify these findings. (2) In addition, since no significant change in freshet discharge has been identified, it would be interesting to differentiate between the proportions of old- and new-water using isotope geochemistry and evaluate the impact of rain-on-snow events on freshet flows (Dou et al., 2021). Based on my research, proportionally more of freshet flows may consist of old-water and there will have been a decrease in new-water contribution to freshet flows over time. Spring rain-on-flow events may also contribute to controlling the amount of new-water that reaches the outlet.

Chapter 6: Conclusion

This 26-year hydrologic dataset of the WCRB provided an opportunity to identify change and large-scale hydrometric relationships within the research basin. It aided in filling a knowledge gap resultant from a lack of long-term hydrological data in northern regions (Laudon et al., 2016). The aim of this study was to identify trends in temperature, precipitation, and discharge, determine some of the underlining mechanisms that could contribute to driving these changes, and note the inter-annual and spatial variability of change across the basin. The key findings from this study are:

(1) Annual temperature is increasing within the basin at a rate (0.05°C per year) comparable to the rest of the Yukon and the global arctic. Changes in precipitation are also trending upward but are currently only significant in winter (0.96 mm per year across the WCRB) and in the summer (1.89 mm per year at Forest).

(2) The timing of peak flow during freshet has shifted to later in the year at the WCRB. This is contrary to many other study sites that follow a nival regime. This is not expected to be related to a delay in melt as there was no significant change in the last day of melt (based on point measurements). It may be related to melt rate, snow distribution across the catchment, or pathway length.

(3) A significant increase in baseflow was related to late-season rainfall (used as a proxy for soil moisture before freeze). It was also significantly related to high

runoff ratios, where runoff ratios are also related to the number of high intensity discharge days, which typically occur during freshet.

These findings highlight that catchment response to climate change are variable spatially and temporally. The trends discussed were significant, but there are many increasing trends that are not significant. The increasing trends that are currently insignificant are aligned with climate change predictions. It will be important to continue to monitor the WCRB and revisit these trends to see if the increases become significant, stabilize, or change over time.

Appendix A

Table A.1: Mean percentage of monthly precipitation at Alpine, Buckbrush, and Forest as snow from 1993 to 2019.

Month	Month Number	Alpine Snow (%)	Buckbrush Snow (%)	Forest Snow (%)
January	1	99.9	99.0	99.7
February	2	100	99.7	99.8
March	3	100	99.1	97.8
April	4	97.3	79.1	51.2
May	5	47.8	18.1	3.9
June	6	0.8	0	0
July	7	0	0	1.0
August	8	1.3	0.9	0
September	9	30.3	11.0	4.1
October	10	92.2	75.7	52.0
November	11	100	98.4	97.5
December	12	99.7	99.3	99.8

References

Ahmed, R., Prowse, T., Dibike, Y., & Bonsal, B. (2021). Effects of climatic drivers and teleconnections on late 20th century trends in spring freshet of four major Arcitc-drainage rivers. *Water, 13,* 179. doi: 10.3390/w13020179

Aigang, L., Shichang, K., Zongxing, L., & Theakstone, W.H. (2010). Altitude effects of climatic variation on Tibetan Plateau and its vicinities. *Journal of Earth Science, 21*(2), 189-198. doi: 10.1007/s12583-010-0017-0

Ala-aho, P., Soulsby, C., Pokrovsy, O.S., Kirpotin, S.N., Karlsson, J., Serikova, S., Vorobyev, S.N., Manasypov, R.M., Loiko, S., & Tetzlaff, D. (2018). Using stable isotopes to assess surface water source dynamics and hydrological connectivity in a high-latitude wetland and permafrost influenced landscape. *Journal of Hydrology, 556,* 279-293.

Allen, S.T., von Freyberg, J., Weiler, M., Goldsmith, G.R., & Kirchner, J.W. (2019). The seasonal origins of streamwater in Switzerland, *Geophysical Research Letters, 46*, 10,425-10,10434. doi: 10.1029/2019GL084552

AMAP (2017). Snow, Water, Ice and Permafrost in the Arctic (SWIPA) 2017. Arctic Monitoring and Assessment Programme (AMAP), Oslo, Norway. xiv + 269 pp Ambaum, M.H.P., Hoskins, B.J., Stephenson, D.B. (2001). Arctic oscillation or North Atlantic Oscillation? *American Meteological Society, 14,* 3495-3507.

Amiro, B. (2009). Measuring boreal forest evapotranspiration using the energy balance residual. *Journal of Hydrology, 366,* 112-118. doi: 10.1016/j.hydrol.2008.12.021

Anderson, L., Birks, J., Rover, J., & Guldager, N. (2013). Controls on recent Alaskan lake changes identified from water isotopes and remote sensing. *Geophysical Research Letters, 40,* 3413-3418. doi:10.1002/grl.50672

Arp, C.D., Whitman, M.S., Kemintz. R., & Stuefer, S.L. (2020). Evidence of Hydrological Intensification and Regime Change from Northern Alaskan Watershed Runoff. *Geophysical Research Letters, 47,* e2020GL089186. doi: 10.1029/2020GL089186.

Barrow, E., Maxwell, B., & Gachon, P. (2004). Climate Variability and Change in Canada: Past, Present, and Future. ACSD Science Assessment Series No. 2, Meteorological Service of Canada, Environment Canada, Toronto, Ontario, 114p.

Beniston, M. (1997) Variations of snow depth and duration in the Swiss Alps over the last 50 years: Links to changes in large-scale climatic forcings. *Climatic Change, 36,* 281-300. doi: 10.1023/A:1005310214361

Beringer, J., Chapin III, F.S., Thompson, C.C., & McGuire, A.D. (2005). Surface energy exchanges along a tundra-forest transition and feedbacks to climate, *Agricultural and Forest Meteorology, 131,* 143-161. doi: 10.1016/j.agrformet.2005.05.006

Betts, R.A., Cox, P.M., Lee, S.E., & Woodward, F.I. (1997). Contrasting physiological and structural vegetation feedbacks in climate change simulations. *Nature, 387,* 796-799.

Bintanja, R., & Andry, O. (2017). Towards a rain-dominated Arctic. *Nature Climate Change, 7,* 263-268. doi: 10.1038/NCLIMATE3240

Bjerknes, J. (1969). Atmospheric teleconnections from the equatorial Pacific. *Monthly Weather Review, 97*(3), 163-172.

Bolduc, C., Lamoureux, S. F., & Franssen, J. (2018). Thermal and isotopic evidence for surface and subsurface water contributions to baseflow in a high Arctic river. *Hydrological Processes, 32(5),* 602-616. doi: 10.1003/hyp.11427

Bonsal, B., & Shabbar, A. (2011). Large-scale climate oscillations influencing Canada, 1900-2008. Canadian Biodiversity: Ecosystem Status and Trends 2010, Technical Tematic Report No. 4. Canadian Councils of Resource Ministers. Ottawa, ON. iii + 15p, http://www.biodivcanada.ca/default.asp?lang=En&n=137E1147-0

Bounoua, L., Hall, F.G., Sellers, P.J., Kumar, A., Collatz, G.J., Tucker, C.J., & Imhoff, M.L. (2010). Quantifying the negative feedback of vegetation to greenhouse warming: A modelling approach. *Geophysical Research Letters, 37,* L23701. doi: 10.1029/2010GL045338

Box, J.E., Colgan, W.T., Chritensen, T.R., Schmidt, N.M., Lund, M., Parmentier, F.-J.W., Brown, R., Bhatt, U.S., Euskirchen, E.S., Romanovsky, V.E., Walsh, J.E., Overland, J.E., Wang, M., Corell, R.W., Meier, W.N., Wouters, B., Mernild, S., Mard, J., Pawlak, J., & Olsen, M.S. (2019). Key indicators of Arctic climate change: 1971-2017. *Environmental Research Letters, 14,* 045010. doi: 10.1088/1748-9326/aafc1b

Bridgman, H.A., Oliver, J.E. (2006). The Global Climate System: Patterns, Processes, and Teleconnections. Cambridge: *Cambridge University Press*

Bring, A., Fedorova, I., Dibike, Y., Hinzman, L., Mard, J., Mernild, S.H., Prowse, T., Semenova, O., Stuefer, S.L., & Woo, M.-K. (2016), Arctic terrestrial hydrology: A synthesis of processes, regional effects, and research challenges, *Journal of Geophysical Research: Biogeosciences, 121,* 621-649. doi: 10.1002/2015JG003131

Burn, D.H. (1994). Hydrologic effects of climatic change in west-central Canada. *Journal of Hydrology, 160(1-4),* 53-70. doi: 10.1016/0022-1694(94)90033-7

Burn, D.H., & Hag Elnur, M.A. (2002). Detection of hydrologic trends and variability. *Journal of Hydrology, 255,* 107-122.

Carey, S.K., Boucher, J.L., & Duarte, C.M. (2013). Inferring groundwater contributions and pathways to streamflow during snowmelt over multiple years in a discontinuous permafrost subarctic environment (Yukon, Canada). *Hydrogeology Journal, 21,* 67-77. doi: 10.1007/s10040-012-0920-9

Carey, S.K., & Quinton, W.L. (2005). Evaluating runoff generation during summer using hydrometric stable isotope and hydrochemical methods in a discontinuous permafrost alpine catchment. Hydrological Processes. doi: 10.1002/hyp.5764

Carey, S.K., & Woo, M.-K. (2000). The role of soil pipes as a slope runoff mechanism, Subarctic Yukon, Canada, *Journal of Hydrology, 233,* 206-222.

Carey SK & Woo M. (2001). Slope runoff processes and flow generation in a subarctic subalpine catchment. *Journal of Hydrology. 253,* 110-129.

Cayan, D.R., Kammerdiener, S.A., Dettinger, M.D., Caprio, J.M., & Peterson, D.H. (2001). Changes in the Onset of Spring in the Western United States, *American Meteorological Society, 82*(3), 399-414

Clark, I., & Fritz, P. (1997). *Environmental isotopes in hydrogeology*. U.S.A.: CRC Press.

Connon, R.F., Quinton, W.L., Craig, J.R., & Hayashi, M. (2014). Changing hydrologic connectivity due to permafrost thaw in the lower Liard River valley, NWT, Canada. *Hydrological Processes, 28,* 4163-4178.

Cunderlik, J.M., & Ouarda, T.B.M.J. (2009). Trends in the timing and magnitude of floods in Canada. *Journal of Hydrology, 275,* 471-480. doi: 10.1016/j.hydrol.2009.06.050

DeBeer, C.M., Wheater, H.S., Carey, S.K., & Chun, K.P. (2016). Reecent climatic, cryospheric, and hydrological changes over the interior of western Canada: a review and synthesis. *Hydrology and Earth System Sciences, 20,* 1573-1598. doi: 10.5194/hess-20-1573-2016

Dingman, SL. (2015). *Physical Hydrology.* Long Grove, Illinois: Waveland Press, Inc.

Dou, T., Xiao, C., L., J., Wang, Q., Pan, S., Su, J., Yuan, X., Ding, M., Zhang, F., Xue, K., Bieniek, P.A.,& Eicken, H. (2021). Trends and spatial variation in rain-on-snow events over the Arctic Ocean during the early melt season. *The Cryosphere, 15,* 883-895. doi: 10.5194/tc-15-883-2021

Essery, R., & Pomeroy, J. (2004). Vegetation and topographic control of wind-blown snow distributions in distributed and aggregated simulations for an Arctic Tundra Basin. *Journal of Hydrometeorology, 5*(5), 735-744. doi: 10.1175/1525-7541(2004)005<0735:VATCOW>2.0.CO;2

Fleming, S.W., & Whitfield, P.H. (2010). Spatiotemporal mapping of ENSO and PDO surface meteorological signals in British Columbia, Yukon, and southeast Alaska. *Atmosphere-Ocean, 48*(2), 122-131. doi: 10.3137/AO1107.2010

Freeze, R.A. (1974). Streamflow Generation. *Reviews of Geophysics and Space Physics, 12*(4), 627-647

Gat JR. (2010). Isotope Hydrology: A Study of the Water Cycle. *Imperial College Press.*

Gershunov, A., & Barnett, T.P. (1998). Interdecadal modulation of ENSO teleconnections. *Bulletin of the American Meteological Society, 79*(12), 2715-2726. doi: 10.1175/1520-0477(1998)079<2715:IMOET>2.0CO;2

Gibson J.J., Edwards T.W.D., Birks S.J., St Amour N.A., Buhay W.M., McEachern P., Wolfe B.B., & Peters D.L. (2005). Progress in isotope tracer hydrology in Canada. *Hydrological Processes, 19*, 303-327. doi:10.10002/hyp.5766

Gibson, J.J., & Reid, R. (2014). Water balance along a chain of tundra lakes: A 20-year isotropic perspective. *Journal of Hydrology, 519*, 2148-2164.

Giorgi, F., Hurrell, J., Marinucci, M.R., & Beniston, M. (1997). Elevation Dependency of the Surface Climate Change Signal: A Model Study. *Journal of Climate, 10*, 288-296.

Government of Yukon (2020). Yukon state of the environment report 2020: A report on environmental indicators, 130 p.

Harris, S.A., French, H.M., Heginbottom, J.A., Johnston, G.H., Ladanyi, B., Sego, D.C., & van Everdingen, R.O. (1988). Glossary of Permafrost Related Ground-Ice Terms. *National Research Council of Canada, 142*, p.157.

Hinton, M.J., Schiff, S. L., & English, M.C. (1994). Examining the contributions of glacial till water to storm runoff using two- and three-component hydrograph separations. *Water Resources Research, 30*(4), 983-993.

Hinzman, L.D., Bettez, N.D., Bolton, W.R., Chapin, F.S. […] Yoshikawa, K. (2005). Evidence and Implications of Recent Climate Change in Northern Alaska and Other Arctic Regions. *Climate Change, 72,* 251-298. doi: 10.1007/s10584-005-5352-2.

Hisdal, H., Holmqvist, E., Hyvarinen, V., Jonsson, P., Kuusisto, E., Larsen, S.E., Lindstrom, G., Ovesen, N.B., & Roald, L.A. (2003). Long time series: A review of Nordic studies. *CWE Long Time Series Group, Report No. 2.*

Hisdal, H., Holmqvist, E., Jonsdottir, J.F., Jonsson, P., Kuusisto, E., Lindstrom, G., & Roald, L.A. (2010). Has streamflow changed in the Nordic countries? *Norwegian Water Resources and Energy Directorate (NVE),* Report No. 1.

Hisdal, H., Roald, L. A., & Beldring, S. (2006). Past and future changes in flood and drought in the Nordic countries, in: Climate Variability and Change: Hydrological Impacts, Publ. No. 308, edited by: Demuth, S., Gustard, A., Planos, E., Seatena, F., Servat, E., IAHS Press, Wallingford, 502-507

Hoeg, S., Uhlenbrook, S., & Leibundgut, C. (2000). Hydrograph separation in a mountainous catchment – combining hydrochemical and isotopic tracers. *Hydrological Processes, 14*, 1199-1216.

Holmes, R. M., Coe, M. T., Fiske, G. J., Gurtovaya, T., McClelland, J. W., Shiklomanov, A. I., Spencer, R. G. M., Tank, S. E., & Zhulidov, A. V. (2012). Climate Change Impacts in the Hydrology and Biogeochemistry of Arctic Rivers. *Climatic Change and Global Warming of Inland Waters: Impacts and Mitigation for Ecosystems and Societies.* Chapter 1. doi : 10.1002/9781118470596.ch1

Hurell, J.W. (1995). Decadal trends in the North Atlantic Oscillation: Regional temperatures and precipitation. *Science, 269*(5224).

IPCC: Global Warming of 1.5 °C. An IPCC Special Report on the impacts of global warming of 1.5 °C above pre-industrial levels and related global greenhouse gas emission pathways, in the context of strengthening the global response to the threat of climate change, sustainable development, and efforts to eradicate poverty, edited by: Masson-Delmotte, V., Zhai, P., Pörtner, H.-O., Roberts, D., Skea, J., Shukla, P. R., Pirani, A., Moufouma-Okia, W., Péan, C., Pidcock, R., Connors, S., Matthews, J. B. R., Chen, Y., Zhou, X., Gomis, M. I., Lonnoy, E., Maycock, T., Tignor, M., and Waterfield, T., in press, 2018.

Jantze, E.J., Laudon, H., Dahlke, H. E., & Lyon, S. W. (2015). Spatial Variability of Dissolved Organic and Inorganic Carbon in Subarctic Headwater Streams. *Arctic, Antarctic, and Alpine Research, 47*(3), 529-546. doi: 10.1657/AAAR0014-044

Jones, N.E., Petreman, I.C., & Schmidt, B.J. (2015). High flows and freshet timing in Canada: Observed Trends. Climate Change and Research Report CCRR—42, 34p.

Jost, G., Weiler, M., Gluns, D.R., & Alila, Y. (2007). The influence of forest and topography on snow accumulation and melt at the watershed-scale. *Journal of Hydrology, 347*, 101-115. doi: 10.1016/j.jhydrol.2007.09.006.

Kane, D.L., McNamara, J.P., Yang, D., Olsson, P.Q., & Gieck, R.E. (2003). An Extreme Rainfall/Runoff Event in Arctic Alaska. *Journal of Hydrometeorology*

Kane D.L., Yang D., Prowse T., Shiklomanov I., Marsh P., Ohata T., & Killingtveit A. (2005). Synthesis of high latitude hydrologic water balances. *Conference: 15th International Northern Research Basins Symposium and Workshop*

Kane, D. L., Hinzman, L. D., Gieck, R. E., McNamara, J. P., Youcha, E. K., & Oatley, J. A. (2008). Contrasting extreme runoff events in areas of continuous permafrost, Arctic Alaska. *Hydrology Research, 39*(4), 287-298. doi: 10.2166/nh.2008.005

Kane, D. L., Hinzman, L. D., & Zarling, J. P. (1991). Thermal response of the active layer to climatic warming in a permafrost environment. *Cold Regions Science and Technology, 19*(2), 111-122. doi:10.1016/0165-232X(91)90002-X

Kiffney, P.M., Bull, J.P., & Feller, M.C. (2002). Climatic and hydrologic variability in a coastal watershed of southwestern British Columbia. *Journal of the American Water Resources Association, 38*(5), 1437-1451.

Kozii, N., Haahti, K., Tor-ngern, P., Chi, J., Hasselquist, E.M., Laudon, H., Launiainen, S., Oren, R., Peichl, M., Wallerman, J., & Hasselquist, N.J. (2020). Partitioning growing season water balance within a forested boreal catchment using sap flux, eddy covariance, and a process-based model, *Hydrology and Earth System Sciences, 24*, 2999-3014. doi: 10.5194/hess-24-2999-2020

Lafrenière M.J. & Lamoureux S.F. (2019). Effects of changing permafrost conditions on hydrological processes and fluvial fluxes. *Earth Science Reviews*, 191, 212-223.

Latif, M., & Barnett, T.P. (1994). Causes of Decadal Climate Variability over the North Pacific and North America. *Science, 266*(5185), 634-637.

Laudon, H., Spence, C., Buttle, J., Carey, S.K., McDonnell, J.J., & McNamara, J.P. (2017). Save northern high-latitude catchments. *Nature geoscience, 10*, 324-325.

Laudon H, Tetezlaff , D, Soulsby C, Carey S, Seibert J, Buttle J, Shanley J, McDonnell JJ, & McGuire K. (2013). Change in winter climate will affect dissolved organic carbon and water fluxes in mid-to-high latitude catchment. *Hydrological Processes, 27*, 700-709.

Leipe, S.C., & Carey, S.K. (2021). Rapid shrub expansion in a subarctic mountain basin revealed by repeat airborne LiDAR. *Enviromenta Research Communications*, in press. doi: 10.1088/2515-7620/ac0e0c

Lewkowicz, A.G., & Endie, M. (2004). Probability mapping of mountain permafrost using the BTS method, Wolf Creek, Yukon Territory, Canada. *Permafrost and Periglacial Processes, 15*, 67-80. doi: 10.1002/ppp.480

Liljedahl, A.K., Hinzman, L.D., Kane, D.L., Oechel, W.C., Tweedie, C.E.,& Zona, D. (2017). Tundra water budget and implications of precipitation underestimation. *Water Resources Research, 53*(8), 6472-6486. doi: 10.1002/2016WR020001

Lyne, V.D., & Hollick, M. (1979). Stochastic time-variable rainfall-runoff modelling. *Hydrology and Water Resources Symposium*, 89-92.

Lyon SW, Destouni G, Giesler R, Humborg M, Seibert J, Karlsson J, & Troch P. A. (2009). Estimation of permafrost thawing rates in a sub-arctic catchment using recession flow analysis. *Hydrology and Earth System Science, 13,* 595-604.

Lyon S. W., Ploum S. W., van der Velde Y., Rocher-Ross G., Morth C., & Giesler, R. (2018). Lessons learned from monitoring the stable water isotopic variability in precipitation and streamflow across a snow-dominated subarctic catchment. *Arctic, Antarctic, and Alpine Research, 50*(1), e1454778. doi: 10.1080/15230430.2018.1454778.

Matti, B., Dahlke, H.E., Dieppois, B., Lawler, D.M., & Lyon, S.W. (2017). Flood seasonality across Scandinavia-Evidence of a shifting hydrograph? *Hydrological Processes, 31,* 4354-4370. doi: 10.1002/hyp.11365

Maule CP, & Stein J. (1990). Hydrologic Flow Path Definition and Partitioning of Spring Meltwater. *Water Resources Research, 26(12),* 2959-2970.

McCartney, S.E., Carey, S.K., & Pomeroy, J.W. (2006). Intra-basin variability of snowmelt water balance calculations in a subarctic catchment. *Hydrological Processes, 20,* 1001-1016. doi: 10.1002/hyp.6125

McDonnell JJ. (2013). Are all runoff processes the same? *Hydrological Processes*. *27*. 4103-4111. doi: 10.1002/hyp.10076

McNeill-Jewer, C.A. (2015). Atmospheric teleconnection intensity correlated with Alaska and Yukon snow water equivalent. *Master's Thesis,* p.71.

McNamara, J.P., Kane, D.L., & Hinzman, L.D. (1998). An analysis of streamflow hydrology in the Kuparuk River Basin, Arctic Alaska: a nested watershed approach. *Journal of Hydrology, 206,* 39-57.

Mekis, E. (2005). Adjustments for trace measurements in Canada. *15th Applied Climatology Conference*.

Meredith, M., M. Sommerkorn, S. Cassotta, C. Derksen, A. Ekaykin, A. Hollowed, G. Kofinas, A. Mackintosh, J. Melbourne-Thomas, M.M.C. Muelbert, G. Ottersen, H. Pritchard, & E.A.G. Schuur (2019). Polar Regions. In: *IPCC Special Report on the Ocean and Cryosphere in a Changing Climate* [H.-O. Pörtner, D.C. Roberts, V. Masson-Delmotte, P. Zhai, M. Tignor, E. Poloczanska, K. Mintenbeck, A. Alegría, M. Nicolai, A. Okem, J. Petzold, B. Rama, N.M. Weyer (eds.)]. In press.

Merio, L.-J., Ala-aho, P., Linjama, J., Hjort, J., Klove, B., & Marttila, H. (2019). Snow to precipitation ratio controls carchment storage and summer flows in boreal headwater catchments. *Water Resources Research, 55,* 4096-4109. doi: 10.1029/2018WR023031

Milewska, E.J., Vincent, L.A., Hartwell, M.M., Charlesworth, K., & Mekis, E. (2019). Adjusting precipitation amounts from Geonor and Pluvio automated weighing gauges to preserve continuity in observations in Canada. *Canadian Water Resources Journal, 44(2),* 127-145. doi: 10.1080/07011784.2018.1530611

Mountain Research Initiative EDW Working Group., Pepin, N., Bradley, R. *et al*. Elevation-dependent warming in mountain regions of the world. *Nature Clim Change* **5,** 424–430 (2015). https://doi.org/10.1038/nclimate2563

Musselman K. N., Clark M. P., Liu C., Ikeda K., & Rasmussen R. (2017). Slower snowmelt in a warmer world. *Nature Climate Change, 7,* 214-220. doi: 10.1038/NCLIMATE3225

Myers-Smith, I.H., & Hik, D.S. (2017). Climate warming as a driver of tundra shrubline advance. *Journal of Ecology, 106,* 547-560. doi: 10.1111/1365-2745.12817

Neal, E.G., Walter, M.T., & Coffeen, C. (2002). Linking the pacific decadal oscillation to seasonal stream discharge patterns in Southeast Alaska. *Journal of Hydrology, 263,* 188-197.

O'Donnell, B., Gruenig, M., & Riedel, A. (2018). Arctic Summer College Yearbook: An Interdisciplinary Look into Arctic Sustainable Development. *Springer.*

Overland, J.E., & Pease, C.H. (1982). Cyclone climatology of the Bering Sea and its relation to sea ice extent. *Monthly Weather Review, 110*(1), 5-13. doi: 10.1175/1520-0493(1982)110<0005:CC0TBS>2.0.CO;2

Oxford University Press. (2004). *The Oxford English dictionary*. Oxford.

Pan, X., Yang, D., Li, Y., Barr, A., Helgason, W., Hayashi, M., Marsh, P., Pomeroy, J., & Janowicz, R. J. (2016). Bias corrections of precipitation measurements across experimental sites in different ecoclimatic regions of western Canada, The Cryosphere, 10, 2347–2360. doi: 10.5194/tc-10-2347-2016.

Pearson, R.G., Phillips, S.J., Loranty, M.M., Beck, P.S.A., Damoulas, T., Knight, S.J., & Goetz, S.J. (2013). Shifts in Arctic vegetation and associated feedbacks under climate change, *Nature Climate Change, 3,* 673-677, doi: 10.1038/NCLIMATE1858

Pepin, N.C., & Lundquist, J.D. (2008). Temperature trends at high elevations: Patterns across the globe. *Geophysical Research Letters, 35*(14), L14701. doi: 10.1029/2008GL034026

Pepin, N.C., & Seidel, D.J. (2005). A global comparison of surface and free-air temperatures at high elevations. *Journal of Geophysical Research, 110,* D03104. doi:10.1029/2004JD005047

Piao, S., Fang, J., Zhou, L., Ciais, P., & Zhu, B. (2006). Variations in satellite-derived phenology in China's temperate vegetation. *Global Change Biology, 12*(4), 672-685. doi: 10.1111/j.1365-2486.2006.01123.x

Ploum S. W., Lyon S. W., Teuling A. J., Laudon H., & van der Velde Y. (2019). Soil frost effects on streamflow recessions in a subarctic catchment. *Hydrological Processes, 33*(9), 1304-1316.

Pomeroy J. W., Bewley, D. S., Essery, R. L. H., Hedstrom, N. R., Link, T., Granger, R. J., Sicart, J. E, Ellis, C. R., & Janowicz, J. R. (2006). Shrub tundra snowmelt. Hydrological Processes. 20, 923-941. doi: 10.1002/hyp.6124

Pomeroy, J.W., & Gray, D.M. (1995). Snowcover: Accumulation, Relocation, and Management. NHRI Science Report No. 7.

Quinton, W.L., & Marsh, P. (1999). A conceptual framework for runoff generation in a permafrost environment. *Hydrological Processes, 13*(16), 2563-2581. doi: 10.1002/(SICI)1099-1085(199911)13:16<2563::AID-HYP942>3.0.CO;2-D

Ramage, J., Jungsberg, L., Wang, S., Westermann, S., Lantuit, H., & Heleniak, T. (2021). Population living on permafrost in the Arctic. *Population and Environment.* doi: 10.1007/s11111-020-00370-6

Rangwala, I., & Miller, J. R. (2012). Climate change in mountains: a review of elevation-dependent warming and its possible causes. *Climatic Change, 114,* 527-547. doi: 10.1007/s10584-012-0419-3.

Rasouli K., Pomeroy J. W., Janowicz J. R., Carey S. K., & Williams T. J. (2014). Hydrological sensitivity of a northern mountain basin to climate change. *Hydrological Processes,* 28, 4191–4208. doi: 10.1002/hyp.10244

Rasouli, K., Pomeroy, J.W., Janowicz, J.R., Williams, T.J., & Carey, S.K. (2019). A long-term hydrometeorological dataset (1993-2014) of a northern mountain basin: Wolf Creek Research Basin, Yukon Territory, Canada. *Earth System Science Data, 11,* 89-100. doi: 10.5194/essd-11-89-2019.

Rasouli, K., Scharold, K., Mahmood, T. H., Glenn, N. F., & Marks, D. (2020). Linking hydrological variations at local scales to regional climate teleconnection patterns. *Hydrological Processes, 34,* 5624-5641. doi: 10.1002/hyp.13982

Rodionov, S. N., Bond, N. A., & Overland, J. E. (2007). The Aleutian low, storm tracks, and winter climate variability in the Bering Sea. *Deep Sea Research Part II: Tropical Studies in Oceanography, 54*(23-26), 2560-2577. doi: 10.1016/j.dsr2.2007.08.002

Rohrer, M., Bronnimann, S., Martius, O., Raible, C. C., & Wild, M. (2019). Decadal variations of blocking and storm tracks in centennial reanalyses. *Tellus A: Dynamic Meteorology and Oceanography, 71*(1), 1586236. doi: 10.1080/16000870.2019.1586236

Rovansek, R. J., Hinzman, L. D., & Kane, D. L. (1996). Hydrology of a tundra wetland complex on the Alaskan Arctic Coastal Plain, *Arctic and Alpine Research, 28*(3), 311-317. doi: 10.1080/00040851.1996.12003183

Rupper, S., Steig, E. J., & Roe, G. (2004). The relationship between snow accumulation at Mt. Logan, Yukon, Canada, and climate variability in the north Pacific. *Journal of Climate, 17,* 4724-4739.

Semmens, K.A., & Ramage, J.M. (2013). Recent changes in spring snowmelt timing in the Yukon River basin detected by passive microwave satellite data. *The Cryosphere, 7,* 905-916. doi: 10.5194/tc-7-905-2013

Semmler, T., Danilov, S., Gierz, P., Goessling, H. F., Hegewald, J., Hinrichs, C., et al. (2020). Simulations for CMIP6 with the AWI climate model AWI-CM-1-1. *Journal of Advances in Modelling Earth Systems, 12,* e2019MS002009. doi: 10.1029/2019MS002009

Shabbar A., & Khandekar, M. (1996). The impact of el Nino-Southern oscillation on the temperature field over Canada: Research note, *Atmosphere-Ocean, 34*(2), 401-416. doi: 10.1080/07055900.1996.9649570

Shur Y., Hinkel K. M., & Nelson F. E. (2005). The Transient Layer: Implication for Geocryology and Climate-Change Science. *Permafrost and Periglacial Processes, 16,* 5-17. doi: 10.1002/ppp.518

Simpson, J. J., Hufford, G. L., Fleming, M. D., Berg, J. S., & Ashton, J. B. (2002). Long-term climate patterns in Alaskan surface temperature and precipitation and their biological consequences. *IEEE Transactions on Geoscience and Remote Sensing, 40*(5), 1164-1184

Smith C. A. S., Meikle J. C., & Roots C. F. (editors) (2004). Ecoregions of the Yukon Territory: Biophysical properties of Yukon landscapes. Agriculture and Agri-Food Canada, PARC Technical Bulletin No. 04-01, Summerland, British Columbia, 313p.

Smith, L. C., Pavelsky, T. M., MacDonald, G. M., Shiklomanov, A. I., & Lammers, R. B. (2007). Rising minimum daily flows in northern Eurasian rivers: A growing influence of groundwater in the high-latitude hydrologic cycle. *Journal of Geophysical Research, 112,* G04S47. doi: 10.1029/2006JG000327

Smith, C. D. (2007). Correcting the wind bias in snowfall measurements made with the

Geonor T-200B precipitation gauge and alter wind shield. Proceedings 14th Symposium on Observations and Instrumentation, American Meteorological Society (AMS) Annual Meeting, San Antonio, Texas

Stewart, I. T., Cayan, D. R., & Detinger, M. D. (2004). Changes toward earlier streamflow timing across western North America. *Journal of Climate, 18,* 1136-1155.

Stuefer S. L., Kane, D. L., & Dean, K. M. (2020). Snow water equivalent measurements in remote Arctic Alaska watersheds, *Water Resource Research, 56*, e2019WR025621. doi: 10.1029/2019WR025621

St. Jacques J.-M., & Sauchyn D. J. (2009). Increasing winter baseflow and mean annual streamflow from possible permafrost thawing in the Northwest Territories, Canada. *Geophysical Research Letters, 36*. doi: 10.1029/2008GL035822

St. Jacques, J.-M., Sauchyn, D. J., & Zhao, Y. (2010). Northern Rocky Mountain streamflow records: Global warming trends, human impacts, or natural variability? *Geophysical Research Letters, 37*, L06407. doi: 10.1029/2009GL042045

Sturm, M., Douglas, T., Racine, C., & Liston, G. E. (2005). Changing snow and shrub conditions affect albedo with global implications. *Journal of Geophysical Research: Biogeosciences, 110*(G1), G01004. doi: 10.1029/2005JG000013

Sturm, M., McFadden, J. P., Liston, G. E., Chapin, F. S., Racine, C. H., & Holmgren, J. (2000). Snow-Shrub Interaction in Arctic Tundra: A Hypothesis with Climatic Implications. *Journal of Climate, 14,* 336-344.

Tallaksen L. M. (1995). A review of baseflow recession analysis. *Journal of Hydrology, 165,* 349-370.

Tetzlaff D., Soulsby C., Buttle J., Capell R., Carey S. K., Laudon, H., McDonell J., McGuire K., Seibert J., & Shanley J. (2013). Catchments on the cusp? Structural and functional change in northern ecohydrology. *Hydrological Processes, 27*, 766-774.

Thornewaite, C. W. (1948). An approach toward a rational classification of climate. *Geographical Review, 38*(1), 55-94. van Everdingen, R. O. (2005). Multi-language glossary of permafrost and related ground-ice terms. *International Permafrost Association.* 159 p.

Vormoor, K., Lawrence, D., Heistermann, M., & Bronstert, A. (2015). Climate change

impacts on the seasonality and generation processes of floods – projections and uncertainties for catchments with mixed snowmelt/rainfall regimes. *Hydrology and Earth System Sciences, 19,* 913-931. doi: 10.5194/hess-19-913-2015

Wan, H., Zhang, X., Zwiers, F., & Min, S-K. (2015). Attributing northern high-latitude precipitation change over the period 1966-2005 to human influence. *Climate Dynamics, 45,* 1713-1726.

Wang, S., Yang, Y., & Rivera, A. (2013). Spatial and seasonal variations in evapotranspiration over Canada's landmass. *Hydrology and Earth System Sciences, 17,* 3561-3575. doi: 10.5194/hess-17-3561-2013

Wang, Q., Fan, X., & Wang, M. (2014). Recent warming amplification over high elevation regions across the globe. *Climate Dynamics, 43,* 87-101.

Walvoord, M. A., & Striegl R. G. (2007). Increased groundwater to stream discharge from permafrost thawing in the Yukon River basin: Potential impacts on lateral export of carbon and nitrogen. *Geophysical Research Letters, 34,* 1-6. doi: 10.1029/2007GL030216

Walvoord, M. A., Voss, C. I., & Wellman, T. P. (2012). Influence of permafrost distribution on groundwater flow in the context of climate-driven permafrost thaw: Example from Yukon Flats Basin, Alaska, United States, *Water Resources Research, 48,* W07524. doi: 10.1029/2011WR011595

Wang, Q., Fan, X., & Wang, M. (2014). Recent warming amplification over high elevation regions across the globe. *Climate Dynamics, 43,* 87-101. doi: 10.1007/s00382-013-1889-3.

Wasko, C., Nathan, R., & Peel, M. C. (2020). Trends in global flood and streamflow timing based on local water year. *Water Resources Research, 56,* e2020WR02733. doi: 10.1029/2020WR027233

Whitfield, P. H., Moore, R. D., Fleming, S. W., & Zawadzki, A. (2010). Pacific Decadal Oscillation and the Hydroclimatology of Western Canada – Review and Prospects, *Canadian Water Resources Journal, 35*(1), 1-28. doi: 10.4296/cwrj3501001

Williamson, S. N., Zdanowicz, C., Anslow, F. S., Clarke, G. K. C., Copland, L., Danby, R. K., Flowers, G. E., Holdsworth, G., Jarosch, A. H., & Hik, D. S. (2020). Evidence for elevation-dependent warming in the St. Elias Mountains, Yukon, Canada. *Journal of Climate, 33*(8), 3253-3269. doi: 10.1175/JCLI-D-19-0405.1

Wittenberg, H. (1999). Baseflow recession and recharge as nonlinear storage processes. *Hydrological Processes, 13,* 715-726.

Wittenberg, H. & Sivapalan, M. (1999). Watershed groundwater balance estimation using

streamflow recession analysis and baseflow separation. *Journal of Hydrology, 219*, 20-33.

Woo, M. (2012). *Permafrost Hydrology*. Berlin: Springer Berlin.

Yamazaki, Y., Kubota, J., Ohata, T., Vuglinsky, V., & Mizuyama, T. (2006). Seasonal changes in runoff characteristics on a permafrost watershed in the southern mountainous region of eastern Siberia. *Hydrological Processes, 20*, 453-467. doi: 10.1002/hyp.5914

Yang, D., & Kane, D. L. (2021). Arctic Hydrology, Permafrost and Ecosystems. Switzerland: Swinger Nature Switzerland. doi: 10.10007/978-3-030-50930-9

Yue, S., & Wang, C. Y. (2002). Applicability of prewhitening to eliminate the influence of serial correlation on the Mann-Kendall test. *Water Resources Research, 38*(6), 1068. doi: 10.1029/2001WR000861

Zhang, X., Harvey, K. D., Hogg, W. D., & Yuzyk, T.R. (2001). Trends in Canada streamflow. *Water Resources Research, 37*(4), 987-998.

Zhang, K., Kimball, J. S., Nemani, R. R., & Running, S. W. (2010). A continuous satellite-derived global record of land surface evapotranspiration from 1983 to 2006. *Water Resources Research, 46*(9), W09522. doi: 10.1029/2009WR008800

Zhang, F.-Y., Lan-Hai, L., Sajjad, A., & Xue-Mei, L. (2014). Using path analysis to identify the influence of climatic factors on spring peak flow dominated by snowmelt in an Alpine watershed. *Journal Mountain Science, 11*(4), 990-1000. doi: 10.1007/s11629-013-2789-z